Functions of Bassoon in hippocampus-dependent learning and memory processes

Dissertation

zur Erlangung des akademischen Grades

doctor rerum naturalium

(Dr. rer. nat.)

genehmigt durch die Fakultät für Naturwissenschaften

Der Otto-von-Guericke-Universität Magdeburg

von **M.Sc., M.Eng. Anil Annamneedi**

geb. am 16. März 1987 in Narasapuram, Indien

Gutachter: Prof. Dr. rer. nat. Eckart D. Gundelfinger

Prof. Dr. med. Markus Missler

eingereicht am: 20-06-2017

verteidigt am: 01-02-2018

Acknowledgements

"If you want to shine like a sun, first burn like a sun" – A.P.J. Abdul Kalam.

"The true sign of intelligence is not knowledge but imagination" – Albert Einstein.

"Any man could, if he were so inclined, be the sculptor of his own brain." – Santiago Ramón y Cajal.

The journey till now would not have been possible without the support, guidance and help of several individuals who in one way or another, contributed and extended their valuable assistance.

First and foremost, my utmost gratitude to Prof. Eckart D. Gundelfinger, for providing the Bassoon protein to the neuroscience community. I am very grateful to him for having faith in me and providing me an opportunity to work in a wonderful institution like Leibniz Institute for Neurobiology (LIN). He has rendered tremendous support to me in every possible way and has been very careful in listening to my views and correcting me. I am very much indebted to Prof. Oliver Stork (IBIO, OvGU), for his supervision through all these years. I am equally grateful to him for his scientific ideas, discussions and encouragement during my thesis work. He has been enormously patient in guiding and correcting me. He supported me throughout my work and assisted in shaping up my thesis, successfully.

I would like to thank Prof. Anna Fejtova and Sabrina Müller for their contribution in establishing the conditional Bsn2 mouse line in our lab. I am very grateful to Dr. Gürsel Caliskan (IBIO, OvGU) for providing the electrophysiology data and great discussions. I would like to especially thank Dr. Jorge Bergado-Acosta for showing and explaining the behavioural experiments at the beginning of my study.

I would like to thank all my lab members, "the Bassooners" for their support, discussions regarding the scientific work and their friendly nature which helped to keep the working atmosphere beautiful throughout these years. I would also like to thank colleagues from IBIO, for their discussions regarding behavioural work, which helped me a lot to understand critical aspects further. I would also like to thank technical assistants and animal facilities from LIN and IBIO for their kind help and maintenance of a good laboratory environment.

I would like to thank my friends here in Magdeburg, including Sampath, Jeet, Maru, Franzi, David, Carolina, Rajeev, Sujoy, Paramesh, Santosh and so on, with whom I shared a lot of beautiful moments during all these years.

Last but not least, I am thankful to my family and friends, for their unconditional love and support, throughout these years.

Ⅰ. Summary

Bassoon is a large scaffolding protein and one of the core components of the cytomatrix at the active zone (CAZ) at presynapses. Bassoon is present in excitatory, inhibitory and modulatory presynapses and plays an important role in various aspects of presynaptic plasticity. Bassoon is involved in regulated neurotransmitter release from glutamatergic synapses and the regulation, specifically of P/Q-type Ca^{2+} channels. Bassoon plays a role in the control of presynaptic autophagy and the recruitment of the transcriptional suppressor protein CtBP1 to presynapses and lack of Bassoon affects synapto-nuclear communication. Mice with constitutive ablation of the *Bassoon* gene display impaired presynaptic function, show sensory deficits and develop severe seizures.

To specifically study the role of Bassoon at different types of synapses and its relevance for control of behavior, two conditional Bassoon mutants, one lacking the protein in excitatory synapses of the forebrain and another one lacking the protein at dopaminergic release sites were generated. Emx1-Cre and DAT-Cre driver mice were used to specifically inactivate floxed exon 2 of the *Bsn* gene to generate conditional knockout of *Bsn* in forebrain excitatory neurons (B2E cKO) and conditional knockout of *Bsn* in mid brain dopaminergic neurons (B2D cKO), respectively. Immunohistochemical stainings confirmed specificities of both cKOs. This study shows that B2E cKO mice are hyperactive in the home cages during all the time, display selectively enhanced background contextual fear memory and improved performance in a pattern separation task. Interestingly, adult B2D cKO mice also display hyperactive behavior in home cages only during dark phase. However, old B2D cKO mice display no behavioral changes compared to respective control mice. In B2E cKO mice, behavioral changes are accompanied by an augmentation of baseline synaptic transmission at medial perforant path (MPP) to dentate gyrus (DG) synapses, as indicated by increased ratio of field excitatory postsynaptic potential (fEPSP) slope to fiber volley (FV) amplitude and a lack of maturation in DG responsiveness between juvenile and adult Bsn cKO mice. An increased complexity of apical dendrites of DG granule cells and alterations in the expression of cellular maturation markers suggest an immature phenotype of the DG and augmented neurogenesis in B2E cKO mice. Taken together, this study suggests that Bassoon expression plays a role in the structural and functional maturation of MPP to DG network, and is required for DG-dependent memory formation.

Ⅱ. Zusammenfassung

Bassoon ist ein großes Gerüstprotein mit einer zentralen Rolle in der sogenannten Cytomatrix an der aktiven Zone (CAZ) in Präsynapsen. Bassoon kommt sowohl in exzitatorischen und inhibitorischen, als auch an modulatorischen präsynaptischen Endigung vor und spielt eine wichtige Rolle bei präsynaptischer Plastizität. Dabei ist Bassoon an der Regulation der Neurotransmitter-Ausschüttung an glutamatergen Synapsen und der synaptischen Lokalisation von P/Q-Typ-Calciumkanälen beteiligt. Weiterhin spielt Bassoon eine Rolle bei präsynaptischen Autophagieprozessen. Kürzlich wurde gezeigt, dass Bassoon für die Rekrutierung des transkriptionellen Repressors CtBP1 in die Präsynapse verantwortlich ist und dass das Fehlen von Bassoon die Synapse-zu-Nukleus Kommunikation beeinträchtigen kann. Ferner zeigen Mäuse mit einer konstitutiven Deletion des *Bassoon*-Gens Beeinträchtigungen der präsynaptischen Funktion sowie sensorische Defizite und können schwere Krampfanfälle entwickeln.

Um die Rolle von Bassoon gezielt in verschiedenen Synapsen zu analysieren und seine Relevanz für das Verhalten zu überprüfen, wurden zwei konditionelle Bassoon-Knock-Out-Mauslinien gezüchtet. Dabei fehlt einer Mutante das Bassoon-Gen in exzitatorischen Synapsen des Vorderhirns und einer weiteren Mutante in dopaminergen Synapsen. Dafür wurden die beiden Cre-exprimierenden Mauslinien Emx1-Cre und DAT-Cre verwendet, um gezielt das gefloxte *Bassoon*-Gen in exzitatorischen Neuronen des Vorderhirns (B2E cKO) beziehungsweise in dopaminergen Neuronen des Mittelhirns (B2D cKO) zu inaktivieren. Mittels immunhistochemischer Färbungen wurde dabei die Spezifität der Knock-Outs bestimmt. Die vorliegende Arbeit zeigt, dass B2E-cKO-Mäuse eine permanente Hyperaktivität aufweisen, eine höhere Reaktion speziell in der Kontext-bedingten Furchtkonditionierung zeigen und die Verschiebung von Objekten in einer „Pattern Separation"-Aufgabe besser erkennen können. Interessanterweise zeigen adulte B2D-cKO-Mäuse ebenfalls hyperaktives Verhalten in ihrem Haltungskäfig, allerdings nur in der Dunkel-Phase. Ältere B2D-cKO-Mäuse zeigen dann keine solchen Verhaltensunterschiede gegenüber ihren Kontrollen mehr. Weiterhin wurde in B2EcKO-Mäusen eine Steigerung der basalen synaptischen Transmission vom medialen Tractus perforans (MPP) zu Synapsen des Gyrus dentatus (DG) festgestellt. Bei den B2E-Mäusen konnte eine Verzögerung des Reifungsprozessen der Synapsen im DG festetellt werden. Eine gesteigerte

Komplexität der apikalen Dendriten der Granularzellen des DG und eine Veränderung in der Expression der zellulären Reifungsmarker deuten auf einen unreifen Phänotyp des DG sowie eine gesteigerte Neurogenese in B2E-cKO-Mäusen hin. Zusammenfassend wurde in dieser Arbeit gezeigt, dass die Expression von Bassoon eine wichtige Rolle sowohl in der strukturellen als auch in der funktionellen Reifung des MPP- und DG-Netzwerkes hat und für die DG-abhängige Gedächtnisbildung von Bedeutung ist.

Ⅲ. Table of contents

1 Introduction

1.1 Learning and memory - Importance of hippocampus and its sub region dentate gyrus (DG)

Learning is a process by which humans and animals acquire new information or modify the existing information based on the individual experience. Retaining and storing such information for shorter or longer time windows is what we call as memory (Goelet et al., 1986). Based on the retention time window of information, memories can be differentiated into short-term (seconds to minutes) and long-term (hours to days and years) memories. Further, both short-term and long-term memories are classified into different sub-classes as mentioned in figure 1.1. The two forms of the short-term memory do not require synthesis of new proteins, whereas, long-term memory require protein synthesis and re-organization. The anatomical structures primarily encoding the memories differ based on the type of memory they encode. For example, the anatomical structures like striatum, neocortex, cerebellum and amygdala mediate the procedural memories whereas, hippocampus, entorhinal cortex and perirhinal cortex process the explicit or declarative memories (Baddeley and Hitch, 1993; Squire and Zola, 1996). Declarative or explicit memory involves three different processes - encoding (or consolidation), storage and retrieval (Schacter et al., 1998). Initial processing of information about the input stimulus and its environment pertains to encoding. Retaining of this information over time is a mechanism of storage. During retrieval, the stored information is used to create a conscious representation to execute a learned response. Though the explicit memories are encoded by the exact location, the mechanism and exact location of the storage of these memories are not clear.

Episodic memory, a subclass of declarative or explicit memory (Figure 1.1) is one of the major cognitive memory systems and said to be unique from the remaining memory systems (Tulving and Markowitsch, 1998). Episodic memory can be defined as a memory representation towards experiences and events in a specific point of time and context, from which we retrieve the actual events that took place (Wood et al., 2012). Episodic memory is widely studied because of its uniqueness, and various findings have shown that episodic memories are encoded by the hippocampus and its sub-regions.

Activity-dependent synaptic plasticity within the hippocampal synapses is a prominent feature involved in episodic memories (Neves et al., 2008).
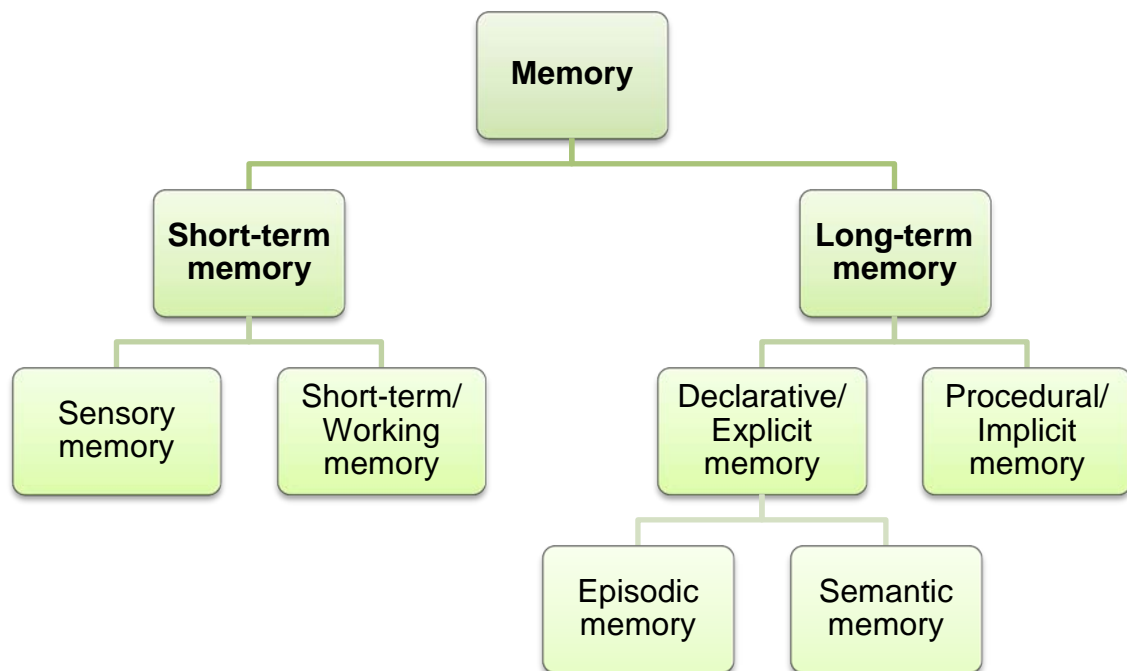
Figure 1.1. Classification of Memory. Memory can be classified in to short-term and long-term based on the retention time. Furthermore, both short-term and long-term memories are classified into different sub classes. Short-term memory is classified into sensory memory and sometimes can be classified as working memory. Long-term memory is classified into declarative and procedural memories. Declarative memory in turn divided into episodic and semantic memory (Baddeley and Hitch, 1993; Squire and Zola, 1996; Wood et al., 2012).

It was shown long back that hippocampus is selectively involved and important for episodic and spatial learning and memory (Scoville and Milner, 1957; Eichenbaum et al., 1999; Burgess et al., 2002). Hippocampal formation and its integrity are very crucial for the creation of cognitive map supporting spatial navigation (Eichenbaum et al., 1990; Sutherland et al., 2001). Previously, it was also shown that hippocampus plays a significant role in contextual fear conditioning, by forming the cognitive representation of context (Selden et al., 1991; Maren et al., 1998; Holland and Bouton, 1999). Lesion studies using animal models revealed that hippocampal lesions result in failure to learn or loss of spatial memory in these animals (Martin et al., 2005; Neves et al., 2008). Especially dorsal hippocampal lesion impairs the spatial information processing in the brain. Because, most of the sensory inputs coming from several cortical areas and the olfactory bulb mainly carry information to the dorsal hippocampus rather than to the ventral hippocampus (Moser et al., 1993). Lesions of the dorsal hippocampus also results in contextual fear conditioning impairments.

Acquisition of fear learning during contextual fear conditioning is impaired, where both unconditioned stimulus (foot shock) and conditioned stimulus are paired (Phillips and LeDoux, 1994).

In recent times, within the hippocampal formation, dentate gyrus (DG) granule cells (GCs) are being shown to be critical players involving in discrimination of contexts and the spatial behavior. The GCs play a role in recalling the context-specific fear response in mice (Hernandez-Rabaza et al., 2008; Liu et al., 2012) through encoding by entorhinal cortical ocean cells which make connections to GCs and CA3 cells. These ocean cells form context representation and activate the CA3 cells and contextual fear memory (Kitamura et al., 2015). The GCs are also necessary for adoption of place strategies (Xavier and Costa, 2009). The dorsal DG is particularly shown to be involved in the processing of spatial features and spatial pattern separation, which is based on the distance between the objects. The processing of the object-spatial information in dorsal DG is mediated through encoding processes (Kesner, 2013). The processing of object-spatial information is mainly due to the specific information processing abilities of inputs coming from the medial and lateral perforant paths to the DG (Eichenbaum et al., 2007; Kesner, 2007). The lesion study at dorsal DG has shown the disruption of object-spatial feature configuration and spatial recognition memories (Kesner et al., 2015). As already mentioned, DG has involved in pattern separation (ability to separate the memory components into the more distinct and unique complex representations which are resistant to confusion) memories (Gilbert et al., 1998; Leutgeb et al., 2007). An additional and important phenomenon occurring at DG, i.e., neurogenesis also plays a role in these specific forms of learning and memory (Aimone et al., 2006).

1.2 Role of neurogenesis in learning and memory

DG of the hippocampal formation is one of the two regions in the mammalian brain, where continuous neurogenesis takes place throughout the life (Altman and Das, 1965; Gage, 2002). This adult hippocampal neurogenesis is one of the complex processes occurs at subgranular zone (SGZ) through the proliferation of neural progenitor cells. It is postulated that endothelial cells and astrocytes promote the proliferation process within the hippocampus (Palmer et al., 1999; Song et al., 2002) and the Bone morphogenic protein (BMP) signaling has been shown to instruct neural progenitor cells to differentiate (Lim et al., 2000). In addition, neurogenesis can also be

enhanced by environmental enrichment, running, hippocampus-dependent learning and under pathological conditions like seizures or ischemic brain injury (Ming and Song, 2005; Deng et al., 2010). The adult-born GCs are continuously incorporated into the hippocampal circuitry and require a long time (several weeks) to develop into mature neurons. They remain in the young and immature state during the development process exhibiting properties like increased excitability, enhanced plasticity and express markers like doublecortin (DCX) and calretinin (Schmidt-Hieber et al., 2004; Zhao et al., 2008). Once mature and become old, adult-born GCs exhibit all the properties of functional neurons in the DG (van Praag et al., 2002). As already mentioned, DG being a part of the hippocampus is involved in contextual fear conditioning and critical pattern separation. Further, ablation of neurogenesis in hippocampus results in impaired contextual fear conditioning and pattern separation in mice (Saxe et al., 2006; Clelland et al., 2009) and regulated ablation of immature GCs results in long-term spatial memory deficits (Deng et al., 2009). On the contrary, augmented adult neurogenesis in mice results in improved pattern separation (Sahay et al., 2011) which is mediated by the immature GCs. Thus, the synaptic transmission and plasticity between entorhinal cortex (EC) and hippocampus have implications in mediating these processes (Nakashiba et al., 2012).

1.3 Mechanisms underlying learning and memory processes

So far knowledge about learning and memory suggests different cellular mechanisms underlying these processes. These include synaptic plasticity, homeostatic changes upon the encoding of memory and structural plasticity. Synaptic plasticity in various brain regions contributing to different memories, points to the possibility that long-term potentiation (LTP) can initially encode, store for a longer time and retrieve different types of information. Hence LTP is considered as major cellular mechanism underlying learning and memory (Cooke and Bliss, 2006). For example, in the hippocampus, the information storage is mediated through the involvement of an activity-dependent LTP, resulting in an increased transmission (Pastalkova et al., 2006; Neves et al., 2008). However, homeostatic changes (or plasticity) at these synaptic connections is considered as another important mechanism. Reversal of the memory should be correlated with the reversal of the changes occurring at the cellular level which should be on par with the conditions prior to the activity or stimulation. During memory encoding process, synaptic changes lead to prolonged changes in excitability of

neurons within a circuit, which can lead to the excitotoxic condition under extreme circumstances. Previous studies have shown the impact of these processes on cell survival or memory storage (Nelson and Turrigiano, 2008; Schacher and Hu, 2014). The homeostatic mechanisms include regulation of presynaptic neurotransmitter release by affecting the structural or functional properties of presynapse (Burrone et al., 2002; Frank et al., 2006) or by regulating excitability through modulation of voltage-gated ion channels (Driscoll et al., 2013). Further, these mechanisms were shown to be involved in the long-term synaptic plasticity which underlies learning and memory (Luscher et al., 1999; Zhang and Linden, 2003).

Another mechanism underlying learning and memory is structural plasticity, which is a form of synaptic change. This includes remodeling of connections between neurons, regulation of dendritic spine and axonal bouton composition and complete structural changes in the dendritic spine and axonal structures. Adult neurogenesis is one of such structural plasticity which requires modification of existing network to accommodate newly born GCs (Sailor et al., 2017). These modifications within the circuitry of the adult hippocampus are known to play a major role in learning and memory. The information processing in the hippocampus is mediated through DG and/or bypassing DG from EC inputs (Figure 1.2).
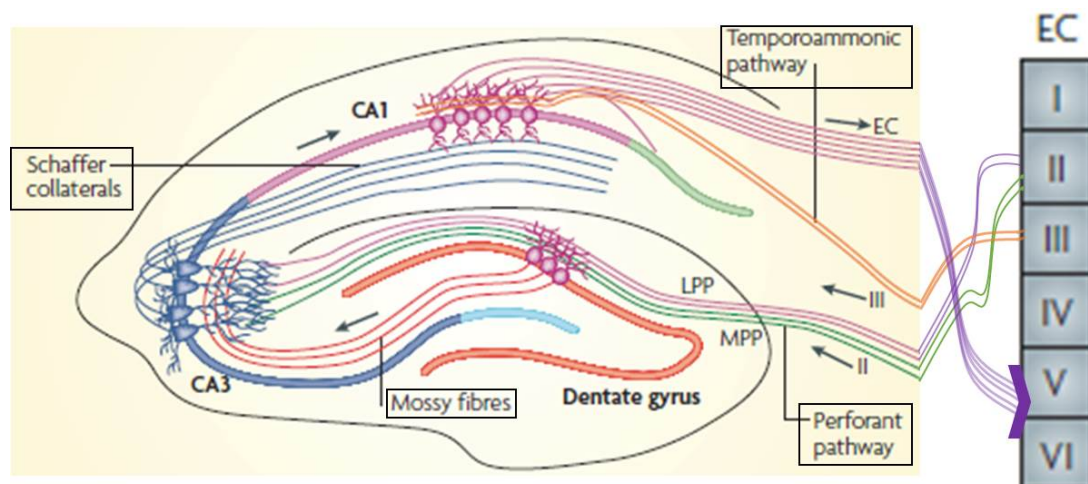
Figure 1.2. Hippocampal circuitry in the rodent brain. The GCs receive inputs from layer II of EC through perforant path (PP). Inner molecular layer at DG receives inputs through medial perforant path (MPP) and outer molecular layer receives inputs through lateral perforant path (LPP). The axonal projections from GCs make synapses with pyramidal cells at CA3 through mossy fiber path. In turn, CA3 sends its projections to CA1 through Schaffer collaterals. The axons from layer II of EC also project directly to CA3 through PP. CA1 receives inputs from layer III of EC through temporoammonic path and sends its axons to layers V of EC. Adapted from Deng et al. (2010)

These pathways within the hippocampus mediate the processes of pattern separation and pattern completion. Synaptic plasticity and transmission in the EC – DG – CA3 pathway have implication in pattern separation. In particular, the young and immature GCs having synapses with perforant path terminals, display higher excitable state and involve in pattern separation (Schmidt-Hieber et al., 2004; Toni and Schinder, 2015). For pattern completion, synaptic plasticity and transmission at a recurrent network of CA3 are proposed to play a major role (Leutgeb et al., 2007; Nakashiba et al., 2012).

1.4 Chemical synapse and the presynaptic active zone (AZ)

Memory formation and maintenance requires changes in neuronal networks connectivity based on modifications in strength and number of synapses. Changes at the synaptic sites, especially strengthening or weakening of the synaptic connections are known to play a major role in memory formation and retention. Chemical synapses are the cell-cell contact sites or biological junctions where the electrical signal arriving at the presynapse changes into chemical signals in the form of neurotransmitter which is released into the synaptic cleft. The postsynapse on the other side of synaptic cleft, then detects this chemical signal and propagates it further as an electric signal at the excitatory synapses or does not propagate further at inhibitory synapses.

The presynaptic bouton is known to be the principal site for the regulation and release of neurotransmitters. The active zone (AZ) is the region of the presynaptic plasma membrane at which neurotransmitter is released into the synaptic cleft. The cytomatrix at the active zone, in short CAZ, is exactly aligned with the post synaptic membrane apparatus known as post synaptic density (PSD). Neurotransmitters are stored in synaptic vesicles (SVs) at the presynaptic site, which maintains the chemical synaptic transmission. SVs undergo vesicle trafficking cycle which consists of different steps (Sudhof, 2004). These includes transport of neurotransmitter into vesicles, clustering of vesicles to presynaptic membrane, docking of the vesicles near the release sites and priming of the docked vesicles to the membrane. Upon influx of Ca^{2+} ions into the presynaptic membrane at the active zone through voltage-gated calcium channels, the docked vesicles are fused to the active zone membrane and release neurotransmitters into the cleft through exocytosis. Compensatory endocytosis of the vesicles takes place

after the release of neurotransmitter next to the active zone, what allows the fast recycling and refilling of SVs (Figure 1.3).
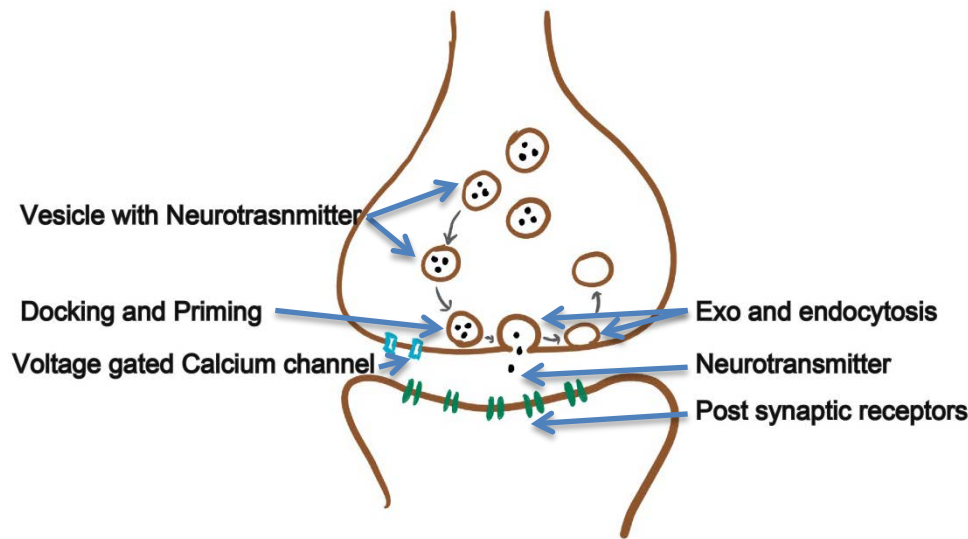
Figure 1.3. Chemical synapse and synaptic vesicle cycle. Diagrammatic representation of events occurring during synaptic vesicle cycle at chemical synapses. This includes docking and priming of vesicles containing neurotransmitter, which upon the influx of Ca^{2+} ions, release neurotransmitter into the synaptic cleft through exocytosis. Further, these vesicles are refilled through endocytosis, which occurs in different ways – recycling with or without an endosomal intermediate, clathrin-mediated endocytosis.

Endocytosis can take place in different pathways – local and fast recycling of the vesicles (kiss-and-stay), rapid endocytosis mediated without clathrin-coated intermediate (kiss-and-run) and slow process involving clathrin-coated intermediates (Sudhof, 2004). The synaptic vesicle pools are classified into three types – the reserve pool, recycling pool and readily releasable pool (RRP). The reserve pool is defined as a large pool of synaptic vesicles (approx~80-90% of the total pool), and release of this pool is triggered upon intense stimulation. Recycling pool is defined as the pool of vesicles, which require moderate stimulation for release. This pool is relatively small (approx~10-15%) and the vesicles in recycling pool participate in exo- and endocytosis. The RRP consists of very few vesicles (approx1% of the total pool) and is defined as the synaptic vesicles that are docked and primed to the pre-synaptic active zone membrane and are readily available for release (Sudhof, 2004; Rizzoli and Betz, 2005).

The CAZ is involved in organizing and regulating the SV cycle. Important protein families involved in the structural and functional organization of the CAZ include large proteins Bassoon and Piccolo together with Munc13s, Rab3-interacting molecules (RIMs), RIM-binding proteins (RBPs), CAST/ELKS proteins, liprins-α

(Fejtova and Gundelfinger, 2006; Schoch and Gundelfinger, 2006; Sigrist and Schmitz, 2011; Ackermann et al., 2015) (Figure 1.4).
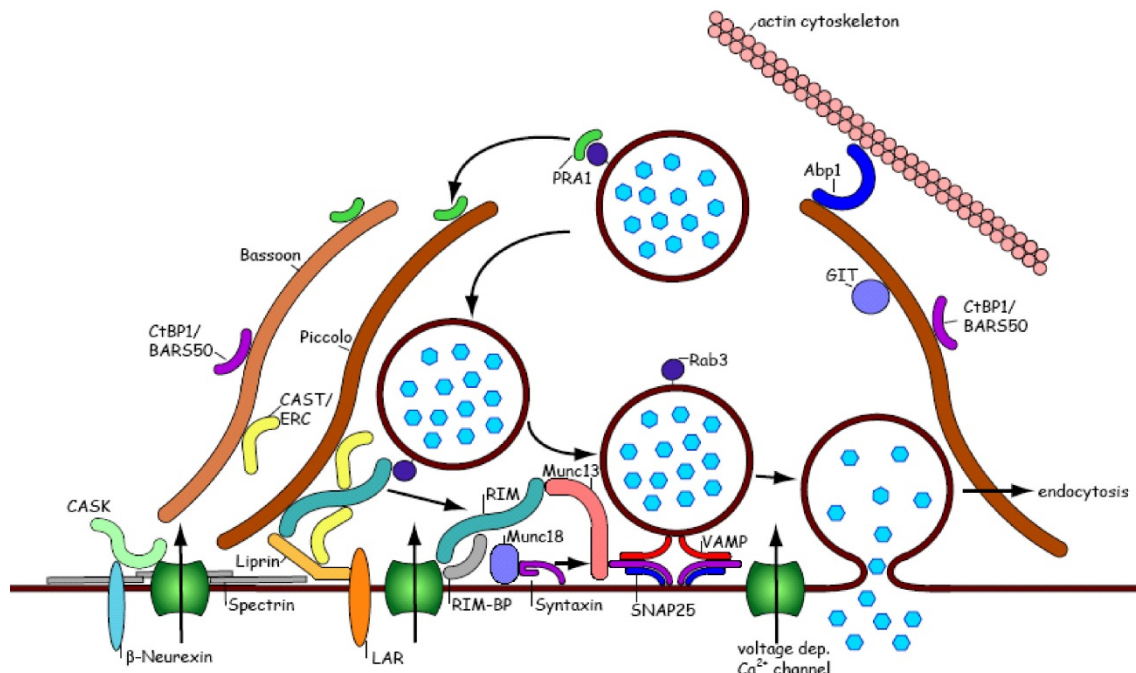
Figure 1.4. Diagrammatic representation of pre-synapse and different proteins present at presynaptic side (Fejtova and Gundelfinger, 2006)**.**

These are multi-domain proteins and perform very important functions at the presynapse like, SV trafficking cycle as mentioned above, Ca^{2+} channel anchoring, regulation of actin-based cytoskeleton, etc. Bassoon and Piccolo are detectable very early during synaptogenesis at the site of neurotransmitter release (Zhai et al., 2001) and exert functions in the developmental assembly of active zone, localization of voltage-gated Ca^{2+} channels and SV priming (Shapira et al., 2003; Ziv and Garner, 2004; Gundelfinger et al., 2016). RIM (Rab3 interacting molecule) family proteins contain four isoforms RIM1α, RIM2α, β and γ, RIM3γ and RIM4γ (Wang and Sudhof, 2003) and regulate synaptic neurotransmitter release at the active zone by interacting with other proteins. RIM1α interacts with Munc13-1 and liprins-α to form a protein scaffold and maintain the normal neurotransmitter release probability (Schoch et al., 2002). Munc13s (Munc13-1 and 2) play a major role in Ca^{2+} binding. Studies have shown that these proteins are also involved in SV priming (Brose et al., 2000). By interacting with Syntaxin, Munc13 forms a loose SNARE complex at the presynaptic membrane allowing Ca^{2+} dependent SV fusion (Rosenmund et al., 2003).

1.5 Bassoon

1.5.1 Bassoon-structure

Bassoon is a large scaffolding protein at the presynaptic site of a chemical synapse, with 420 kDa molecular weight, discovered in late 1990's (tom Dieck et al., 1998). It localizes specifically to the CAZ, where neurotransmitters are being released into the synaptic cleft. From previous studies, it is evident that a fraction of Bassoon is membrane associated and is also associated with vesicular structures. Together these data suggest that at least a fraction of Bassoon is associated with a membranous compartment in neurons (Sanmarti-Vila et al., 2000). Bassoon is expressed widely in different synaptic populations including excitatory and inhibitory (Richter et al., 1999), cholinergic and catecholaminergic presynaptic sites (Juranek et al., 2006).

Bsn gene is localized to chromosomes 3p21 in humans and 9F in rodents. *Bsn* gene contains 12 exons, with a large central exon 5 (6.6 kb) spanning most of the genomic region (tom Dieck et al., 1998; Winter et al., 1999) (Figure 1.5). *Bsn* gene is very well conserved among the different species of vertebrates including humans (Wang et al., 1999; Winter et al., 1999) and so far no mutations have been identified in *Bsn* gene which can be linked to a human disease.

— Genomic region
▯ Untranslated region
▮ Coding exons

Figure 1.5. *Bsn* gene structure. Schematic representation of Bsn gene showing coding and non-coding sequences.
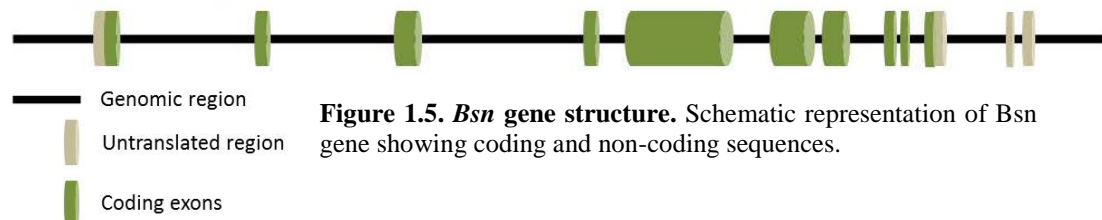
The structural organization of Bassoon protein contains two double zinc finger (Znf 1 and Znf 2) motifs and three coiled coil (CC1, CC2 and CC3) domains and these are highly conserved in humans and rodents (Winter et al., 1999). Among them CC2 is the largest domain which is associated with important functional impact. All three coiled-coil domains serve as multiple interacting sites for many other proteins, involving in various important functions such as assembly of CAZ core complex, voltage-gated calcium channel regulation, trafficking of AZ material, synapto-nuclear communication and presynaptic ubiquitination (tom Dieck et al., 2005; Fejtova et al., 2009; Waites et al., 2013; Davydova et al., 2014; Ivanova et al., 2015; Gundelfinger et al., 2016). Apart from the protein-protein interaction domains, a heptad-repeat region is

also present next to the Znf 2 domain. This heptad-region acts as a common phosphorylation site for proline-directed protein kinases, which functions in diverse cellular processes such as cell cycle, transcription etc. (tom Dieck et al., 1998) (Figure 1.6).

Figure 1.6. Structure of Bassoon protein. Schematic representation of Bassoon protein showing different regions including Zinc finger motifs, coiled coil domains, heptad repeat and poly-Q regions.
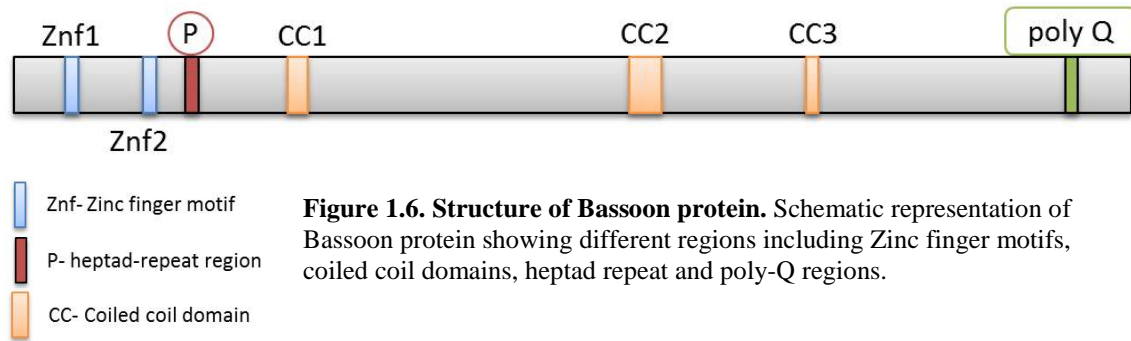
1.5.2 Bassoon functions and mutant mice

Important functions of Bassoon protein can be elucidated by using knockout mice and from the neuronal cultures derived from these mutant mice. So far two different constitutive knockout mice were analyzed: $Bsn^{\Delta Ex4/5}$ mice, generated by disrupting the *Bsn* gene, in which parts of exon 4 and the entire exon 5 were deleted (Altrock et al., 2003). The second mutant was Bsn^{gt} mice, generated using gene trap method, lacking Bassoon at most of the synapses in the brain (Hallermann et al., 2010). Both these Bassoon mutants display similar phenotype in terms of seizures and sensory impairments. More than 50% of the homozygous $Bsn^{\Delta Ex4/5}$ mice die within the first six months after birth due to spontaneous epileptic seizures (Altrock et al., 2003) (Figure 1.7a).

Analysis of both the Bassoon mutants explains its important involvement in anchoring of ribbon synapses, which consists of highly specialized forms of CAZ. For instance, it was reported that photoreceptor ribbons lacking Bassoon are not anchored to the presynaptic active zones (Figure 1.7b,c), which results in an impaired photoreceptor synaptic transmission hence suggesting a role of Bassoon in the formation and the function of photoreceptor ribbon synapses of the mammalian retina (Dick et al., 2003; tom Dieck et al., 2005). It was also shown that Bassoon mutant mice show impairment in ribbon anchoring at cochlear inner hair cell synapses (Figure 1.7d,e), what results in impaired auditory signaling (Khimich et al., 2005; Frank et al., 2010).
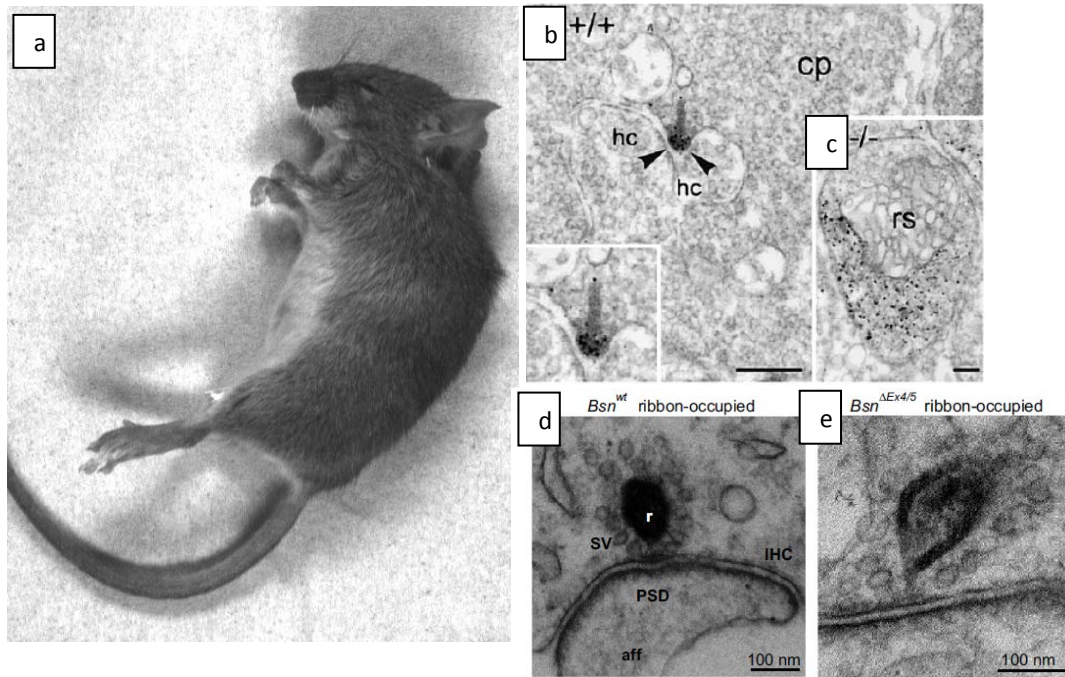
Figure 1.7. Bassoon mutant mice ($Bsn^{\Delta Ex4/5}$). a, $Bsn^{\Delta Ex4/5}$ mice died due to epileptic seizures. **b,c** retinal structure in WT (+/+) and $Bsn^{\Delta Ex4/5}$ mice (-/-).. **d,e** ribbon occupied IHC ribbon synapses. Panel (a) is provided by Prof. Gundelfinger. b-d, Adapted from Dick et al. (2003) and Frank et al. (2010)

Another important function of Bassoon is its involvement in regulating presynaptic voltage-gated calcium channels. Bassoon is involved in the localization of presynaptic voltage-gated Ca^{2+} channels, specifically of $Ca_V2.1$ (P/Q-type) channels, at hippocampal excitatory synapses through interaction with RIM-binding proteins (RBPs) (Davydova et al., 2014). A similar phenotype has also been observed at inner ear hair cell synapses, where the mutant synapses lacking the ribbon exhibited fewer $Ca_V1.3$ Ca^{2+} channels in abnormally shaped clusters (Frank et al., 2010). It was evident that these ribbon-less hair cell synapses also have reduced numbers of functional release sites, with impairments in their refilling, and consequently a smaller RRP. Similarly, the deficit in the replenishment with synaptic vesicles was observed at synapses with particularly high firing rates, such as the cerebellar mossy fiber synapse or the endbulb of Held in the auditory system (Hallermann et al., 2010; Mendoza Schulz et al., 2014).

Bassoon is also involved in the transport of the active zone material to the presynaptic sites. It was shown that Bassoon together with Piccolo constitutes the core components of the CAZ and are transported for assembling the nascent synapses in association with Golgi-derived membranous organelles, called Piccolo-Bassoon transport vesicles (PTVs) (Zhai et al., 2001). Bassoon interacts with dynein light chains

(DLCs) and the disruption of this binding result in impaired axonal trafficking of PTVs (Fejtova et al., 2009). Apart from this, recent studies regarding Bassoon functions have shown that Bassoon plays a role in synapto-nuclear communication. Bassoon is involved in the recruitment of the transcriptional co-repressor protein CtBP1 to presynapses, in an activity-dependent manner (Ivanova et al., 2015; Ivanova et al., 2016). And it was also shown that the absence of Bassoon disturbs the synapto-nuclear communication via CtBP1 and, in turn, gene expression in neurons.

Recently, it was shown that Bassoon together with Piccolo regulates presynaptic ubiquitination and proteostasis. shRNA-mediated knockdown of Bassoon and Piccolo from glutamatergic synapses results in the disruption of synaptic protein homeostasis and integrity in older cultures (12 and 14-16 days *in vitro*, DIV) (Figure 1.8).
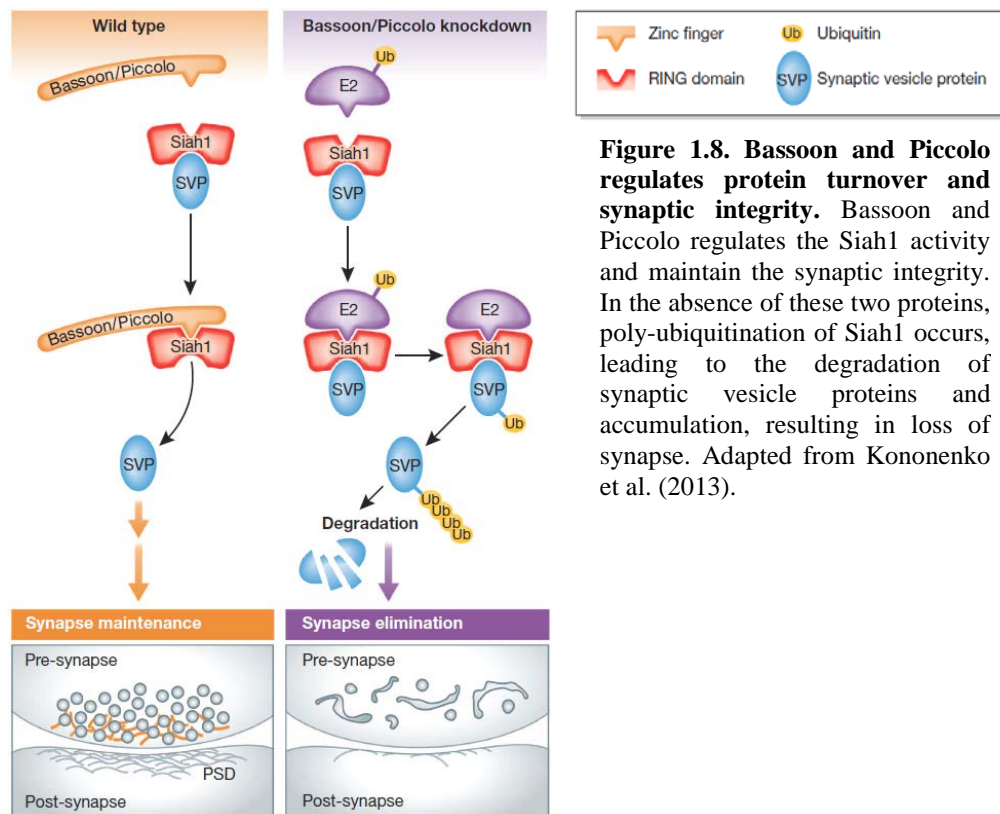
Figure 1.8. Bassoon and Piccolo regulates protein turnover and synaptic integrity. Bassoon and Piccolo regulates the Siah1 activity and maintain the synaptic integrity. In the absence of these two proteins, poly-ubiquitination of Siah1 occurs, leading to the degradation of synaptic vesicle proteins and accumulation, resulting in loss of synapse. Adapted from Kononenko et al. (2013).

Bassoon together with Piccolo maintains the protein turnover by controlling the activity of the E3 ubiquitin ligase Siah1, which apparently plays an important role in the maintenance of the presynaptic structure and function (Kononenko et al., 2013; Waites et al., 2013). Very recently it was shown that Bassoon alone could control the presynaptic autophagy by interacting with Atg5. This process is known to be a poly-ubiquitination dependent, but not through Siah1 (Okerlund et al., 2017).

$Bsn^{\Delta Ex4/5}$ mutants show enlargement of some brain structures like cortex and hippocampus (Figure 1.9), which is a peculiar phenotype (Angenstein et al., 2007). The enlarged brain structures further correlated with elevated BDNF levels in the hippocampus and other forebrain regions. Further studies on $Bsn^{\Delta Ex4/5}$ mice had revealed a correlation between increased hippocampal size with enhanced neurogenesis. Apart from enhanced neurogenesis, reduced apoptosis was also observed in $Bsn^{\Delta Ex4/5}$ mutant mice (Heyden et al., 2011).
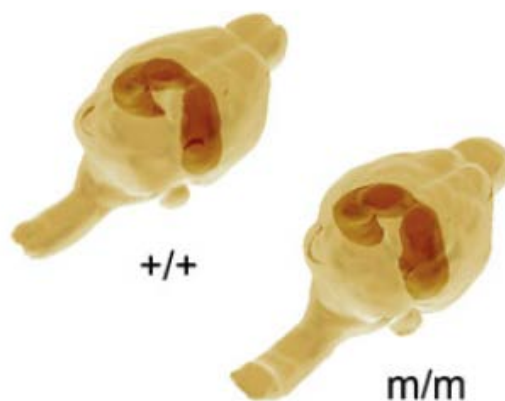
Figure 1.9. Anatomical changes in $Bsn^{\Delta Ex4/5}$ mice. Enlarged hippocampus in $Bsn^{\Delta Ex4/5}$ mice (m/m) compared to WT mice (+/+). Adapted from Heyden et al. (2011).

Furthermore $Bsn^{\Delta Ex4/5}$ mice display a significantly reduced excitability and synaptic depression accompanied by spontaneous epileptic seizures (Altrock et al., 2003), impaired long-term potentiation (LTP) at CA1 synapses; with morphological changes being observed at CA1 pyramidal neurons (Sgobio et al., 2010). In addition, reduced apical dendritic length and spine density was observed in $Bsn^{\Delta Ex4/5}$ mice. Analysis of mossy fiber (MF) synapses at CA3 region indicated a disturbance of synaptic maturation and development in $Bsn^{\Delta Ex4/5}$ mice (Lanore et al., 2010). An Increased MF-EPSCs amplitude in $Bsn^{\Delta Ex4/5}$ mice which was observed at postnatal day 7 (P7) was reduced at P14, suggesting an inactivation of subset of glutamatergic synaptic sites, similar to what was observed by Altrock and co-workers at conventional hippocampal synapses (2003). At the ultra-structural level, hippocampal CA1 synapses of $Bsn^{\Delta Ex4/5}$ mice displayed no changes in parameters like extension of active zone or docked SVs (Altrock et al., 2003). However, at CA3 mossy fiber bouton (MFB) profile of $Bsn^{\Delta Ex4/5}$ mice displayed a large surface area, increased number of SVs and multiple

contacts with CA3 complex. An increased size of MFBs in $Bsn^{\Delta Ex4/5}$ mice was also reported by Dieni and colleagues (2015).

An abnormal synaptic plasticity was observed in $Bsn^{\Delta Ex4/5}$ mice in the striatum. LTP was reduced in medium spiny (MS) neurons of $Bsn^{\Delta Ex4/5}$ mice. However, fast-spiking (FS) interneurons showed increased short-term potentiation in mutant mice (Ghiglieri et al., 2009). Furthermore, morphological analysis of MS neurons revealed an increased dendritic branching in $Bsn^{\Delta Ex4/5}$ mice with a shift in the proportion of immature vs. mature spines. Analysis of cerebellar mossy fiber to granule cell synapses in both Bassoon mutants ($Bsn^{\Delta Ex4/5}$ mice and Bsn^{gt} mice), revealed an enhanced short-term synaptic depression and unchanged basal transmission at these synapses (Hallermann et al., 2010). This study also demonstrated that in the absence of Bassoon the vesicle reloading rate was halved.

1.6 Role of CAZ proteins in learning and memory – a behavioral perspective

Learning and memory processes lead to changes at the regulation of synaptic proteins. Thus, it was shown recently that auditory discrimination learning in mice lead to changes of synaptic proteins, especially Bassoon and Piccolo, in different brain regions including auditory cortex, frontal cortex, hippocampus and striatum (Kahne et al., 2012). Studies on the CAZ proteins using various mutant mouse models had revealed interesting roles about these proteins in different behavioral paradigms. Knockdown of Piccolo in the hippocampus using antisense oligonucleotide impairs hippocampus-dependent spatial learning and memory in mice (Ibi et al., 2010). Over-expression of Piccolo C2A domain (which is an important calcium sensor and binds with synaptotagmin-1) induces depression-like behavior in mice (Furukawa-Hibi et al., 2010). RIM1$\alpha^{-/-}$ mutant mice displayed impairment in both cue and contextual fear conditioning and hyperactive behavior towards the novelty. These mice also displayed impaired spatial learning (Powell et al., 2004) and region specific deletion of RIM1α had limited the abnormalities seen in constitutive RIM1$\alpha^{-/-}$ mice (Haws et al., 2012), indicating its importance for cognitive processes. A study on Munc13-3-deficient mice has disclosed a role for this protein in motor learning, i.e., mutant mice displayed impaired ability in learning complex motor tasks (Augustin et al., 2001). A more recent study provided detailed information about the role of Munc13-3 in several learning

paradigms and showed that the complete deletion of Munc13-3 leads to decrease in the acoustic startle response (Netrakanti et al., 2015).

With respect to Bassoon functions in learning and memory, we have very limited knowledge due to the development of epilepsy as well as visual and auditory impairments (Dick et al., 2003; Khimich et al., 2005). However, one study has shown the performance of $Bsn^{\Delta Ex4/5}$ mice which was altered in a socially transmitted food preference task (Sgobio et al., 2010). Another study has reported an improved performance of $Bsn^{\Delta Ex4/5}$ mice in a two-way active avoidance paradigm that could be normalized by a TrkB antagonist (Ghiglieri et al., 2010). However, the underlying cellular processes and an interpretation of these results are difficult because of the described impairments and due to a potential gain of function effects by the residual Bassoon fragment lacking its central part, i.e., about two-thirds of the entire protein (Altrock et al., 2003).

1.7 Objectives of the study

The main objective of this work is to study the role of Bassoon, more precisely the effect of Bassoon deficiency in particular synapses involved in learning and memory processes. For the past decade, several discoveries have been made regarding the different functions and importance of Bassoon for functional and plasticity-relevant processes in the pre-synapse, mostly *in vitro*. It is necessary to study the functions of this scaffolding protein in a living biological system to understand the detailed function. As the constitutive homozygous mutant mice ($Bsn^{\Delta Ex4/5}$ mice) develop severe epileptic seizures and frequently die at young age (Altrock et al., 2003), our lab have begun to generate conditional Bsn mutants). In this study, I investigated the role of Bassoon in different learning and memory paradigms using both the Bsn conditional mutants (excitatory forebrain Bassoon knockout, B2E cKO and dopaminergic Bassoon knockout, B2D cKO).

The main strategies for this work are as follows.

➢ Generation of Bsn conditional knockout mice in different neuronal systems like forebrain gulatamatergic and dopaminergic systems using Cre-*loxP* system.
➢ Characterization of Bassoon expression in these conditional mutants using immunohistochemistry, quantitative western blot analysis.

➢ Investigation of Bassoon role at excitatory synapses using excitatory forebrain Bassoon cKO (B2E cKO) in different hippocampus- and cortex-dependent behavioral paradigms for learning and memory, activity, exploratory behavior, and anxiety-related responses.

➢ Analysis of neurogenesis rate in cKO mice as $Bsn^{\Delta Ex4/5}$ mice displayed increased neurogenesis, which have implications in different learning and memory paradigms.

➢ Investigation of Bassoon role in dopamine mediated functions like motor coordination, motor strength and depression, using dopaminergic Bassoon cKO (B2D cKO adult and old) mice, together with the above mentioned behavioral paradigms.

2 Materials and Methods

2.1 Materials

2.1.1 Antibodies

Table 2.1. List of primary and secondary antibodies used for immunohistochemistry (IHC) and western blotting (WB).

Primary antibodies	Species	Company	Dilution
Bassoon (SAP7F)	Mouse Rabbit	Enzo Life Sciences Inc, New York, USA Homemade (LIN)	1:1000 (IHC and WB) 1:1000 (WB)
Calbindin	Rabbit	Swant, Marly1, Switzerland	1:1500 (IHC)
Calretinin	Rabbit	Swant, Marly1, Switzerland	1:1250 (IHC)
CtBP1	Mouse	BD Transduction Laboratories, San Diego, USA	1:1000 (IHC)
Dopamine transporter (DAT)	Rat	Abcam, Cambridge, UK	1:500 (IHC)
Doublecortin	Goat	Santacruz Biotechnology Inc, Dallas, USA	1:100 (IHC)
Ki67	Rabbit	Abcam, Cambridge, UK	1:500 (IHC)
Parvalbumin	Mouse	Immunological sciences, Rome, Italy	1:500 (IHC)
Tubulin-β	Mouse	Sigma-Aldrich, Missouri, USA	1:1000 (WB)
VGAT	Rabbit	Synaptic systems GmbH, Göttingen, German	1:500 (IHC)
VGLUT 1	Rabbit	Synaptic systems GmbH, Göttingen, German	1:500 (IHC)

Secondary antibodies			
anti-mouse Cy3	Goat/ Donkey	Jackson Immuno Research Labs, Pennsylvania, USA	1:500 (IHC)
anti-rabbit Alexa 488	Goat/ Donkey	Invitrogen, California, USA	1:500 (IHC)
anti-rabbit Cy3	Goat/ Donkey	Jackson Immuno Research Labs, Pennsylvania, USA	1:500 (IHC)
anti-goat Cy3	Donkey	Jackson Immuno Research Labs, Pennsylvania, USA	1:250 (IHC)
anti-mouse Alexa 488	Goat/ Donkey	Invitrogen, California, USA	1:500 (IHC)
anti-rabbit Alexa 680 and 770	Goat	Invitrogen, California, USA	1:20000 (WB)
anti-rat Alexa 488	Goat	Invitrogen, California, USA	1:200 (IHC)
anti-rat Alexa 680	Goat	Invitrogen, California, USA	1:20000 (WB)

2.1.2 Animals

All experiments throughout the study were conducted in accordance with the European and German regulations for animal experiments and were approved by the local authorities (under licenses: Tierversuchsgenehmigung, Number: 42502-2-988 LIN and 42502-2-1303 LIN). Animals were obtained from the animal facility of the Leibniz Institute for Neurobiology, Magdeburg. Two different Bassoon conditional knock out mice and their littermate wild-type mice were used in this study.

1. Bassoon conditional knockout in excitatory forebrain synapses (in short B2E cKO) and wildtype littermates (in short B2E WT) (age between 2-4 months) (Figure. 2.1 and 2.2)

2. Bassoon conditional knockout in dopaminergic synapses (in short B2D cKO) and littermate controls (in short B2D CTL) (adult mice between 2-4 months and old mice >1 year of age) (Figure. 2.1 and 2.3)

2.1.3 Reagents used in polymerase chain reaction (PCR)

Lysis buffer (tail cut lysis buffer) containing 10mM TrisHCl (pH 8.0) and 100mM NaCl, Proteinase K solution (Sigma Catalog# P6556), Taq polymerase (One Taq polymerase, New England BioLabs Inc, catalog#M0480X, Qiagen Taq polymerase, Qiagen, catalog#201207), dNTP set (Thermo Catalog#R0182) were used.

2.1.4 Buffers, Solutions and Media

PBS	10 mM Na_2HPO_4
	2 mM KH_2PO_4
	0,137 M NaCl
	2,7 mM KCl
Amido black solution	23 mM amido black in methanol : acetic acid (9:1)
Brain embedding solution	Egg yellow and sucrose 10:1 (g/g) cold mix at 4°C
	25% glutaraldehyde and egg mix 1:20 (mL/mL)
Cryoprotection solution (1L)	300 mL distilled water
	300 mL glycerol
	300 mL ethyleneglycol
	100 mL PBS
Sucrose solution	1 M sucrose in PBS
	0.5 M sucrose in PBS
PFA 4%	1 L PBS (warm up to 60°C)
	40 g PFA
	400 µL 5M NaOH + 150 µL 37% HCl pH 7.5
	Cool down to 4°C before use

2.2 Methods

2.2.1 Generation and genotyping of Bassoon conditional knockout mice

***2.2.1a Conditional knockout of Bassoon in forebrain excitatory neurons*:** Generation of conditional knockout (cKO) of Bassoon in forebrain excitatory neurons was achieved by crossing *Bsn2$^{lx/lx}$* mice (obtained from Taconic Artemis GmbH, Germany) and mice expressing Cre recombinase under the control of *empty spiracle homeobox-1* (Emx1) promoter (Knock-in Emx1$^{Cre/+}$; B6.129S2-Emx1$^{tm1(cre)Krj}$, The Jackson Laboratory; Gorski et al., 2002).
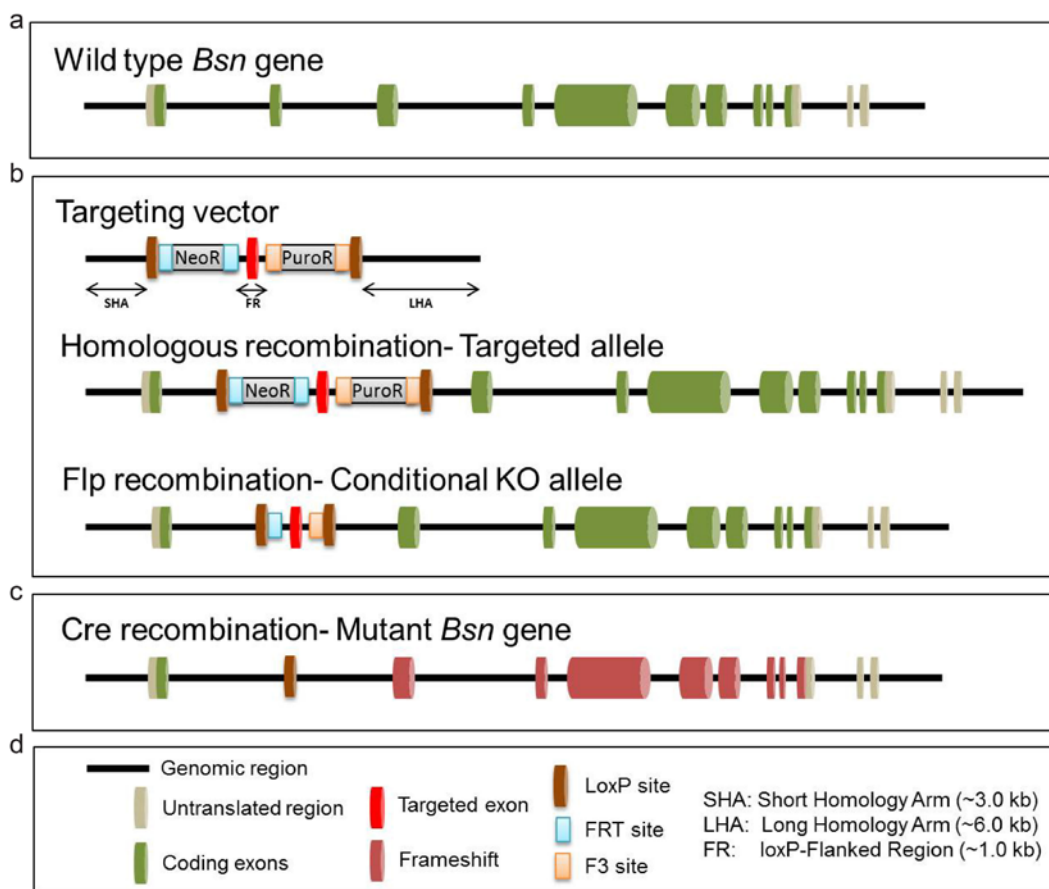
Figure 2.1. Schematic representation showing generation of Bsn2$^{lx/lx}$ mice. a, Schema showing the wild type Bsn gene which contains 12 exons. **b,** Representation of targeting vector containing loxP sites, which results in conditional cKO allele, upon homologous and Flp mediated recombination. **c,** Mutant Bsn gene upon Cre mediated recombination. **d,** Explanations for the abbreviations and symbols used in the schematic representation.

Bsn2$^{lx/lx}$ mice was generated by Taconic Artemis GmbH by inserting loxP sites flanking exon 2 of the *Bsn* gene (Figure. 2.1a,b). A targeting vector containing loxP sites on both sides of exon 2 along with a flippase recognition target (FRT)-flanked neomycin resistance gene (NeoR) in intron 1 and a F3-flanked puromycin resistance

gene (PuroR) in intron 2 was constructed and used for homologous recombination and to select positive clones. The targeting vector was generated using clones from the C57BL/6J RPCIB-731 BAC library and transfected into Taconic Artemis C57BL/6 Tac embryonic stem cell line. The $Bsn2^{lx/lx}$ cKO allele was obtained after Flp recombinase-mediated removal of Neo and Puro resistance genes. It can act as a substrate for Cre-mediated recombination. The recombination leads to deletion of the N-terminal part of Bassoon's 1st Zinc finger domain and causes a frameshift and the generation of premature stop codon in exon 3 (tom Dieck et al., 1998; Winter et al., 1999) (Figure. 2.1c). Both $Bsn2^{lx/lx}$ and Emx1 Cre driver lines were backcrossed to C57BL/6NCrl for at least 10 generations. Breeding was done at Leibniz Institute for Neurobiology, Magdeburg and mice were maintained under 12 hours light-dark cycle, with lights on at 06:00 a.m. with food and water ad libitum (22° ± 2°C). Littermate experimental animals were obtained from $Bsn2^{lx/lx}Emx1^{Cre/+}$ x $Bsn2^{lx/lx}Emx1^{+/+}$ breeding couples (Figure. 2.2) (the mouse line was established by Dr. Anna Fejtova and Sabrina Müller).
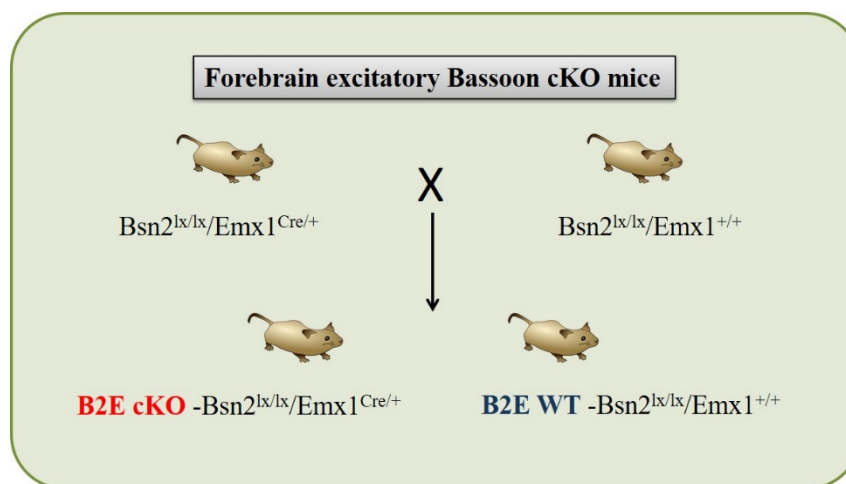
Figure 2.2. Diagrammatic representation of breeding strategy for B2E mice

*2.2.1b Conditional knockout of Bassoon in dopaminergic neurons***:** Conditional knockout of Bassoon in dopaminergic neurons was generated using driver mice expressing Cre recombinase under *dopamine transporter* (DAT) promoter and $Bsn2^{lx/lx}$ mice as described above. DAT Cre driver mice (Backman et al., 2006), (Slc6a3$^{tm1.1(cre)Bkmn}$, The Jackson Laboratory) drive Cre recombinase activity in dopaminergic neurons. By crossing with $Bsn2^{lx/lx}$ mice, it is possible to knockout *Bsn* specifically in dopaminergic neurons, B2D cKO mice ($Bsn2^{lx/lx}/DAT^{Cre/+}$). Littermate experimental animals were obtained from $Bsn2^{wt/lx}DAT^{Cre/Cre}$ x $Bsn2^{wt/lx}DAT^{+/+}$

breeding couples (Figure. 2.3). Here, a different breeding scheme was followed to generate experimental mice. It was reported that Cre insertion within DAT 3´-untranslated region (3´UTR) shows biochemical changes like reduced expression of DAT protein levels in striatum of homozygous Cre and heterozygous Cre mice compared to wild-type mice (Backman et al., 2006). Furthermore, behavioral analysis of heterozygous Cre and wild-type mice in different parameters revealed an increased motor activity in heterozygous Cre mice compared to wild-type mice (Figure 3.36).
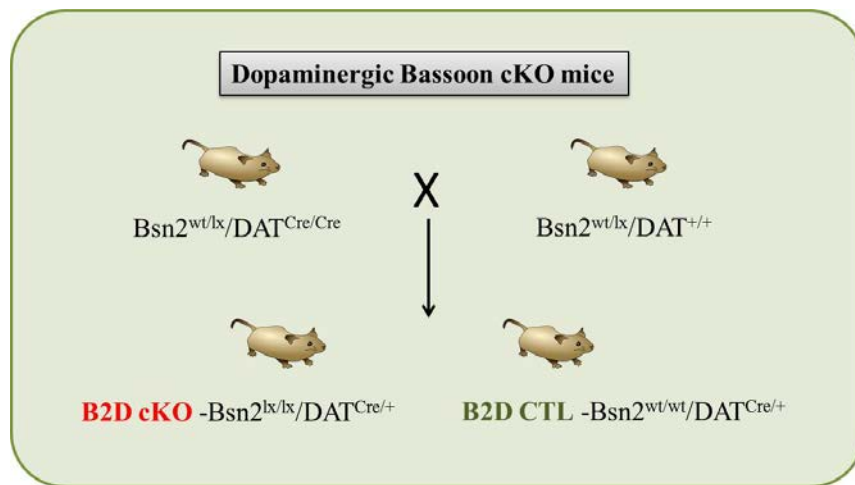
Figure 2.3. Diagrammatic representation of breeding strategy for B2D mice

2.2.2 Genotyping details

Genotyping for the Bsn2$^{lx/lx}$ mice was done with polymerase chain reaction (PCR) using the forward primer (GCAGATTCTAGTCGGTGATCTAGC), reverse primer (GTTGCCTAATGTATGCAGAGTCC) and One Taq polymerase (New England BioLabs Inc, catalog#M0480X). The PCR protocol included an initial denaturation for 3 minutes at 95°C followed by 35 cycles of (30 seconds denaturation at 95°C, 30 seconds annealing at 60°C, and 30 seconds synthesis 68°C, with final synthesis phase of 5 minutes at 68°C. This results in a 220bp wild-type (WT) and 337bp product for the floxed allele. Genotyping for Emx1 Cre was done as described by the supplier using One Taq polymerase (New England BioLabs Inc, catalog#M0480X) and a PCR program 3 minutes at 94°C, 35x (30 seconds at 94°C, 45 seconds at 62.3°C, 45 seconds at 68°C) and final 5 minutes at 68°C. Genotyping for DAT Cre was done as described in Jackson labs (Slc6a3$^{tm1.1(cre)Bkmn}$) with changes in temperatures and

Polymerase (Qiagen Taq polymerase, Qiagen, catalog#201207) used as described here. PCR program set to 94°C 3 minutes, 35x (30 seconds at 94°C, 30 seconds at 62°C, 30 seconds at 72°C) and final 5 minutes at 72°C.

2.2.3 Perfusion and cryo-sectioning of brains

Mice were anesthetized with isoflurane and perfused transcardially with phosphate-buffered saline (PBS) initially for 20 minutes followed by 4% paraformaldehyde (PFA) for another 20 minutes. Heads were cut off with fine scissors and the skull was removed carefully without damaging the brain structures. Brains were post fixed for overnight in the same fixative at 4°C and cryoprotected by incubating them in 0.5M sucrose in PBS and then in 1M sucrose in PBS. Brains were frozen using Isopentane, cooled by liquid nitrogen and stored at −80°C until analyzed. Then brains were transferred to −20°C the day before sectioning and 30-40μm thick sagittal or coronal sections were cut on a cryostat, collected free floating and used for immunological stainings or stored in a cryoprotection solution at −20°C until utilized.

2.2.4 Immunohistochemistry

Immunohistochemical staining was done essentially as described previously (Hubler et al., 2012). Free-floating sections were first washed with PBS (10-15 minutes) and then incubated with blocking solution (10% normal goat serum (NGS), 0.3% Triton X-100 in PBS) for 1hr at room temperature. Then the sections were incubated in primary antibody solution (same blocking solution) overnight to 48 hrs at 4°C. Later, the sections were washed in PBS (three times, 10 minutes each). After washing, brain sections were blocked again with 0.4% bovine serum album (BSA), 0.3% Triton X-100 in PBS for 60 minutes followed by overnight incubation at 4°C, with appropriate secondary antibodies diluted in the same blocking solution. Then, the sections were washed again with PBS (three times, 10 minutes each). The sections were mounted on glass slides and covered with coverslips using fluoromount g or fluoromount g DAPI (Southern biotech, USA) for nuclear counterstaining.

2.2.4a Doublecortin (DCX) and calretinin immunohistochemistry

Free floating sections were first washed with PBS (10-15 minutes) and then incubated with blocking solution (5% BSA, 0.3% Triton X-100 in PBS) for 1hr at room temperature. Then the sections were incubated in primary antibody solution (2% BSA,

0.1% Triton X-100 in PBS), 48 hrs at 4°C. Later, the sections were washed in PBS (three times, 10 minutes each) followed by overnight incubation at 4°C, with appropriate secondary antibodies diluted in the same incubating solution, like primary antibody. Then, the sections were washed with PBS (three times, 10 minutes each). The sections were mounted on glass slides and covered with coverslips using fluoromount g DAPI (Southern biotech, USA).

2.2.5 Microscopy and quantification

Overview pictures of single sagittal brain sections were obtained using Zeiss Axio Imager light microscope. Images were acquired in blocks (covering entire section), using the 2.5X objective. All the blocks were arranged using Adobe InDesign CS6. The brightness and contrast levels of the presented images were minimally adjusted either using Image J software (version 1.50i, National Institutes of Health) or Adobe Photoshop CS6. Quantification of Parvalbumin (PV)-positive cells in the cortex was done by visualizing the nuclei with DAPI staining to define the different layers in the cortex. Images were captured using Zeiss Axio Imager light microscope, with a 20X objective. Images were analyzed using Image J. For quantification of mature and immature markers, serial sections including one in every 5th section (120µm apart) was stained as described above and confocal stacks of 0.65µm Z-step size (~12µm Z-stack volume) were taken with a Leica SP5 confocal microscope using 40X oil immersion objective (1.25-0.75 NA) and LCS software (Leica, Wetzlar, Germany). Total 4-6 coronal sections from dorsal dentate gyrus (DG) per mouse (N=5-6 mice per genotype) were analyzed. Maximal projection images from each stack were obtained using Z-project function in Image-J software. Granule cell layer was marked as region of interest (ROI) in DAPI channel using free hand tool in Image-J and this ROI was applied to the respective channel for other markers. Cell numbers were counted manually using Cell Counter plugin and integrated density values were measured in respective channel using Image-J. Cell numbers were expressed as cells per 100µm² and integrated density (ID) values were normalized to the mean of WT values. To measure adult neurogenesis Ki67 expression was investigated in the DG using Leica microscope (40X/0.75 NA objective) with motorized stage. A total of 5 coronal sections from the dorsal DG were analyzed per mouse (N=5 mice per genotype). The granule cell layer was tracked and marked using DAPI labeled nuclei and Ki67 positive cells were marked and reconstructed using Neurolucida software (MBF Bioscience). Ki67 positive cell

numbers were analyzed using the marker analysis tool in Neuroexplorer software (MBF Bioscience).

2.2.6 Quantitative immunoblot analysis

Cell fractionation and quantitative western blotting was done as described previously by Altrock et al. (2003) and (Lazarevic et al., 2011), respectively. Mice were killed by cervical dislocation and brains were dissected into forebrain (containing cerebral cortex and hippocampus) and cerebellum. Dissected parts were homogenized in a buffer containing 0.32M sucrose and 2.5mM Tris-Hcl (pH 7.4) supplemented with complete Protease Inhibitor (Roche) and PhosSTOP Phosphatase Inhibitor Cocktail (Roche) at 4°C. This was the homogenate fraction for western blot analysis. Further, this homogenate fraction was centrifuged at 1000g for 10 minutes and the supernatant was collected (S1 fraction). This was centrifuged again at 12000g for 20 minutes. Supernatant of this step (S2) was carefully separated without disturbing the pellet (P2). This pellet was resuspended completely in loading buffer containing β-mercaptoethanol, resulting in P2 fraction, which was used for quantitative western blot analysis. Concentration of proteins was estimated using colorimetric Amido black assay (Serva Feinbiochemica GmbH, Heidelberg, Germany) and 10 µg protein per lane was loaded onto Tris-Acetate (TA) polyacrylamide gradient gels (8-4%). TA gel was ran at 10 mA of current and transferred onto the Immobilon-FL PVDF (Millipore) membranes. Blots were then incubated with primary antibodies (in PBS containing 5% BSA, 0.1% Tween and 0.025% sodium azide) 4°C overnight and with secondary antibodies (in PBS containing 1% BSA, 0.1% Tween) 4°C overnight or 1.5 to 2hrs at room temperature. Using Odyssey Infrared Scanner (LI-COR), immunodetection and measurements of integrated densities (ID) of signals was performed. Identical rectangular ROIs were set around the bands to measure the ID values. Values were normalized to loading controls and to the mean value of the WT group for each individual membrane.

2.2.7 Morphological analysis

Using the Golgi impregnation method, morphological characteristics of different hippocampal neurons were analyzed. Impregnation with Golgi-Cox solution was done as described previously (Mylius et al., 2013; Rehberg et al., 2014) without any modifications. Granule cells of the dentate gyrus and pyramidal neurons at the CA1 region of the hippocampus were analyzed using a light microscope (Leica, 100X

objective) with motorized stage. Neuronal tracking and reconstruction was done using Neurolucida software (MBF Bioscience). Quantitative measurements of dendrite length and complexity were done using the Sholl analysis method (with 10µm increasing radius from the center of the soma) tool in Neuroexplorer software (MBF Bioscience). All the analyses were done in DG granule cells, within the proximal range between 0-120 µm from soma, in order to ensure a consistent reconstruction of Golgi impregnated structures in golgi preparations. Golgi staining and slide preparations were done at Eike Budinger's lab at Leibniz Institute for Neurobiology.

2.2.8 Behavioral experiments

Adult male mice were used in all experiments. Animals were obtained at an age between 5-7 weeks (Animal facility, Leibniz Institute for Neurobiology, Magdeburg) and transferred to Institute of Biology, Otto von Guericke University, Magdeburg, where all the behavioral experiments were performed, except for Morris water maze experiment. A separate batch of mice was tested in Morris water maze paradigm at Leibniz Institute for Neurobiology. After transfer, mice were habituated at least for one week in individual cages under a reverse 12h light/12 h dark cycle with lights on at 7:00 p.m., room temperature 22 ± 2 °C and food and water provided ad libitum. All experiments were performed between 9:00 a.m. and 5:00 p.m. (during dark cycle). All the experiments with B2E mice were performed in different test batteries. Test battery one included home cage activity monitoring, light-dark test, open field, object recognition and back ground fear conditioning. Test battery two included open field, object recognition and active avoidance. Test battery three included home cage activity monitoring, pattern separation and foreground contextual fear conditioning. In case of B2D mice, all tests were conducted in a single battery including home cage activity monitoring, light-dark test, elevated plus maze, open field, object recognition, sucrose drinking test, inverted grip strength test, rota rod, social recognition memory and back ground fear conditioning. For old B2D mice, tests were also conducted in a single battery including home cage activity monitoring, light-dark test, elevated plus maze, inverted grip strength test, open field, object recognition, sucrose drinking test, rota rod, social recognition memory. Care was taken to arrange tests avoiding the interferences and providing sufficient recovery time in between.

2.2.8a Home cage activity monitoring

As previously discussed in Bergado-Acosta et al. (2014), mice were monitored for 3-4 consecutive days in their home cages. Activity was measured using infrared-thermo sensors (Home Cage Activity System, Coulbourn Instruments, Allentown PA), mounted on the top of each cage, which detect the changes in body heat for movement of the mice. Small movement lower limit recorded for 100 milliseconds and upper limit recorded for 500 milliseconds. Movement measured between lower and upper limits and the raw values for each 15 seconds were summed up to detect activity periods in 5 minute bins per hour (total 12 active periods per hour). The percentages of active periods were calculated per hour and the mean values for each hour per genotype over 3-4 consecutive days were plotted.

2.2.8b Light-Dark test

Anxiety like behavior was tested in a two-compartment light-dark test. Mice were placed in light compartment (19 cm (l) x 21 cm (w) x 20 cm (d)) first and allowed to explore the entire apparatus also including the connected dark compartment (17 cm (l) x 21 cm (w) x 20 cm (d)) for 5 min. Both the compartments connected with an opening of 5 cm x 5 cm. The total time spent in compartments, distance covered and activity in different compartments, together with the number of transitions between compartments were detected with photo beams (TSE System, Bad Homburg, Germany) (Stork et al., 2000).

2.2.8c Elevated plus maze (EPM)

Mice were tested in an elevated plus maze to measure anxiety levels. The EPM apparatus consists of two closed arms measuring 35 cm (l) x 5 cm (w) x 15 cm (h) and two open arms measuring 35 cm (l) x 5 cm (w), which is elevated 40 cm above ground surface. Experiment was performed under red light (40 watts or 5 Lux, i.e. low light conditions). Mice were placed at the end of one of the open arm and allowed to explore whole apparatus for 5 minutes. Total distance, number of center entries, time spent and number of entries to the closed and open arm were tracked using ANY-maze Video tracking system (version 4.50, Stoelting Co, Wood Dale, IL, USA).

2.2.8d Open field exploration

To further assess the novel environment exploration and anxiety like behavior in mice, we tested the mice in an open field for two consecutive days, in an arena measuring 50 cm (l) x 50 cm (w) x 35 cm (d), 20 minutes each. On day 1, red light (5 Lux low light conditions) and on day 2 bright light (100 Lux) was used. Each chamber was divided into different regions like corners (12.5 cm x 12.5 cm), rims (25 cm x 12.5 cm) and center (25 cm x 25 cm). Exploration of mice in each region was monitored using a video-tracking system (ANY-maze, Stoelting Co, USA) interfaced with computer. Distance moved by mice and percentage of time spent in different regions were measured.

2.2.8e Novel object recognition

A novel object recognition task was done as described previously (Stefanko et al., 2009) in two phases either on same day with 2 hrs inter-phase interval to test short-term memory or 24 hrs inter-phase interval to test long-term memory. Phase 1 was the habituation, where the mice encounter two identical objects (O1 and O2) (made from Lego blocks, with cumin as a mild olfactory cue) in different locations (each location was assigned to each corner and equidistant (10 cm) from two sides of respective corners of an open field arena). Phase 2 was the testing phase, where one of the identical objects was replaced by a novel object (O3, with Cinnamon as an olfactory cue) and mice encounter a familiar object and a novel object (Figure 2.4).
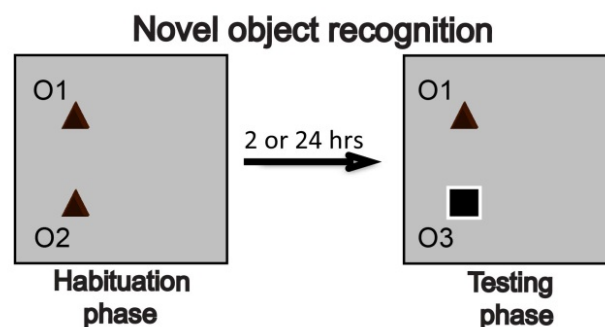

Figure 2.4. Schematic representation of novel object recognition paradigm

Exploration of objects by each mouse was monitored for 20 min during each session using a video-tracking system (ANY-maze, Stoelting Co, USA) and the

exploration time at the novel and familiar locations was measured and a discrimination index was calculated using the below formula.

$$DI = \frac{(Tn - Tf)}{(Tn + Tf)}$$

DI= Discrimination index; Tn= Time spent with novel object; Tf= Time spent with familiar object

2.2.8f Novel object location

This spatial version of the object recognition task was employed as described previously (Roozendaal et al., 2010) with slight modifications. The task was carried in an open field arena one day after the exploration in the field during bright light. On the first day of the experiment, mice were habituated to two identical objects (made from Lego blocks, with cumin as a mild olfactory cue) placed at different locations (each location was assigned to each corner and equidistant (10 cm) from two sides of respective corners of an open field arena) B1 and B2. During day 2, twenty-four hours later, mice encountered one of the objects at novel location B4 (Figure 2.5).
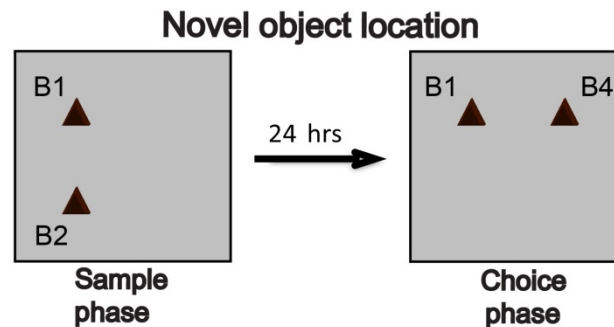

Figure 2.5. Schematic representation of novel object location paradigm

Exploration of objects by each mouse was monitored for 20 min during each session using a video-tracking system (ANY-maze, Stoelting Co, USA) and the exploration time at the novel and familiar locations was measured and a discrimination index was calculated the below formula.

$$DI = \frac{(ETn - ETf)}{(ETn + ETf)}$$

DI= Discrimination index; ETn= Exploration time at novel location; ETf= Exploration time at familiar location

2.2.8g Pattern separation

The pattern separation task was done as described previously (Bekinschtein et al., 2013) with slight modifications. To explain the procedure briefly, a day after habituating to the open field arena for two sessions (10 min each), mice encounter three identical objects placed in locations A1, A2 and A3 during sample phase (10 min session). A1 was equally and more distanced (24 cm) from A2 and A3, whereas A2 and A3 were 14 cm apart from each other and towards the opposite corner of the arena. 24 hours later during choice phase, instead of A2 and A3, another identical object placed at slightly changed location, A4. Mice will encounter familiar object at A1 and another identical object at novel location at A4 (Figure 2.6). Exploration time at different locations for 10 min was recorded and analyzed using ANY-maze and a discrimination index was calculated, as described above.
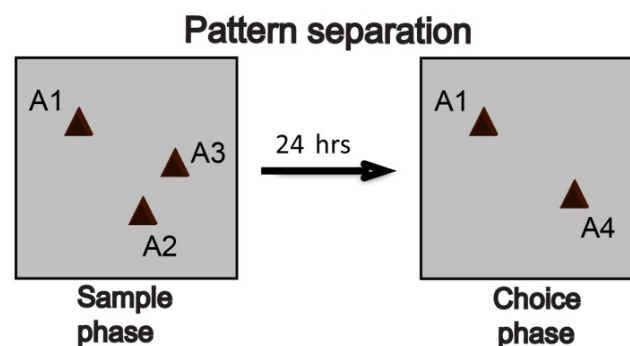
Figure 2.6. Schematic representation of pattern separation paradigm

2.2.8h Social recognition and memory

Social memory interaction can be used to study autistic-like behavior in mice and other social deficits (Silverman et al., 2010). Sociability can be determined by measuring the time spent by the test mouse in chamber containing unfamiliar stranger mouse vs chamber with non-animated object. Social memory can be determined by evaluating discrimination in terms of time spent by test mouse between familiar and newly introduced unfamiliar stranger in another chamber. Social behavior was

evaluated as described by Won et al. (2012), in a three-compartment apparatus made of 60 cm (l) x 30 cm (w) x 40 cm (d) clear cage, separated by partitions for the mice to enter each chambers. The two lateral compartments contained wire cylindrical cages with numerous mesh-like holes (13 cm (h) x 4 cm (r)) yielding olfactory cues where the stranger mice (C57BL/6 male mice) were placed (Figure 2.7). Mouse activity was measured by a video-camera and analyzed with the same video-tracking system (ANY-maze, Stoelting Co, USA). Parameters like rearing and entry into different chambers were also entered manually. Each mouse was placed inside the central compartment and explored the apparatus for a 5 minutes habituation period. In the sociability test, an unfamiliar male stranger mouse 1 and non-animated mouse like object made of Lego blocks were introduced inside the wire cylindrical cages of the lateral compartments for 5 minutes. To test the social memory, stranger mouse 2 was introduced into the cylinder containing object and observed for 5 more minutes. Discrimination index during sociability and social memory was measured using formula below.

$$DI \ (sociability) = \frac{(Ts1-To)}{(Ts1+To)} \qquad DI \ (Social \ memory) = \frac{(Ts2-Ts1)}{(Ts2+Ts1)}$$

DI= Discrimination index; Ts1 and Ts2= Time spent with stranger mice S1 and S2; To= Time spent with object
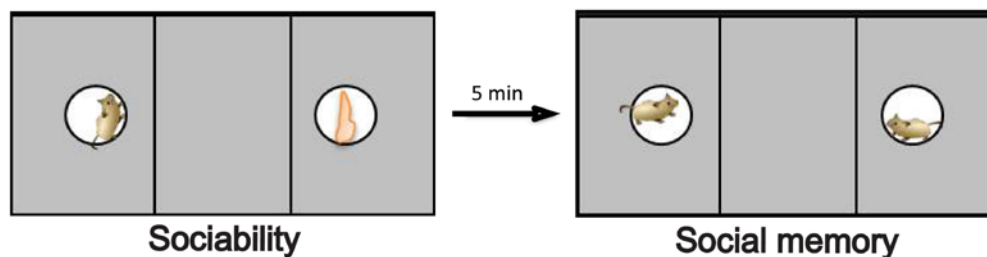
Figure 2.7. Schematic representation of social recognition and memory paradigm

2.2.8i Inverted grip strength test

The inverted grip strength test was done to assess the muscular strength based on the ability of mice to remain hanging to the inverted cage lid. Each mouse was placed on the large rat cage lid and inverted. This inverted lid was placed at 35-40 cm height from the ground level. Bedding material or big rat cage was placed under the lid in

order to protect the mouse from injuries, if fallen. Hanging time was measured for 2 minutes and expressed as % of time hanging.

2.2.8j Rotarod

Motor coordination and balance was measured in mice using rotarod system (Ugo Basile Rota-Rod model#57604). Mice were placed on a rotating drum (3 cm per single mouse; 5 mice can be tested each time) with a constant speed of 4 rpm for 2 minutes during two training sessions with 24 hours interval in between. During the test, mice were placed on accelerating rotarod from 4 to 40 rpm for 5 minutes. This was done in two sessions and average values from these two sessions were considered for measuring the duration the mice spent on accelerating rotarod and maximum speed they withstand.

2.2.8k Sucrose preference test

To test depression-like behavior, mice were tested in sucrose preference test. Protocol was adopted from Strekalova et al. (2004). Three days before the start of the experiment, mice were habituated to the 15 ml falcon tubes containing tap water. During test, for 4 days, mice were provided with two falcon tubes one containing 1% sucrose solution and other containing tap water. Care was taken to prevent probable effects of side preference; the position of two falcon tubes was switched every 24 hours. Sucrose preference was calculated using the flowing formula.

$$\% \, of \, sucrose \, consumption = \frac{amount \, of \, sucrose \, intake}{amount \, of \, sucrose \, intake + amount \, of \, water \, intake} * 100$$

2.2.8l Fear conditioning

2.2.8l.I Cue fear conditioning: Mice were tested in a classical auditory cued conditioning (combined context/cue conditioning) paradigm described earlier (Laxmi et al., 2003). The training apparatus (TSE System, Bad Homburg, Germany) comprised of acrylic glass arena (16 cm (l) X 32 cm (w) X 20 cm (d)) with a grid floor for delivery of

mild electric foot shocks. The entire arena was enclosed in a big cubicle containing speaker, ventilation fan and background noise (70 dB), connected to a computer to measure the different parameters, using a photo beam system. Habituation, training and testing sessions were done as described previously (Bergado-Acosta et al., 2008) with minor modifications.

Briefly to explain, mice were habituated to training apparatus with six neutral acoustic stimuli (CS- 2.5-kHz, 10 seconds with 20 seconds inter stimulus intervals, ISIs) in 2 sets separated by 120 seconds. During next day, mice were trained with three presentations of conditional stimuli (CS+ 10-kHz, 10 seconds with 20 seconds ISIs) each terminated with 1 second unconditional stimulus (US, scrambled foot shock of 0.4 mA) in 2 sets again with 120 seconds pause. Fear memory towards context (24 hrs after training) was tested in training context without any kind of presentations for 8 minutes. Fear memory towards different tones (48 hrs after training) was tested in a neutral context (standard home cage with bedding) by presenting both CS- and CS+, respectively as shown in the Figure 2.8. Fear memory was expressed as freezing (lack of movements except for respiration) behavior and expressed as percentage of time spent freezing during the retrieval sessions.
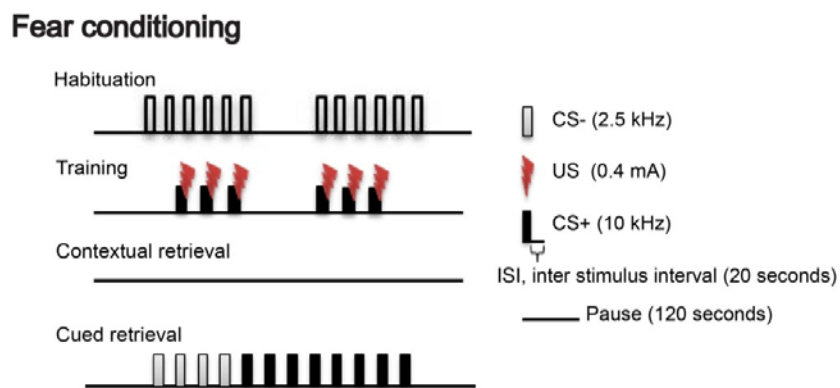
Figure 2.8. Schematic representation of cue fear conditioning

2.2.8l.II Foreground contextual fear conditioning: In order to test more specifically the contextual fear memory, mice were tested in foreground contextual fear conditioning paradigm. Training and retrieval were performed in the apparatus (TSE System, Bad Homburg, Germany) described above. Mice were trained in the fear conditioning chamber in three daily sessions, each consisting of 2 min habituation, two

US (0.4 mA, 1 second) with 30 seconds interval and 30 seconds final rest. On the fourth day, memory retrieval was tested over a period of 10 min in the training context, without US exposure (Figure 2.9). The first 2 min of retrieval day were used to measure the fear memory.
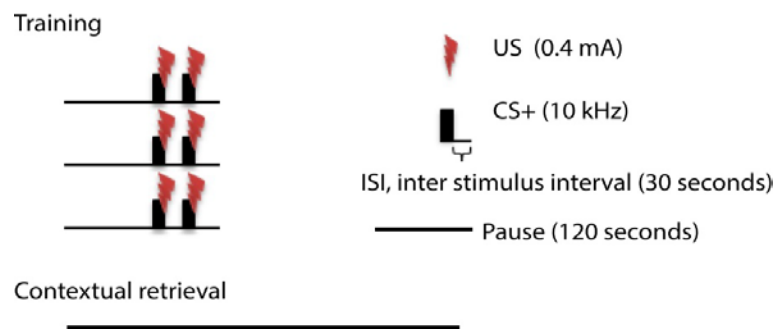

Figure 2.9. Schematic representation of foreground contextual fear conditioning

2.2.8m Active avoidance

Mice were tested in another aversive avoidance paradigm in shuttle box as described previously (Sparkman et al., 2005) with minor changes. Test was done in a shuttle box (TSE System, Bad Homburg, Germany) containing a Plexiglas compartment with 36 cm (l) x 21 cm (w) x 20 cm (d) dimensions and with a separator in the middle with 4x4 cm opening equipped with a grid floor for delivery of mild foot shocks. Mice were habituated to the apparatus for 3 minutes on each training day. Conditioned stimuli (CS) (tone: 10 kHz, 65 dB) was presented for 20 seconds in total. After the first 5sec of each tone presentation an unconditioned stimulus (US) (foot shock: 0.10 mA) was co-presented and foot shock intensity was increased to 0.30 mA if the mice did not shuttle to the other compartment within the 10sec after the presentation of US. The test was performed for 5 consecutive days with 50 trials presented per day with inter-trial intervals of 20 seconds. As conditioned responses, crossing to the other chamber with the onset of CS before delivery of the foot shock (0.1 mA) (Avoidance learning), were measured with photo beam detection (TSE System, Bad Homburg, Germany).

2.2.8n Morris water maze

To assess the spatial learning and memory, mice were tested in a Morris water maze submerged platform task, in large circular basin (130 cm) containing opaque

water (24-26°C) and circular platform (10 cm diameter) placed approximately 1.5 cm below the water level. The task was done as described previously (Montag-Sallaz and Montag, 2003) with minor modifications. During the acquisition phase, mice were subjected to hidden platform (at fixed position, South-East) for three consecutive days. The following two days were retrieval/reversal phase with platform position at North-West. A total of 6 trials per day were carried for a maximum of 120 seconds per each trial. Mice were guided to the platform, if they failed to reach the platform within the 120 seconds duration. The first two trails during the reversal phase were considered as probe trails in order to assess the spatial memory. All trials were videotaped using the VideoMot 2 system (TSE). The latency to reach the platform and path length moved were measured using Wintrack open source software.

2.2.9 Electrophysiology

Electrophysiological recordings were performed and analysed by Dr. Gürsel Caliskan at Institute of Biology, OvGU, Magdeburg. Adult (3-4 months old) and young (27-33 days old) male B2E cKO mice and their WT littermates were used for electrophysiological experiments (12-hr light-dark cycle, lights on at 7p.m.; room temperature 22 ± 2°C). Adult male mice were deeply anesthetized with isoflurane and decapitated. Brains were rapidly (~30-60 sec) removed and placed in cold (4-8°C) carbogenated (5% CO_2/ 95% O_2) artificial cerebrospinal fluid (aCSF) containing (in mM) 129 NaCl, 21 $NaHCO_3$, 3 KCl, 1.6 $CaCl_2$, 1.8 $MgSO_4$, 1.25 NaH_2PO_4 and 10 glucose. Dorsal hippocampal transverse slices (400 µm) were obtained from the septal pole by cutting parasagittal slices at an angle of about 12° using an angled platform. Three to four most dorsal slices were transferred to an interface chamber perfused with aCSF at 34.0 ± 1.0°C (flow rate: 2.0 ± 0.2 ml / min, pH 7.4, osmolarity ~300 mosmol / kg). Slices were incubated for at least 1 hr before starting recordings. The experimenter was blind to the genotype of mice. Extracellular field recordings were obtained with a glass electrode filled with ACSF (~1MΩ). For DG electrophysiology, the recording electrode was placed at the inner molecular layer at 70-100 µm depth. Stimulation activating medial fibers in the MPP was performed using a bipolar tungsten wire electrode with exposed tips of ~20 µm and tip separations of ~75 µm (electrode resistance in ACSF: ~0.1 MOhm). Position of stimulating and recording electrodes at

the inner molecular layer of the DG was confirmed by the verification of paired-pulse depression at 50 ms interpulse interval. For CA1 electrophysiology, the recording electrode was placed at the stratum radiatum (SR) of the CA1 sub region while the stimulation electrode was placed at the proximal CA1 stimulating Schaffer collaterals. Signals were pre-amplified using a custom-made amplifier and low-pass filtered at 3 kHz. Signals were sampled at a frequency of 10 kHz and stored on a computer hard disc for off-line analysis. Before obtaining an input-output (I/O) curve, 10-20 min of baseline responses were recorded (0.033 Hz, pulse duration: 100 µs). Once the responses were stabilized, seven intensities ranging from 5 µA to 50 µA were used to obtain an input/output (I/O) curve.

2.2.10 Data analysis and statistics

All the behavioral data were analyzed and graphs were plotted using MS-Office excel (versions 2010 and 2016) and GraphPad Prism5. Data was evaluated by unpaired Student t-Test or Mann -Whitney U test (two group comparisons) based on the Shapiro-Wilk normality test and Chi square (χ2) test. Multiple group comparisons were evaluated using two-way ANOVA and two-way repeated measures ANOVA, followed by Bonferroni's post hoc test. Outliers were identified using either the free calculator from Graphpad based on the Grubb's test (Grubbs, 1969) or Dean and Dixon test (Dean and Dixon, 1951). All data are represented as Mean ± SEM. Probability values of <0.05 were considered as significant.

3. Results

3.1 B2E mice

3.1.1 B2E cKO mice lack Bassoon expression in excitatory synapses, specifically in the forebrain region

B2E (Bsn2$^{lx/lx}$/Emx1$^{Cre/+}$) mice express Cre recombinase in glutamatergic neurons of the forebrain, based on the Emx1 promoter activation (Gorski et al., 2002), and thus should lack Bassoon at excitatory synapses in the forebrain region including cerebral cortex and hippocampus. To assess the expression pattern of Bassoon in these mice, sagittal brain sections from both WT and cKO mice were stained using antibody against Bassoon. As expected, a clearly reduced staining intensity was observed in the forebrain region of cKO mice (Figure 3.1a), when compared to the cerebellum.
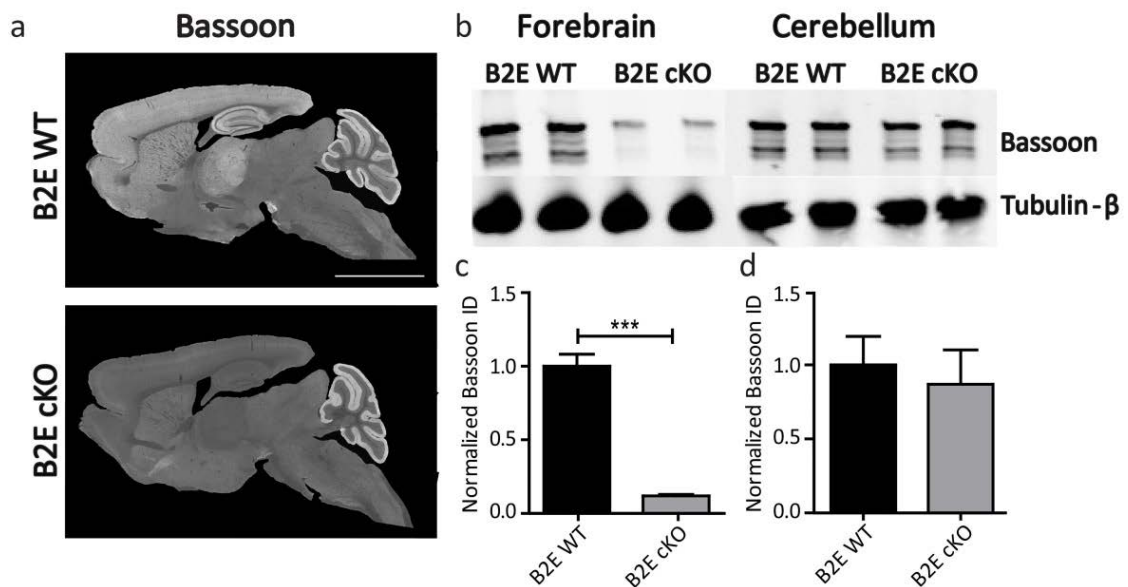

Figure 3.1. B2E cKO mice display strongly reduced Bassoon immunoreactivity in forebrain regions. a, Sagittal brain sections from B2E wild-type (WT) and littermate B2E cKO mice stained for Bassoon. Reduced expression of Bassoon was observed in the B2E cKO forebrain regions (cerebral cortex, hippocampus), whereas no difference in expression of Bassoon was observed in cerebellum, midbrain and brain stem from both genotypes. **b,** Western blots (10µg protein/lane) probed with Bassoon antibody and Tubulin-β (loading control) from forebrain and cerebellum homogenates of B2E WT and B2E cKO brains. **c,** A nearly 85% loss of Bassoon is evident in the forebrain of B2E cKO mice, as revealed by quantification of Bassoon expression in the forebrain of cKO mice (Integrated density values normalized to WT), **d,** whereas no change in Bassoon expression was observed in cerebellum of WT and cKO mice. (N=5). Scale bar in **a** is 3 mm. All values are mean ± SEM; ***$P \leq 0.001$, Student's t-test.

Furthermore, quantitative western blot analysis was done to check the levels of Bassoon protein in forebrain and cerebellum lysates. Results show that Bassoon

expression levels were reduced in forebrain lysate (Figure 3.1b, n=5 each, p< 0.0001, unpaired t-Test) of cKO mice when compared to WT mice (Figure 3.1c). Whereas, Bassoon levels were unchanged between the genotypes in cerebellar lysates (Figure 3.1d).

To assess the synapse-type specificity of Cre recombinase activity in cKO mice, I stained the sections showing regions cortex and hippocampus using antibodies against Bassoon, VGLUT1 (marker for excitatory presynapses) (Figure 3.2a and c) and VGAT (marker for inhibitory presynapses) (Figure 3.2b and d).
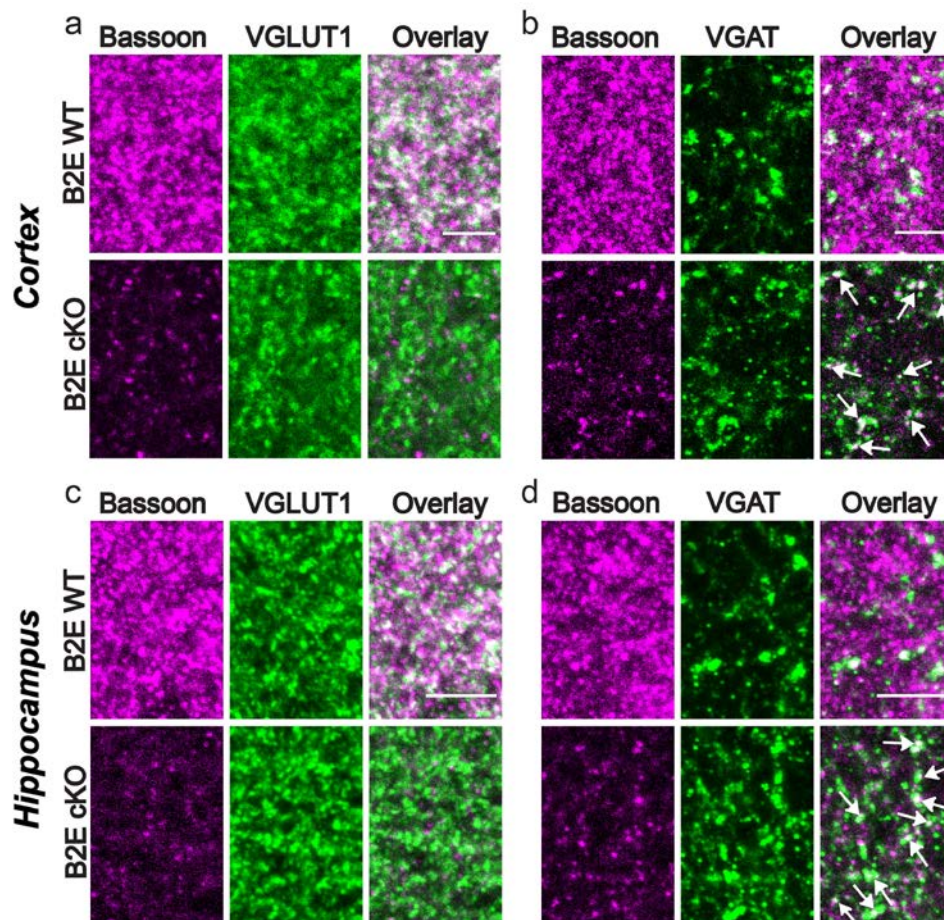

Figure 3.2. B2E cKO mice lack Bassoon in forebrain excitatory synapses. Brain sections showing cortex (visual cortex area V1) **(a)** and hippocampus (molecular layer of dentate gyrus) **(c)** from B2E WT and cKO mice depict the localization of Bassoon at excitatory VGLUT1-positive synapses in B2E WT and strongly reduced colocalization in B2E cKO mice (Overlay panels). Assessment of colocalization of Bassoon and VGAT in the cortex **(b)** and hippocampus **(d)** of both B2E WT and cKO mice indicates significant colocalization (Overlay panels) as Bassoon is still expressed in inhibitory synapses (white spots indicated by white arrows). Scale bar is 5µm in all panels.

Overlay images (visual cortex, area V1 and molecular layer of DG) showing basically no co-localization between Bassoon and VGLUT1 and high co-localization

between Bassoon and VGAT (white spots indicated by white arrows) confirm the lack of Bassoon in excitatory synapses. There is an expression of residual Bassoon observed in some non-glutamatergic or non-GABAergic synapses, potentially from neuromodulatory afferences (Gasbarri et al., 1997; Picciotto et al., 2012). With the immunohistochemical and quantitative western blot analyses together, it is evident that knockout of Bassoon is restricted to forebrain in these cKO mice.

3.1.1a B2E cKO mice survive normally in comparison with WT littermates

B2E mice were observed for 1 year to detect potential differences in their survival rate. Both B2E cKO (N=20) and WT (N=19) mice displayed basically no differences in their survival (Figure 3.3a), what is in contrast to previously studied constitutive mutants which frequently die from epileptic seizures (Bsn$^{\Delta Ex4/5}$ mice; Altrock et al., 2003).
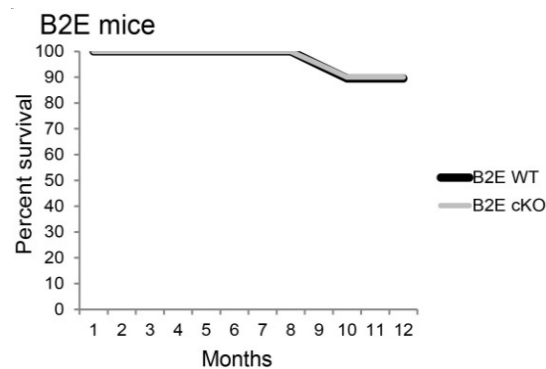

Figure 3.3. Normal survival rate of B2E cKO mice. Survival plot indicating comparable survival rates of B2E cKO (N=20) and WT (N=19) mice.

3.1.2 Behavioral assessment of B2E cKO mice

Male B2E cKO mice and WT littermates were analyzed in various behavioral paradigms to assess for potential neurological as well as learning and memory deficits caused by the lack of Bassoon at excitatory forebrain synapses.

3.1.2a B2E cKO mice displayed hyperactive behavior in home cage activity monitoring but no change in open field activity

B2E cKO and WT mice were monitored in home cage activity, where a significant effect of the day time was observed with strongly increased activity during

the 12 hrs of dark phase of the diurnal cycle (Figure. 3.4a; $F_{(23,851)}=95.97$, $p<0.0001$, two-way repeated measures ANOVA). However, a significant genotype effect $(F_{(1,37)}=9.88$, $p=0.0033)$ that did not show an interaction with day time $(F_{(23,851)}=0.49$, $p=0.9795)$ revealed that home cage activity was increased in B2E cKO as compared to WT mice in both dark (WT: $53.59 \pm 2.69967\%$; cKO: $63.53 \pm 3.022\%$, $T_{(37)}=2.461$, $p=0.0187$, Student t-Test) and light phases (WT: $15.21 \pm 1.672\%$; $24.21 \pm 2.024\%$, $T_{(37)}=3.440$, $p=0.0015$, Student t-Test).

Further, B2E cKO and WT mice were analyzed for novelty induced exploratory activity in an open field, which was tested during the dark phase of the cycle using low light and bright light test sessions. Two-way repeated measures ANOVA revealed an effect of the test session $(F_{(1,41)}=15.78$, $p=0.0003)$ but no effect of genotype $(F_{(1,41)}=3.22$, $p=0.0803)$ or genotype x session interaction $(F_{(1,41)}=0.64$, $p=0.4276)$ concerning the distance travelled in the open field (Figure 3.4b).
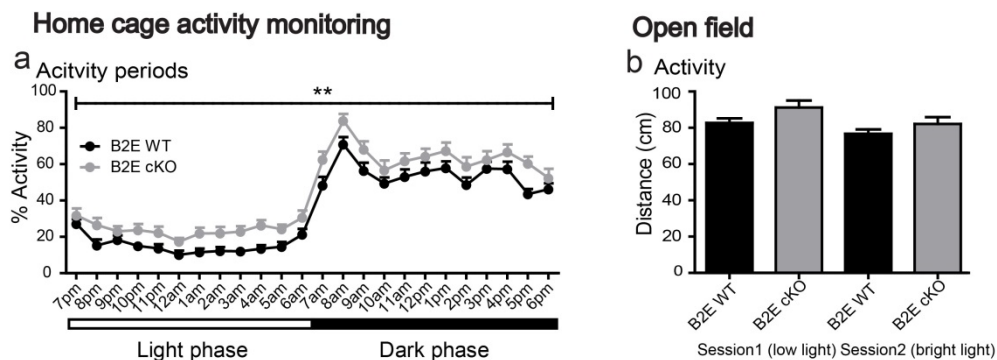

Figure 3.4. Increased home cage activity in B2E cKO mice. **a,** B2E cKO (N=19) and WT (N=20) mice were tested in their home cages for activity. Both the B2E cKO and WT mice display normal circadian activity with increased activity during dark phase. However, B2E cKO mice compared to WT mice displayed increased activity during both light and dark phases. **b,** No change in novelty induced activity (distance explored) was observed between B2E cKO (N=19) and WT (N=24) mice in two sessions at different light conditions. All values are mean $\pm$ SEM; $**P \leq 0.01$, two-way repeated measures ANOVA with Bonferroni post hoc test.

3.1.2b B2E cKO mice display unaltered anxiety levels compared to WT mice

Next, I compared the time B2E cKO and WT mice spent exploring the center of the open field arena as a measure for anxiety related behavior. As shown in Figure 3.5a, there was an effect of the test session $(F_{(1,41)}=15.01$, $p=0.0004)$, but no genotype effect

(F(1,41)=0.07, p=0.7940) or genotype x session interaction (F(1,41)=1.04, p=0.3137). This indicates an unaltered novelty induced anxiety in cKO mice.
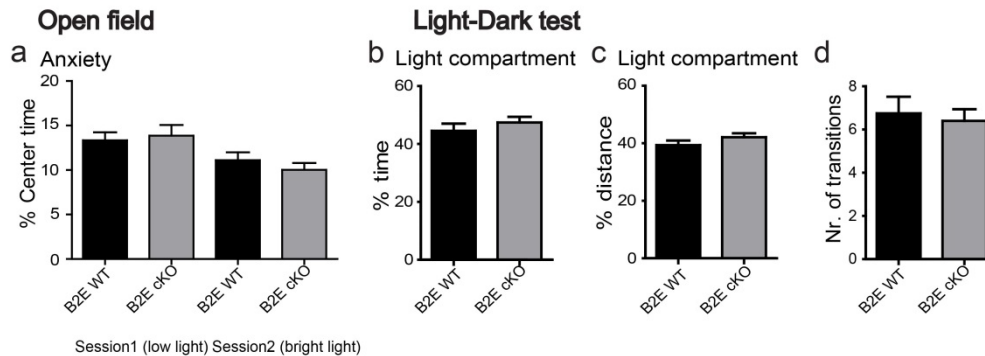

Figure 3.5. Unaltered anxiety levels in B2E cKO mice. **a,** No change in anxiety (time spent in center region of the open field) observed between B2E cKO (N=19) and WT (N=24) mice in the open field arena. **b,c,** Anxiety levels were unchanged in B2E cKO mice as indicated by the percentage of time spent or distance travelled in light chamber during the light-dark test (B2E cKO: N=10; WT: N=12). **d,** Number of transitions between the two compartments were also unchanged between genotypes. All values are mean ± SEM; two-way repeated measures ANOVA with Bonferroni post hoc test (**a**), Student's t-test (**b,c,d**).

Similarly, in the light-dark test for anxiety-like behavior, cKO mice spent a comparable time in the illuminated compartment as WT mice (Figure. 3.5b; WT: 44.54 ± 2.49%; cKO: 47.41 ± 1.98; U=53.50, p=0.6923, Mann-Whitney U test). The distance (expressed as %) travelled in the illuminated compartment (Figure. 3.5c; WT: 39.38 ± 1.62%; cKO: 42.14 ± 1.32%; U=42, p=0.2485) as well as the number of transitions between illuminated and dark compartments were also not different between the genotypes (Figure. 3.5d; WT: 6.75 ± 0.77; cKO: 6.40 ± 0.54; U=50.50, p=0.5469).

3.1.2c B2E cKO mice exhibits altered background contextual fear conditioning

To assess the behavior of B2E cKO and WT mice towards the aversive fear conditioning, mice were further tested in a combined contextual and cued fear conditioning paradigm, where mice learned to display fear response in the form of freezing towards the context where an aversive event (foot shock) occurred and towards the cue (auditory tone) which is paired with the aversive event.
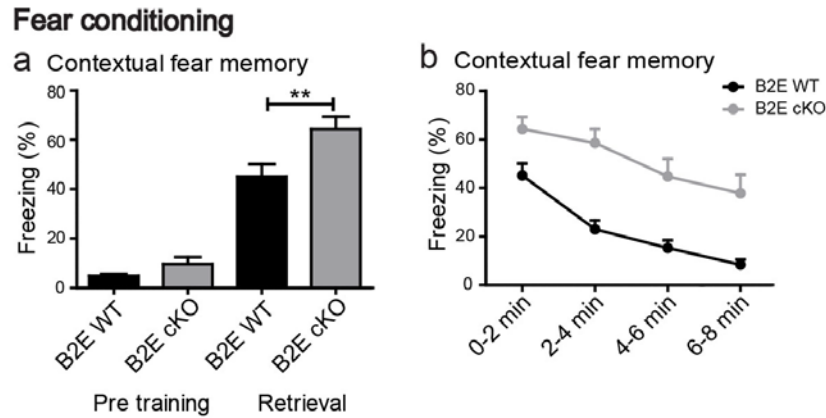
Fear conditioning

Figure 3.6. Altered background contextual fear memory in B2E cKO mice. **a,** B2E cKO (N=11) and WT mice (N=13) display enhanced fear response expressed as percent of freezing (1st two minutes of the respective session) to shock context during retrieval when compared to pre training. However, B2E cKO mice in comparison with WT mice display increased contextual fear response 24 hrs after the training session (indication for memory). **b,** Freezing (%) values throughout the session, where B2E cKO mice displayed increased fear response compared to WT mice. All values are mean ± SEM; **$P \le 0.01$, ***$P \le 0.001$, two-way repeated measures ANOVA with Bonferroni post hoc test (**b**), Student's t-test (**a**).

Significant differences between B2E cKO and WT mice were detectable in background contextual fear conditioning (Figure 3.6a). Freezing analysis using two-way repeated measures ANOVA, revealed increased freezing levels in both genotypes during contextual retrieval (1st two minutes as an indication towards contextual memory) when compared to baseline freezing levels prior to training (effect of test session: $F_{(1,22)}=175.86$, p<0.0001). This analysis further indicated a significant effect of genotype ($F_{(1,22)}=9.34$, p=0.0058), whereas the genotype x session interaction slightly missed the statistical significance ($F_{(1,22)}=4.07$, p=0.0561). Post hoc comparison of genotypes revealed a significant difference between genotypes during contextual retrieval (WT: 45.19 ± 4.89%; cKO: 64.39 ± 4.96%; p<0.01, Bonferroni test) but not during pre-training (WT: 4.94 ± 0.76%; cKO: 9.70 ± 2.79%; p>0.05). Fear response throughout the contextual retrieval session (in 2 min bins) indicates an highly significant increase in fear memory towards the context in B2E cKO mice (Figure 3.6b; genotype effect: $F_{(1,22)}=20.81$, p=0.0002; genotype x session duration interaction: $F_{(3,66)}=2.82$, p=0.0454).

Furthermore, mice were tested in a neutral context, 24 hrs after contextual retrieval session, to assess the memory towards auditory cue (i.e., CS) (Figure 3.7a). Both genotypes showed relatively low freezing levels to the neutral context alone or to the non-conditioned auditory test stimulus (CS-), but stronger freezing in response to

the CS+ (effect of test stimulus: $F_{(1,22)}=17.09$, p=0.0004, two-way repeated measures ANOVA); however, no evidence was found for a genotype effect ($F_{(1,22)}=0.06$, p=0.8123) or a genotype x test stimulus interaction ($F_{(1,22)}=0.32$, p=0.5794). Analysis throughout the session including inter stimulus intervals (ISIs) revealed comparable freezing levels between the genotypes (Figure 3.7b; genotype effect: $F_{(1,22)}=0.11$, p=0.7420).
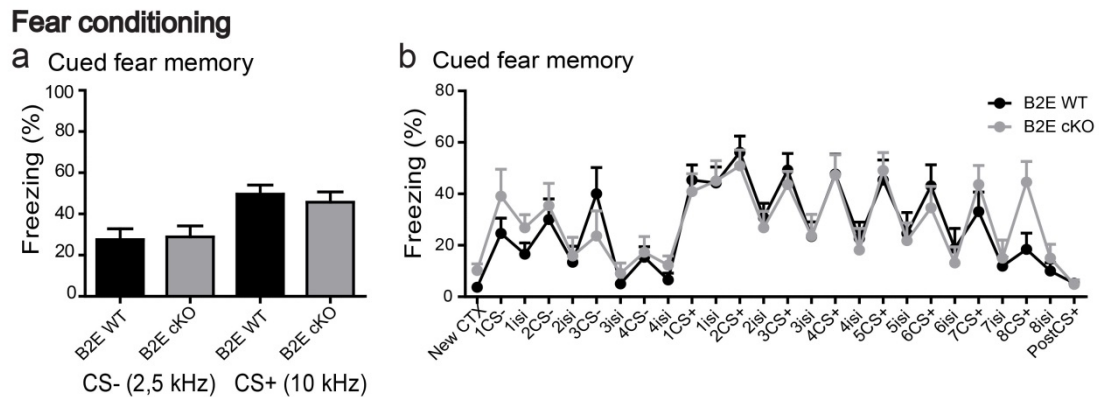

Figure 3.7. Normal cued fear memory in B2E cKO mice. **a,** B2E cKO mice (N=11) in comparison with WT mice (N=13) displayed similar fear responses expressed as percent of freezing (during tone presentation, as a memory indicator). **b,** Freezing (%) values throughout the session, where B2E cKO and WT mice displayed similar fear response, less freezing to CS- compared to CS+. All values are mean ± SEM; two-way repeated measures ANOVA with Bonferroni post hoc test.

To delineate dorsal and ventral hippocampus-dependent effects of contextual fear conditioning in B2E mice, cKO and WT mice were tested in foreground contextual fear conditioning paradigm, which essentially involves the ventral hippocampus (Phillips and LeDoux, 1994).

Freezing analysis between baseline/pre-training (on day1) and retrieval session (24hrs after the last training session on day 3) revealed a significant session effect (Figure 3.8a; $F_{(1,15)}=40.09$, p<0.0001, two-way repeated measures ANOVA). However, no effect of genotype ($F_{(1,15)}=0.55$, p=0.4693) or genotype x session interaction ($F_{(1,15)}=0.61$, p=0.4481) could be observed. Fear response throughout the contextual retrieval session (in 2 min bins) indicates no change in fear memory towards the foreground context in B2E cKO mice (Figure 3.8b; genotype effect: $F_{(1,15)}=1.68$, p=0.2142; genotype x session duration interaction: $F_{(3,45)}=0.65$, p=0.5859).
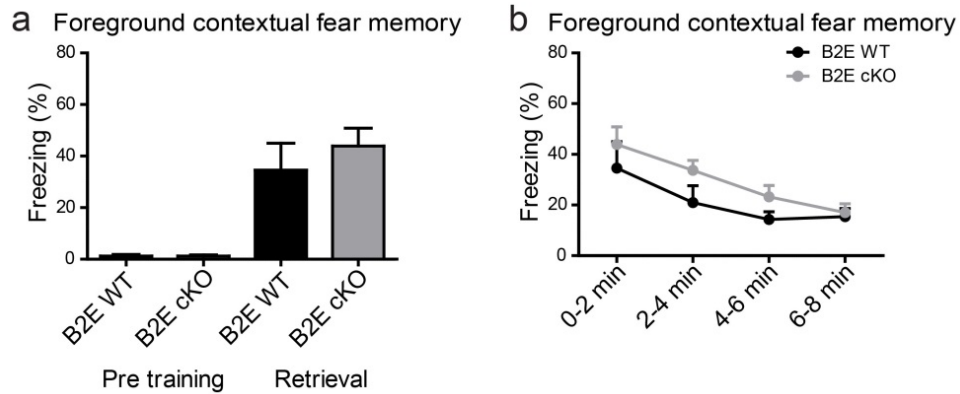
Figure 3.8. Unaltered foreground contextual fear memory in B2E cKO mice. **a,** B2E cKO mice (N=9) in comparison with WT mice (N=8) displayed comparable fear responses expressed as percent of freezing (during tone presentation, as a memory indicator). **b,** Freezing (%) values throughout the session, where B2E cKO and WT mice displayed similar fear response, less freezing to CS- compared to CS+. All values are mean ± SEM; two-way repeated measures ANOVA with Bonferroni post hoc test.

3.1.2d B2E cKO mice shows normal active avoidance learning and unaltered foot shock sensitivity

Since Bsn$^{\Delta Ex4/5}$ mice were shown to display increased performance in an active avoidance task (Ghiglieri et al., 2010), I also tested B2E cKO mice in this paradigm. However, both the cKO and WT mice learned the task effectively showing an increase of avoidance reactions over time (F(4,72)=39.06, p<0.0001, two-way repeated measures ANOVA), and no genotype differences (F(1,18)=0.13, p=0.7226) or session x genotype interactions (F(4,72)=1.06, p=0.3813) were apparent (Figure 3.9).
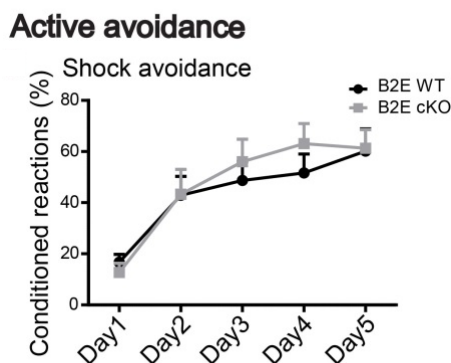
Figure 3.9. B2E cKO mice displayed normal active avoidance learning. B2E cKO (N=9) and WT (N=11) displayed similar avoidance responses (expressed as %) per day resulting in comparable learning curves in both genotypes. All values are mean ± SEM; two-way repeated measures ANOVA with Bonferroni post hoc test.

Furthermore, mice were exposed to a series of foot shocks with increasing intensities (from 0.1, 0.2 and 0.3mA) to control for a bias due to pain sensitivity differences. A significant effect of shock intensity was observed with respect to freezing

response (Figure 3.10a; F(2,36)=25.83, p<0.0001, two-way repeated measures ANOVA), but no main effect of genotype (F(1,18)=0.16, p=0.6897,) or shock intensity x genotype interaction (F(2,36)=1.21, p=0.3088). Different other parameters like flinching (Figure 3.10b; 54.5 % of WT (n=11) and 22.2 % of cKO (n=9), observed only during the 0.1mA stimulus; p=0.1421, χ2 test) and vocalization (Figure 3.10c; at 0.1mA stimulus – 18.2 % of WT, 11.1 % of cKO, p=0.6595; at 0.2mA stimulus – 54.5 % of WT, 33.3 % of cKO, p=0.3428; at 0.3mA stimulus – 90.9 % of WT, 77.8 % of cKO, p=0.4132; mice exhibited vocalization), were not different between genotypes.
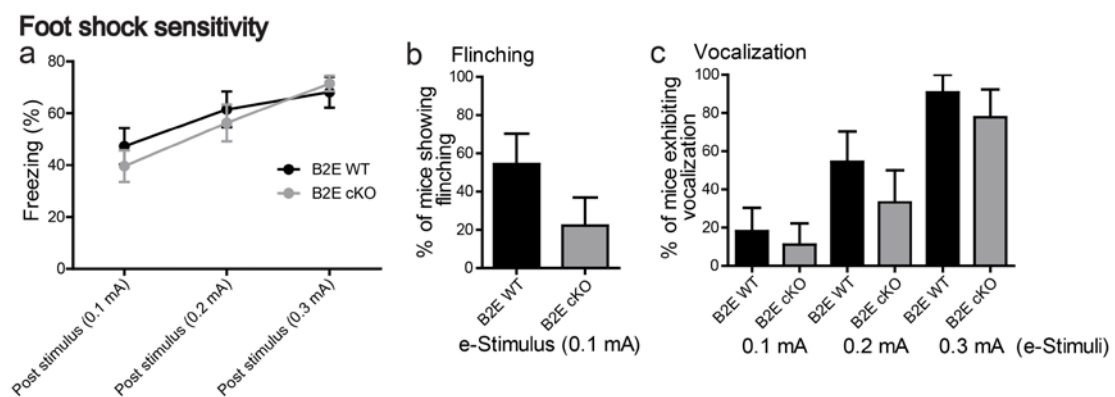

Figure 3.10. Unaltered foot shock sensitivity in B2E cKO mice. a, B2E mice (WT: N=11, cKO: N=9) were presented with increased intensities of foot shock to check differences in sensitivity between B2E WT and cKO mice. Increased and comparable freezing levels were observed in both the groups with increased foot shock intensity. Other parameters like flinching score **(b)** at 0.1 mA stimulus and vocalization **(c)** at all the presented stimuli showed no significant differences between the genotypes. All values are mean ± SEM; two-way repeated measures ANOVA **(a)** and Chi-square test **(b,c)**.

3.1.2e B2E cKO mice display improved performance in dentate gyrus (DG)-dependent pattern separation

The observed changes in background contextual fear conditioning suggest functional alterations of the dorsal hippocampus of B2E cKO mice. To further investigate this, I tested B2E mice in an additional task involving hippocampal structure, i.e. DG-dependent pattern separation. This task is mainly based on the rodent innate behavior to explore the novel spatial alterations (Ennaceur and Delacour, 1988).
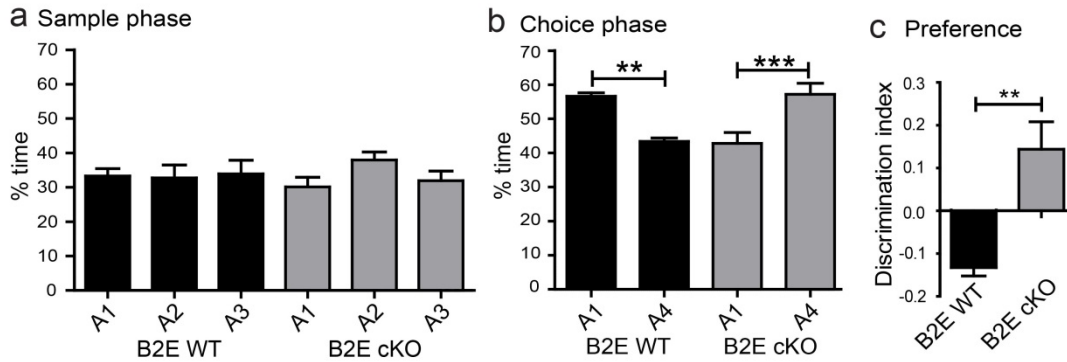
Figure 3.11. Improved performance of B2E cKO mice in a dentate gyrus-dependent pattern separation paradigm. a, B2E cKO mice (N=9) and WT mice (N=7) displayed comparable exploration time (%) at all the locations during the sample phase. **b,** Exploration times of B2E cKO and WT mice at novel and familiar locations during the choice phase. WT mice spent more time with the familiar object than with the object at the novel location. In contrast, B2E cKO mice spent more time with the object at the novel location. **c,** Higher discrimination index in B2E cKO mice, indicating significantly altered performance compared to WT mice. All values are mean ± SEM; **$P \leq 0.01$, ***$P \leq 0.001$, two-way ANOVA with Bonferroni post hoc test (**a,b**), Student's t-test (**c**).

In the pattern separation task, both B2E cKO and WT mice explored all the three locations equally well during sample phase (Figure. 3.11a; $F_{(2,42)}=0.78$, p=0.4669, two-way ANOVA) with no main effect of genotype ($F_{(1,42)}=0.00$, p=1.000) genotype x location interaction ($F_{(2,42)}=1.15$, p=0.3263), indicating no location bias. During the choice phase (Figure 3.11b), again no significant effects of genotype ($F_{(1,28)}=0.00$, p=1.0000) and location ($F_{(1,28)}=0.05$, p=0.8319) were observed but, importantly, a significant genotype x location interaction ($F_{(1,28)}=26.94$, p<0.0001). Bonferroni post hoc tests revealed a significant change in the exploration of familiar and novel locations within the B2E cKO mice (p<0.001), where cKO mice spent more time exploring the novel location when compared to the familiar location. By contrast, B2E WT mice preferred the familiar location (p<0.01). Further discrimination indices were also calculated to illustrate the relative preference for either location; these differed significantly between WT and cKO mice (Figure 3.11c; t(14)=3.670, p=0.0025, Student's t-Test). These results indicate that, B2E cKO mice could perform the pattern separation between the two close positions avoiding the confusion. This better performance in DG-dependent pattern separation is in concert with the altered behavior observed in background fear conditioning in B2E cKO mice.

3.1.2f B2E cKO mice display better performance in a novel object location task with no change in novel object recognition memory

In the novel object location task, during sample phase, B2E cKO and WT mice were habituated to two identical objects in different locations and no significant effect of location (Figure 3.12a; $F_{(1,26)}=3.96$, p=0.0574, two-way ANOVA), no effect of genotype ($F_{(1,26)}=0.79$, p=0.3819) and location x genotype interaction ($F_{(1,26)}=0.08$, p=0.7730) was observed. During the choice phase 24h later (Figure 3.12b), there was a significant effect of location ($F_{(1,26)}=11.80$, p=0.002) as mice generally preferred the novel location. No main effect of genotype was found ($F_{(1,26)}=0.11$, p=0.7397), but a significant location x genotype interaction ($F_{(1,26)}=5.04$, p=0.0335). Bonferroni post hoc test revealed a preference of B2E cKO mice (p<0.01) for the novel location, for which the WT showed only a non-significant trend. The calculation of the discrimination index revealed a non-significant trend for enhanced performance in cKO mice, when compared to WT mice (Figure 3.12c; t(13)=1.838, p=0.0890, Student's t-test).
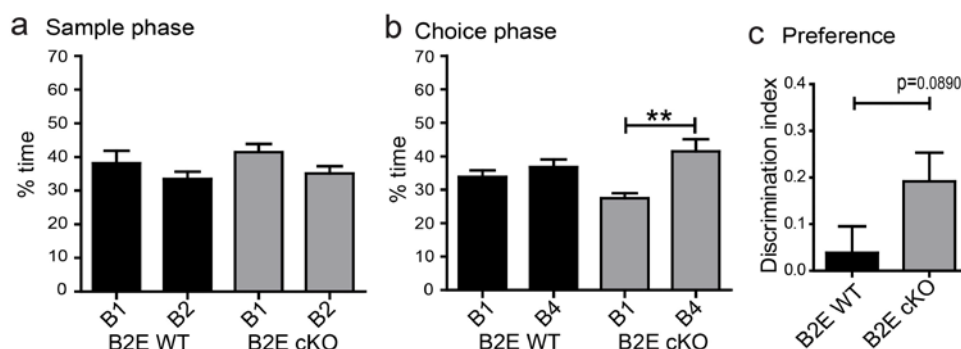

Figure 3.12. Better performance of B2E cKO mice in novel object location task. a, B2E cKO mice (N=7) and WT mice (N=8) displayed comparable exploration times (%) at all the locations the during sample phase. **b,** Exploration time at novel and familiar locations by B2E cKO and WT mice during choice phase. WT mice have a slight preference for the object at the novel location than for the one at the familiar location. In contrast, B2E cKO mice spent more time with the object at the novel location. **c,** A non-significant trend towards higher discrimination index was detected in B2E cKO mice compared to WT mice. All values are mean ± SEM; **$*P \leq 0.01$, two-way ANOVA with Bonferroni post hoc test (**a,b**), Student's t-test (**c**).

In novel object recognition task, mice were tested for both short-term and long-term memory. During long-term memory testing, B2E cKO and WT mice encounter two identical objects (O1 and O2) during habituation phase (Figure 3.13a). There was no effect of genotype ($F_{(1,28)}=0.00$, p=1.0000) or genotype x object interaction ($F_{(1,28)}=1.10$, p=0.3031). However, the effect of object ($F_{(1,28)}=9.09$, p=0.0054) was

observed. Bonferroni post hoc test revealed a significant preference of WT mice towards one of the objects, O1 (p<0.05). 24 hrs later, during testing phase, one of the objects was replaced with a novel object (O3) (Figure 3.13b). No main effect of genotype (F(1,28)=0.00, p=1.0000) or genotype x object interaction (F(1,28)=0.40, p=0.5315) was observed. As expected, a significant effect of object (F(1,28)=45.54, p<0.0001) was detectable. Bonferroni post hoc test revealed a significant preference of both B2E cKO and WT mice for the novel object over the familiar object (cKO: p<0.001; WT: p<0.001), resulting in similar discrimination indices (Figure 3.13c).

Long-term memory
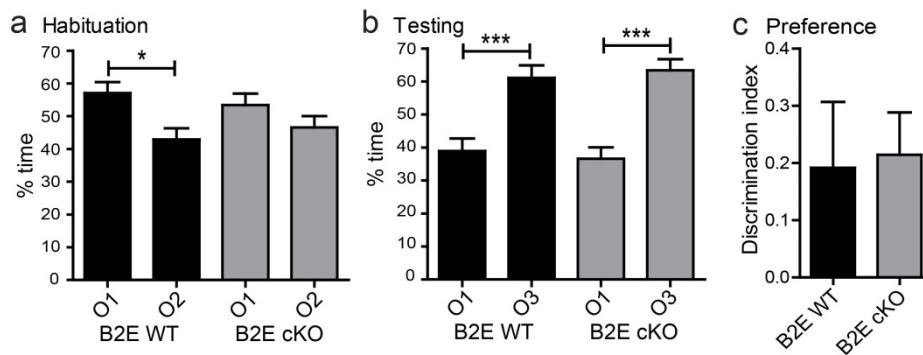
Short-term memory

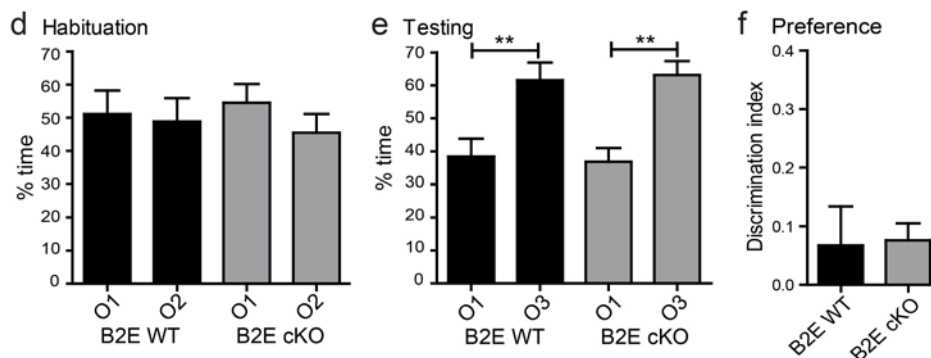**Figure 3.13. Unaltered novel object recognition memory in B2E cKO mice. a,** In a test for long-term memory, B2E cKO mice (N=9) displayed comparable exploration times (%) at both locations during habituation. However, WT mice (N=7) spent more time at one of the objects. **b,** Exploration times at novel and familiar objects by B2E cKO and WT mice during testing phase. Both B2E cKO and WT mice prefer the novel over the familiar object. **c,** Similar discrimination indices observed in B2E cKO and WT mice. **d,** While testing for short-term memory, both B2E cKO (N=6) and WT mice (N=7) displayed equal exploration times at both locations during habituation phase. **e,** During testing, both groups prefer the novel object. **f,** Similar discrimination indices between both groups were observed during the testing phase. All values are mean ± SEM; **$P \leq 0.01$, two-way ANOVA with Bonferroni post hoc test (**a,b,d,e**), Student's t-test (**c,f**).

In a test for short-term memory, both the groups of mice encounter two identical objects (O1 and O2) during habituation phase and explored both the objects equally without any bias (Figure 3.13 d. $F_{(1,22)}=0.74$, $p=0.3975$). There was no effect of genotype ($F_{(1,22)}=-0.00$, $p=1.0000$) or genotype x object interaction ($F_{(1,22)}=0.26$, $p=0.6136$) observed. Two hrs later, during testing phase, one of the objects was replaced by a novel object (O3). Both genotypes prefer the novel over the familiar one (Figure 3.13e; $F_{(1,22)}=-0.00$, $p=1.0000$). No effect of genotype x object interaction ($F_{(1,22)}=0.11$, $p=0.7481$) was observed. As expected, a significant preference for the novel object ($F_{(1,22)}=25.07$, $p<0.0001$) was observed. Bonferroni post hoc test revealed a significant effect for both B2E cKO and WT mice (cKO: $p<0.01$; WT: $p<0.01$), resulting in similar discrimination indices (Figure 3.13f). These results indicate that long-term as well as short-term memories for familiar vs. novel objects were unchanged in B2E cKO mice.

3.1.2g B2E cKO mice display unaltered performance in Morris Water Maze

B2E cKO and WT mice were further examined for spatial learning and memory in the Morris Water Maze (Figure 3.14). During the acquisition phase, a significant learning rate was observed over the three training days with gradually decreasing escape latencies to find the platform (effect of training day: $F_{(2,32)}=7.32$, $p=0.0024$, two-way repeated measures ANOVA) and reduction of path length (effect of training day: $F_{(2,32)}=17.55$, $p<0.0001$) in both the groups (days 1-3 in Figure 3.14a,b). Main effects of genotype were observed neither for the escape latency ($F_{(1,16)}=2.55$, $p=0.1297$) nor for the total path length ($F_{(1,16)}=1.94$, $p=0.1832$,) and no genotype x training day interaction was observed for escape latency ($F_{(2,32)}=0.05$, $p=0.9477$) nor for path length ($F_{(2,32)}=0.13$, $p=0.8751$). During the probe trails (Figure 3.14c,d), both WT and cKO mice spent comparable times (%) in the old platform quadrant (probe trail1: $t_{(16)}=0.4694$, $p=0.6451$; probe trail2: $t_{(16)}=0.8809$, $p=0.3914$, Student's t-test) when compared to the quadrant of the new platform (probe trail1: $t_{(16)}=0.4289$, $p=0.6737$; probe trail2: $t_{(16)}=0.3163$, $p=0.7559$) (Figure 3.13c,d). During reversal training (days 4-5 in Figure 3.14 a,b), with the platform shifted to a new position, no significant effect of genotype in escape latency ($F_{(1,16)}=1.68$, $p=0.2130$) and path length ($F_{(1,16)}=0.93$, $p=0.3492$) or genotype x training day interaction effect in escape latency ($F_{(1,16)}=2.69$, $p=0.1202$) and path length ($F_{(1,16)}=2.95$, $p=0.1054$) were found.
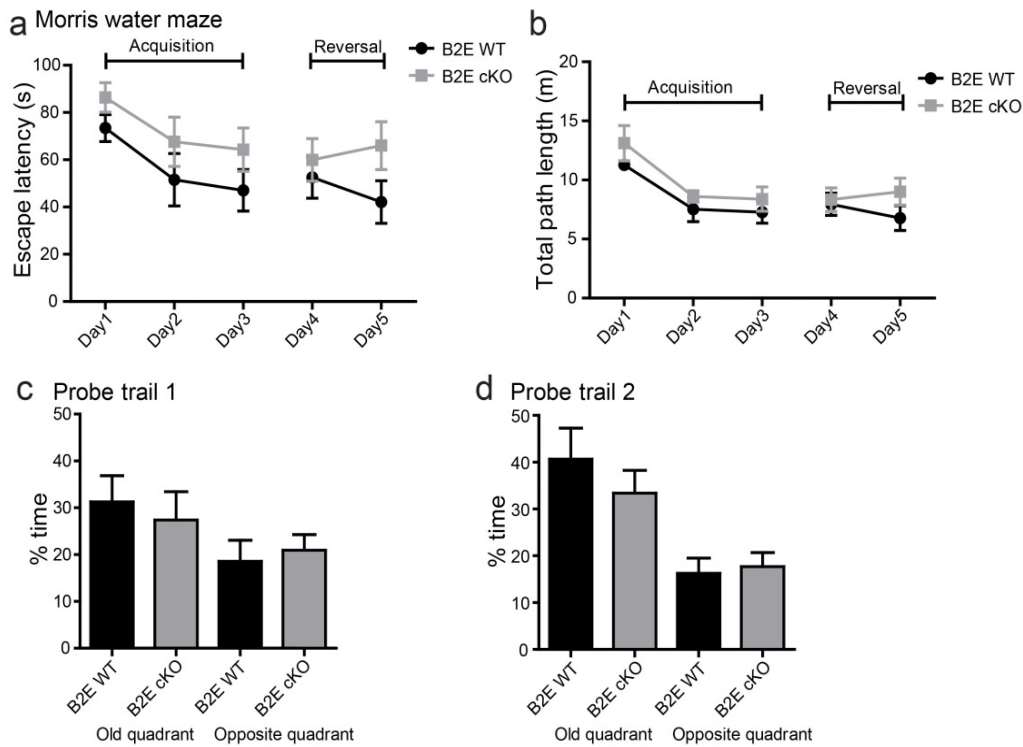
Figure 3.14. Normal spatial learning and memory in B2E cKO mice. a, B2E cKO mice (N=9) and WT mice (N=9) displayed comparable escape latencies and **b,** total path length to reach the hidden platform during the first 3 days of acquisition and the next 2 days of reversal phase. **c,** Both B2E cKO and WT mice spent relatively more time (%) at the old platform quadrant than the opposite platform quadrant during the two probe trails on day 4. All values are mean ± SEM; two-way repeated measures ANOVA with Bonferroni post hoc test (**a,b**), Student's t-test (**c,d**).

3.1.3 No behavioral changes were found in different Emx1 control groups

To control for genetic background, Cre expression and Emx1 haplodeficiency, I also tested Emx1$^{+/+}$ (without Cre) and Emx1$^{Cre/+}$ mice in the behavioral paradigms used for the characterization of B2E cKO mice. None of the analyzed parameters was different between the two driver line genotypes (Figure 3.15).

In home cage activity analysis, a significant effect of the day time was observed in both groups with increased activity during the 12 hrs of dark phase of the cycle (Figure 3.15a; $F_{(23,345)}=32.55$, $p<0.0001$, two-way repeated measures ANOVA). No significant genotype effect ($F_{(1,15)}=0.37$, $p=0.5512$) and no interaction with day time ($F_{(23,345)}=0.92$, $p=0.5780$) was observed. Comparison of activity during 12 hrs of dark phase and 12 hrs of light phase were also unchanged between the groups (dark phase:

Emx1$^{+/+}$: 46.85 ± 6.04%; Emx1$^{Cre/+}$: 44.54 ± 2.75%, t(15)=0.3621, p=0.7224, Student's t-test and light phase: Emx1$^{+/+}$: 21.22 ± 2.89%; Emx1$^{Cre/+}$: 17.94 ± 2.58%, t(15)=0.8511, p=0.4081).
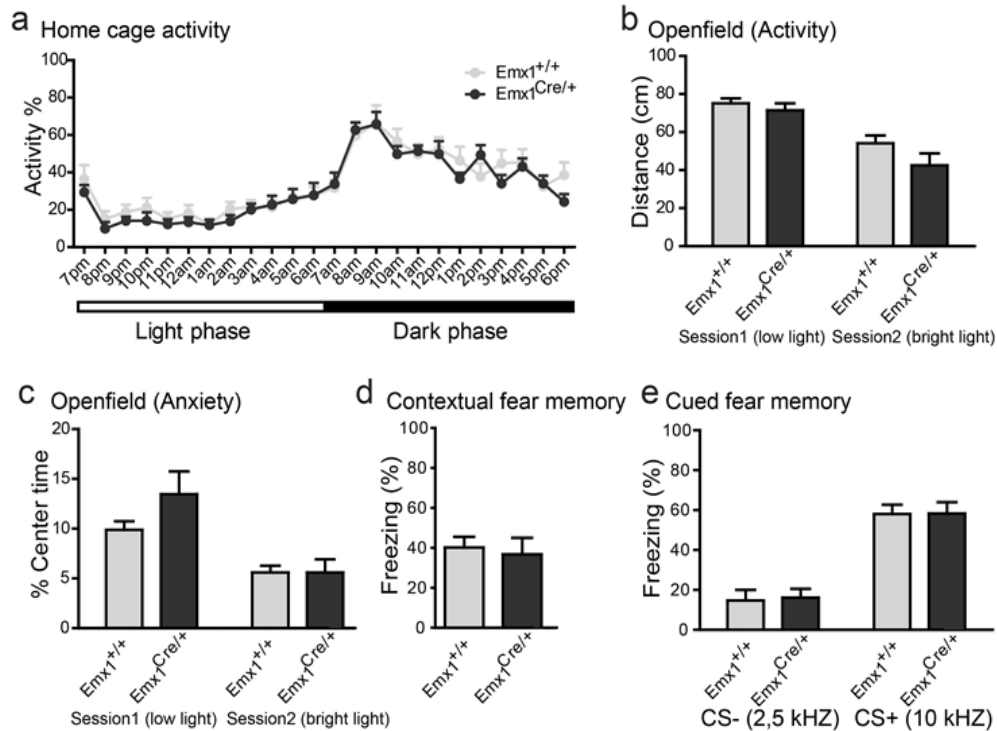

Figure 3.15. No change in the behavior of different Emx1 control groups. a, (Emx1$^{+/+}$: N=8, Emx1$^{Cre/+}$: N=9) displayed un altered home cage activity **b,** In open field exploration both the groups (Emx1$^{+/+}$: N=9, Emx1$^{Cre/+}$: N=9) ran the same distance. **c,** Anxiety levels were also unchanged between the groups with respect to time they spent in the center of the open field. **d,** During contextual retrieval both the control (Emx1$^{+/+}$: N=9, Emx1$^{Cre/+}$: N=9) groups spent comparable time freezing in the shock context 24 hrs after training. **e,** Both groups displayed less and comparable freezing towards CS- and profound freezing towards the CS+. All values are mean ± SEM; two-way repeated measures ANOVA with Bonferroni post hoc test.

Open-field analysis of distance travelled using low light and bright light test sessions revealed significant effect of the test session (Figure 3.15b; F(1,16)=51.16, p<0.0001, two-way repeated measures ANOVA) but no genotype effect (F(1,16)=2.28, p=0.1508) or genotype x session interaction (F(1,16)=1.28, p=0.2743). In addition, time spent in the center was analyzed as a measure of anxiety. There was a significant effect of the test session (Figure 3.15c; F(1,16)=23.70, p=0.0002), but no genotype effect (F(1,16)=1.26, p=0.2783) or genotype x session interaction (F(1,16)=2.07, p=0.1695) was observed.

Furthermore, mice (Emx1$^{+/+}$: N=9, Emx1$^{Cre/+}$: N=9) were tested in combined contextual and cued fear conditioning paradigm. Both the groups displayed comparable

pre-training baseline freezing levels and increased freezing levels in the shock context 24 hrs later. This results in a significant session effect (Figure 3.15d; $F_{(1,16)}=47.68$, p<0.0001), but no genotype effect ($F_{(1,16)}=0.07$, p=0.7986) or genotype x session interaction ($F_{(1,16)}=0.19$, p=0.6718). 24 hrs after the contextual retrieval mice were tested in neutral context for auditory cued memory (Figure 3.15e). Both genotypes showed low freezing levels to the non-conditioned auditory test stimulus (CS-), but strong freezing to the CS+ (effect of test stimulus: $F_{(1,16)}=75.77$, p<0.0001). No change was evident for effect of genotype ($F_{(1,16)}=0.03$, p=0.8728) or genotype x test stimulus interaction ($F_{(1,16)}=0.01$, p=0.9114).

3.1.4 B2E cKO mice display morphological changes of dentate gyrus granule cells

Hippocampal neurons in $Bsn^{\Delta Ex4/5}$ mice were reported to display morphological changes (Sgobio et al., 2010). Based on the previous finding and observed behavioral phenotype in B2E cKO mice, which implicates the dorsal hippocampus and specifically the DG I next analyzed the morphology of DG granule cells using the Golgi impregnation method (Figure 3.16a). Sholl analysis revealed an increased arborization of DG granule cell dendrites in B2E cKO mice (Figure 3.16b; $F_{(1,9)}=10.43$, p=0.0103, two-way repeated measures ANOVA). Specifically, dendritic complexity was higher in the region 60-120µm distant from the cell soma ($t_{(9)}=3.481$, p=0.0069, Student's t-test). The total dendritic branch length was also significantly increased in cKO mice as compared to WT mice (Figure 3.16c; $t_{(9)}=2.546$, p=0.0314). Further analysis of the order of apical dendritic branching revealed an increased mean number of 1st order branching's per cell in B2E cKO mice as compared to WT mice (Figure 3.16c; $t_{(9)}=2.890$, p=0.0179). Based on these findings, I further investigated the density of spines in the dendritic region between 60-120 µm away from the soma. This revealed a lower spine density in cKO mice compared to their WT littermates (Figure 3.16d; $t_{(6)}=3.904$, p=0.0079).

To check whether these changes might global or region-specific, I also analyzed CA1 pyramidal neurons from WT and cKO mice (Figure 3.17a). There was no significant genotype effect observed in the number of intersections (Figure 3.17b; $F_{(1,10)}=0.03$, p=0.8671) from both basal and apical dendrites.
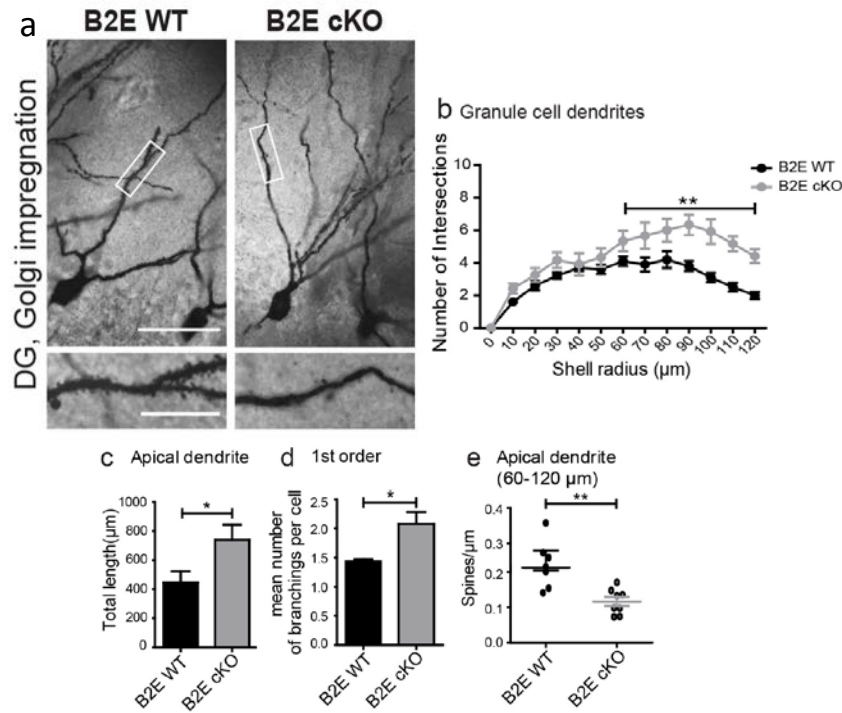
Figure 3.16. Morphological changes of DG granule cells in B2E cKO mice. a, Example images of Golgi impregnation of dentate gyrus (DG) granule cells from WT and B2E cKO mice (high magnification of entangled area in lower panel showing spine density). **b,** Sholl analysis of apical dendrites shows an increased number of intersections in B2E cKO mice compared to WT mice, indicating an enhanced dendritic arborization in B2E cKO in a region 60-120 µm away from soma. **c,** Increased cumulative length of dendrites in cKO mice compared to WT mice (B2E WT: N=5 mice, n=10 cells; B2E cKO: N=6 mice, n=11 cells). **d,** Increase in mean number of 1st order branching in B2E cKO mice. **e,** The density of spines measured in the region of increased dendritic arborization in cKO is reduced when compared WT littermates (N=4 mice each; WT: n=7 cells, cKO: n=8 cells). Scale bar is 15 µm in **a** and 5 µm in lower panel. All values are mean ± SEM; *$P \leq 0.05$, **$P \leq 0.01$, two-way repeated measures ANOVA (**b**) and Student's t-test (**c,d,e**).

Further analysis on dendritic branch length at CA1 pyramidal neurons revealed no significant genotype effect (Figure 3.17c; $F_{(1,10)}=0.01$, p=0.9193).

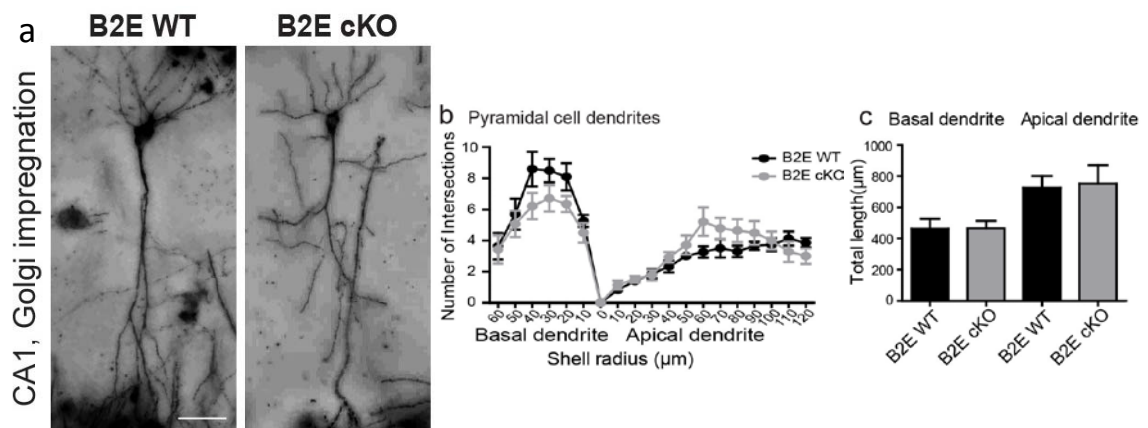**Figure 3.17. Unaltered morphological properties of CA1 pyramidal cells in B2E cKO mice. a,** Example images of Golgi impregnation of CA1 pyramidal cells from B2E WT and cKO mice. **b,** Sholl analysis revealed no change in dendritic arborization in B2E cKO mice. **c,** Total dendritic branch length did also not differ between genotypes. Scale bar is 15 µm in **a.** All values are mean ± SEM; two-way repeated measures ANOVA.

3.1.5 Increased excitability and lack of maturation-induced decrease in excitability at medial perforant path to dentate gyrus (MPP-DG) synapses of B2E cKO mice

For an assessment of physiological correlates of these behavioral and structural deviations in B2E cKO mice, electrophysiological properties of hippocampal synapses of B2E cKO mice in the dorsal hippocampus were analyzed by Dr. Gürsel Caliskan from Institute of Biology, Magdeburg.
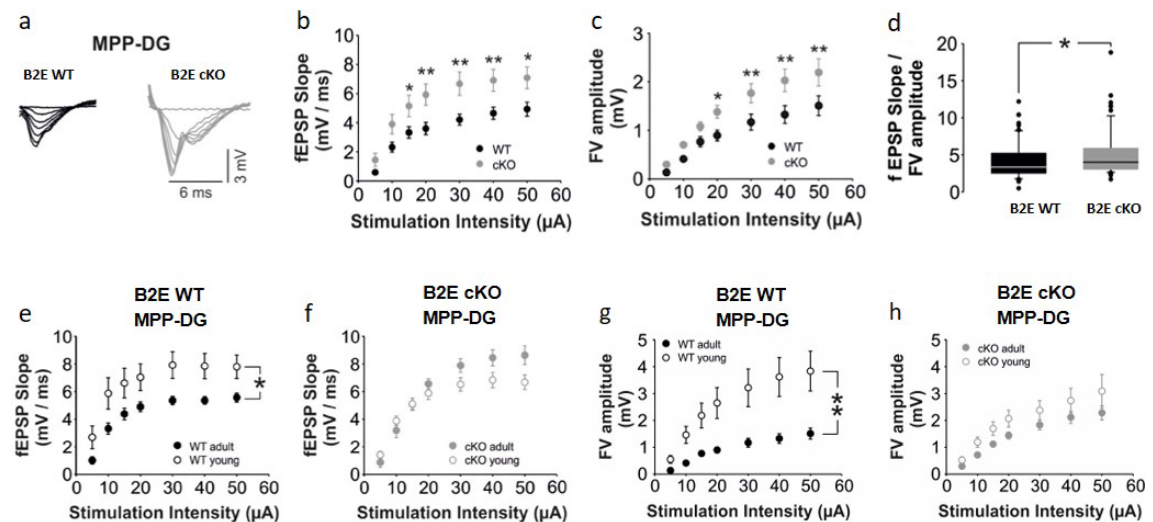

Figure 3.18. Increased baseline transmission and lack of age-dependent maturation of granule cells in DG of B2E cKO mice at MPP-DG. a, Example traces of field excitatory postsynaptic potential (fEPSP) responses to increasing stimulation strengths (5-50 µA) at the MPP-DG. **b,** Summary graphs indicating increased synaptic excitability in MPP-PP synapses of B2E cKO mice (DG: N = 5 mice, n = 22 slices) compared to WT mice (DG: N = 6 mice, n = 21 slices). **c,** Summary graphs indicating increased presynaptic fiber volley (FV) amplitude in MPP-PP synapses of B2E cKO mice (DG: N = 5 mice, n = 9 slices) compared to WT mice (DG: N = 6 mice, n = 11 slices). **d,** Summary graphs showing fEPSP slope to FV amplitude ratio in MPP-DG pathway, which is increased in B2E cKO mice. **e,** Age-dependent decrease in baseline excitability in the MPP-DG synapse of B2E WT mice (WT adult: N = 4 mice, n = 11 slices, WT young: N = 5 mice, n = 11 slices). **f,** Lack of an age-dependent decrease in baseline excitability in the MPP-DG synapse of B2E cKO mice (cKO adult: N = 4 mice, n = 11 slices, cKO young: N = 5 mice, n = 11 slices). **g,** Summary graph showing a maturation-induced decrease in FV amplitudes in the MPP-DG synapse of WT mice (WT adult: N = 5 mice, n = 11 slices, WT young: N = 5 mice, n =9 slices). **h,** Summary graph illustrating the lack of an age-dependent decrease in FV amplitudes in the MPP-DG synapse of cKO mice (cKO adult: N = 4 mice, n = 9 slices, cKO young: N = 5 mice, n = 10 slices). All values are mean ± SEM; $*P \leq 0.05$, $**P \leq 0.01$; two-way repeated measures ANOVA and Student's t-test. MPP: Medial Perforant Path, DG: Dentate gyrus. (This data and figure panels were provided by Dr. Gürsel Caliskan).

Field-excitatory postsynaptic potential (fEPSP) slopes and fiber volley (FV) amplitudes obtained from input-output (I-O) curves (Figure 3.18a) were analyzed to determine the baseline excitability and synaptic efficacy in the MPP-DG pathway. At

MPP-DG synapses, a significant increase not only in the fEPSP slopes (Figure 3.18b; MPP-DG: $F_{(1,41)}=6.063$, p=0.018, two-way repeated measures ANOVA), but also in the FV amplitudes (Figure 3.18c; MPP-DG: $F_{(1,18)}=5.598$, p=0.029) was observed in B2E cKO vs. WT slices. Further, to elucidate the changes in the baseline synaptic efficacy in B2E cKO and WT mice, fEPSP slope to FV amplitude ratios were calculated. In the MPP-DG synapse, the fEPSP to FV amplitude ratio is significantly increased indicating an augmented baseline transmission (Figure 3.18d; WT: 4090.4 ± 289.6, B2E cKO: 5139.2 ± 404.7; U=1739.0, p=0.02, Mann-Whitney U test). Based on the above findings and previous observations regarding the excitable state of GCs (Schmidt-Hieber et al., 2004; Zhao et al., 2008), it is hypothesized that lack of Bassoon may impair maturation of the dentate gyrus and, therefore, compared electrophysiological properties of young (~4-5 weeks) and adult (~12-16 weeks) WT and cKO mice. In WT mice the excitability of MPP-DG synapses was reduced during maturation as fEPSP slopes were significantly smaller in adult WT mice than in young WT mice (Figure 3.18e; $F_{(1, 22)}=7.131$, p=0.014, two-way repeated measures ANOVA). By contrast, the high MPP-DG synapse excitability of cKO mice was maintained during maturation, and no significant alteration between I-O curves of the young and adult cKO mice became evident (Figure 3.18f; $F_{(1, 20)}=1.592$, p=0.222). Furthermore, to check whether the lack of maturation-induced decrease in fFPSP slopes at the MPP-DG synapse of adult cKO mice was associated with any adaptive presynaptic change, the FV amplitudes obtained from MPP-DG synapse of young vs. adult WT and cKO mice were compared. Indeed, in WT animals, a significant decrease in FV amplitudes during maturation was observed (Figure 3.18g; $F_{(1, 18)}=10.275$, p=0.005). During development, similar to unaltered postsynaptic excitability in B2E cKO mice no change in presynaptic FV amplitudes was observed (Figure 3.18h; $F_{(1, 18)}=2.479$, p=0.133), indicating the maintenance of an immature-like state of DG in B2E cKO mice.

3.1.6 B2E cKO mice maintain an immature state of dentate gyrus granule cells

Based on these anatomical and electrophysiological findings, I further tested for the expression of various maturation markers in the DG. First, I analyzed the expression of calbindin as a marker for mature granular cells (Figure. 3.19a). In the granule cell layer (GCL) of cKO mice, the immunohistochemical labeling of calbindin (integrated density values) was reduced, when compared to WT mice (Figure. 3.19c; t(10)=2.274,

p=0.0462, Student's t-test), resembling the effect in constitutive *Bsn*$^{\Delta Ex4/5}$ mutants (Dieni et al., 2015).

Next, sections were stained for immature cells in the GCL using calretinin and doublecortin (DCX) as markers (Figure. 3.19b). I found that the number of cells positive for either calretinin (p<0.001, Bonferroni posttest) or DCX (p<0.01) were strongly increased in the granule cell layer of cKO mice (Figure. 3.19d; $F_{(1,9)}$=18.86, p=0.0019, two-way repeated measures ANOVA). The number of cells double positive for calretinin and DCX were also significantly increased (Figure. 3.19e; $t_{(9)}$=3.501, p=0.0067), but the proportion of calretinin positive cells that were also positive for DCX were not changed between the genotypes (WT: 74.33 ± 2.662%; cKO: 81.06 ± 3.76%).
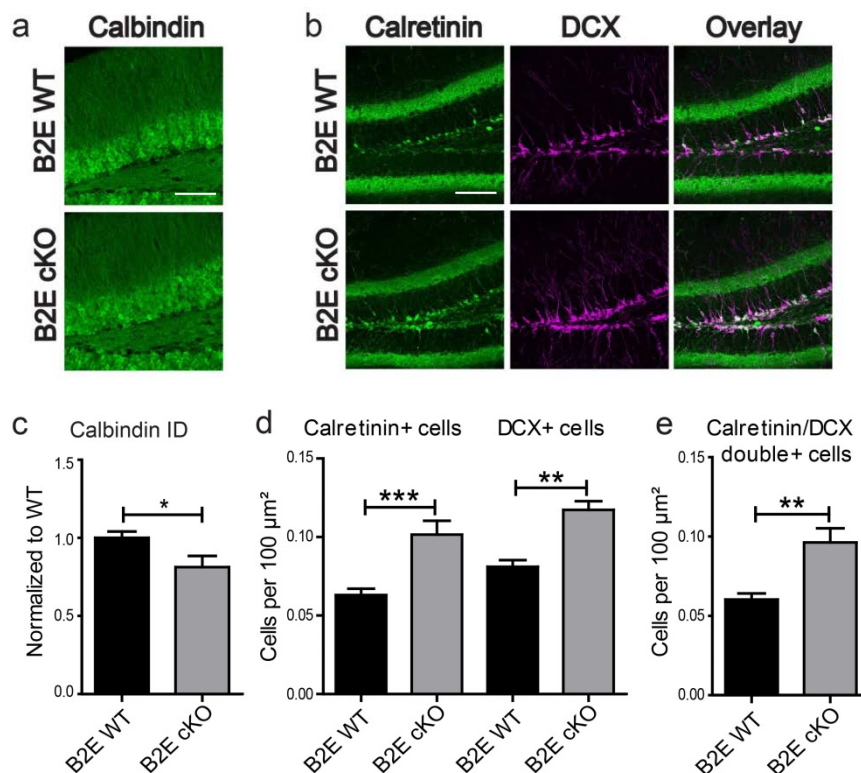

Figure 3.19. Delayed maturation of granule cells in DG of B2E cKO mice. a, Representative dorsal of mature granule cells and the quantification of calbindin labeling (integrated density values) confirms a reduced expression in B2E cKO mice (**c**). **b,** Representative dorsal hippocampus sections from WT (N=5) and cKO (N=6) mice were stained for calretinin and doublecortin (DCX) as markers of immature granule cells. An increased labeling for both markers is evident in B2E cKO mice. **d** The densities of immature cells positive for calretinin or DCX, as well as **e,** double positive cells are significantly increased in B2E cKO mice. Scale bar, 100µm. All values are mean ± SEM; *$P \leq 0.05$, **$P \leq 0.01$, ***$P \leq 0.001$, two-way repeated ANOVA followed by Bonferroni post hoc test (**d**) and Student's t-test (**c,e**).

3.1.7 Increased neurogenesis was observed in B2E cKO mice

Furthermore, rate of neurogenesis was investigated in B2E cKO mice, as it might contribute to the increased number of immature cells in the DG of cKO mice. A similar observation was also described earlier regarding enhanced neurogenesis in $Bsn^{\Delta Ex4/5}$ mice (Heyden et al., 2011). To this end, I used Ki67 as a marker to identify proliferating cells in the DG (Figure 3.20a). I found that Ki67 positive cells in GCL of Bsn cKO mice were significantly more when compared to WT mice (Figure 3.20b; t(8)=4.102, p=0.0034).
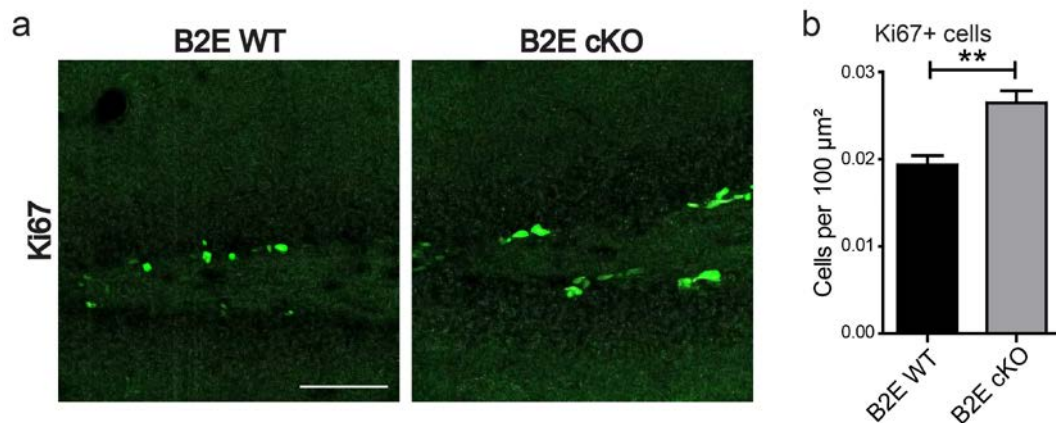

Figure 3.20. Elevated neurogenesis observed in B2E cKO mice. **a,** Dorsal hippocampus sections from B2E cKO (N=5) and WT (N=5) mice were stained using Ki67 antibody. **b,** Quantification of Ki67 positive cells show increased number in B2E cKO mice compared to WT mice. Scale bar, 100µm. All values are mean ± SEM; **$*P \leq 0.01$, Student's t-test.

3.2 B2D mice

3.2.1 B2D cKO mice lack Bassoon expression in dopaminergic terminals

Another conditional mouse model of Bassoon lacking exon 2 of the Bsn gene specifically in dopaminergic neurons was established. To generate this cKO, Bsn2$^{lx/lx}$ mice were bred with a driver line expressing Cre recombinase under the control of promoter of the dopamine transporter gene (DAT-Cre) (Backman et al., 2006). This allows to specifically knockout *Bsn* in dopaminergic neurons in these mice. Mice with successful Cre recombination are B2D cKO mice (Bsn2$^{lx/lx}$DAT$^{Cre/+}$) and littermates B2D CTL mice does not contain the floxed allele of *Bsn* gene (Bsn2$^{+/+}$DAT$^{Cre/+}$).

To assess the specificity of Cre recombinase activity in B2D cKO mice, striatal sections were stained using antibodies against Bassoon and DAT (dopaminergic marker) (Figure 3.21a). Overlay images and high magnifications of overlays showing less co-localization between Bassoon and DAT confirms the lack of Bassoon in dopaminergic release sites. However, Bassoon staining in the cKO striatum is still strong, due to the glutamatergic inputs coming from different other brain regions like neocortex, hippocampus and amygdala (Berke and Hyman, 2000). With the immunohistochemical stainings it is evident that knockout of Bassoon is restricted to dopaminergic terminals in these cKO mice. Survival rates of B2D mice was monitored and analyzed for 1 year. Both B2D cKO (N=16) and CTL (N=17) mice survive in a same proportion without any differences in the survival rate between the genotypes (Figure 3.21b).
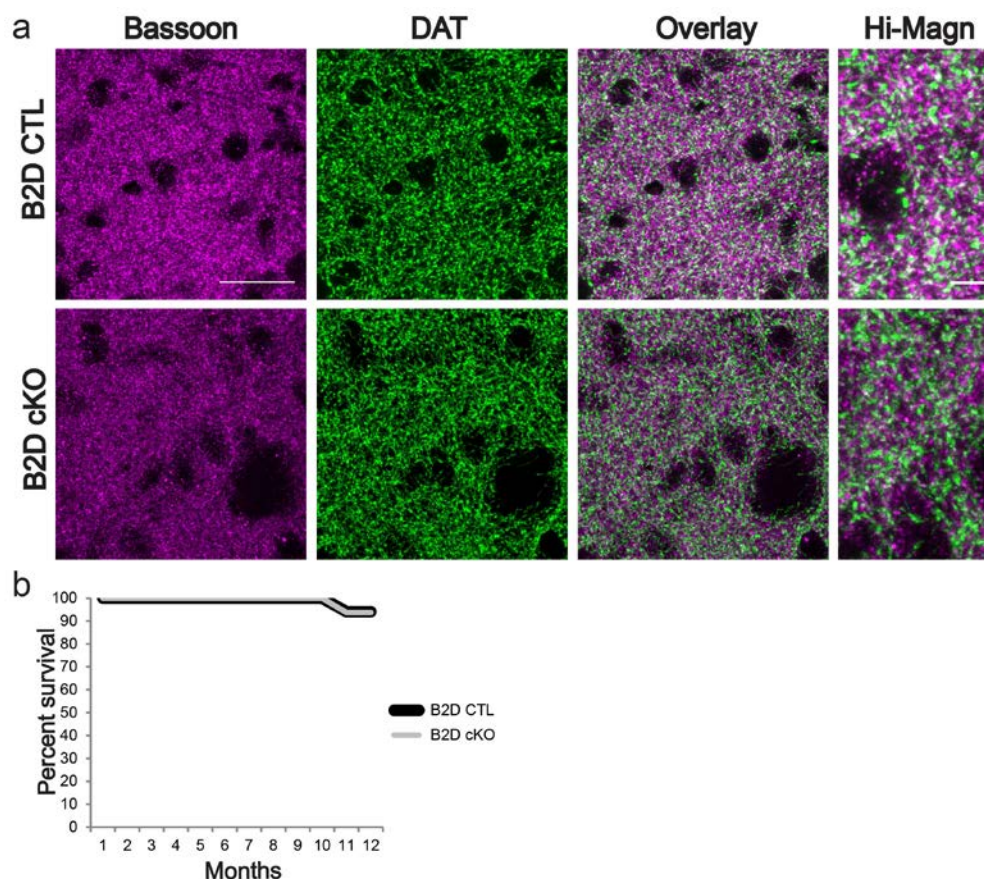

Figure 3.21. B2D cKO mice lack Bassoon in dopaminergic terminals and display normal survival rates. a, Staining of striatal sections from B2D CTL and cKO mice with anti-Bassoon and anti-DAT antibodies shows the localization of Bassoon at dopaminergic synapses in B2D CTL and strongly reduced colocalization in B2D cKO mice (Overlay and Hi-Magn- high magnification panels). Scale bar in **a** is 25µm and high magnification is 5µm. **b,** Survival plot indicating comparable survival rates of B2D cKO (N=16) mice compared to CTL (N=17) mice.

3.2.2 Behavioral analysis of B2D cKO mice

Adult (3-4 months) and old (>1 year of age) male B2D cKO mice and CTL littermates were analyzed in different behavioral paradigms as described below.

3.2.2a B2D cKO mice displayed increased activity during the dark phase of the cycle in home cage activity monitoring

Activity of B2D cKO and CTL mice was monitored in the home cages of the mice. A significant of effect of phase or day time was observed with increased activity during the dark phase of the cycle (Figure 3.22a; $F_{(23,299)}=23.43$, $p<0.0001$, two-way repeated measures ANOVA). Interestingly, there was a significant effect of genotype effect ($F_{(1,13)}=5.00$, $p=0.0435$) and genotype x phase interaction ($F_{(23,299)}=2.10$, $p=0.0027$) observed. Phase-wise comparison of activity (%) revealed an increased activity of B2D cKO mice during dark phase of the cycle when compared to CTL mice (CTL: $35.22 \pm 5.872\%$, N=7; B2D cKO: $55.99 \pm 5.563\%$, N=8; $t_{(13)}=2.566$, $p=0.0235$, Student's t-test). No change in activity was observed during the light phase of the cycle (CTL: $17.46 \pm 3.680\%$; B2D cKO: $21.73 \pm 2.079\%$; $t_{(13)}=1.045$, $p=0.3150$).
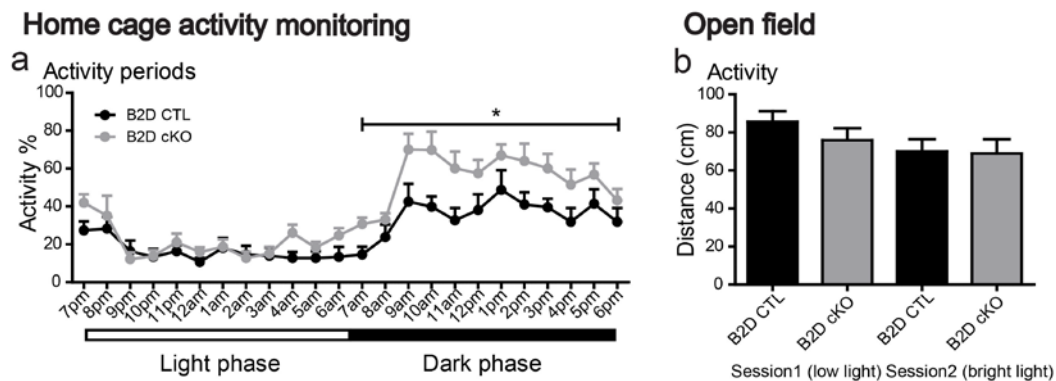

Figure 3.22. Increased home cage activity in B2D cKO mice during dark phase of cycle. a, B2D cKO (N=8) and CTL (N=7) mice were tested in their home cages to measures activity. Both groups display normal circadian activity with increased activity during dark phase. However, B2D cKO mice compared to CTL mice displayed increased active periods, which are represented as activity %, specifically during dark phase. **b,** No change in novelty induced activity (distance explored) was observed between B2E cKO (N=8) and CTL (N=7) mice in two sessions differing by light conditions. All values are mean ± SEM; *$P \leq 0.05$, two-way repeated measures ANOVA with Bonferroni post hoc test, Student's t-test.

Next, B2D cKO and CTL mice were tested in an open field arena to analyze novelty induced exploratory behavior. This was done during the dark phase of the cycle under low light and bright light test conditions. A significant effect of test session was

observed (Figure 3.22b; $F_{(1,13)}=10.82$, p=0.0059, two-way repeated measures ANOVA). However, no effect of genotype ($F_{(1,13)}=0.39$, p=0.5445) or genotype x test session interaction ($F_{(1,13)}=1.58$, p=0.2314) observed.

3.2.2b No change of anxiety in B2D cKO mice

Further, the time spent in center region of the open field was compared between B2D cKO and CTL mice as an indication for anxiety (Figure 3.23a). No effect of genotype ($F_{(1,13)}=1.72$, p=0.2126, two-way repeated measures ANOVA) or genotype x test session interaction ($F_{(1,13)}=0.58$, p=0.4615) could be observed.

In the elevated plus maze, B2D cKO mice showed similar preference like CTL mice for an open arm in terms of number of entries (Figure 3.23b; $t_{(12)}=0.6457$, p=0.5306, Student's t-test) or time (%) spent in an open arm (Figure 3.23c; $t_{(12)}=0.7687$, p=0.4569).
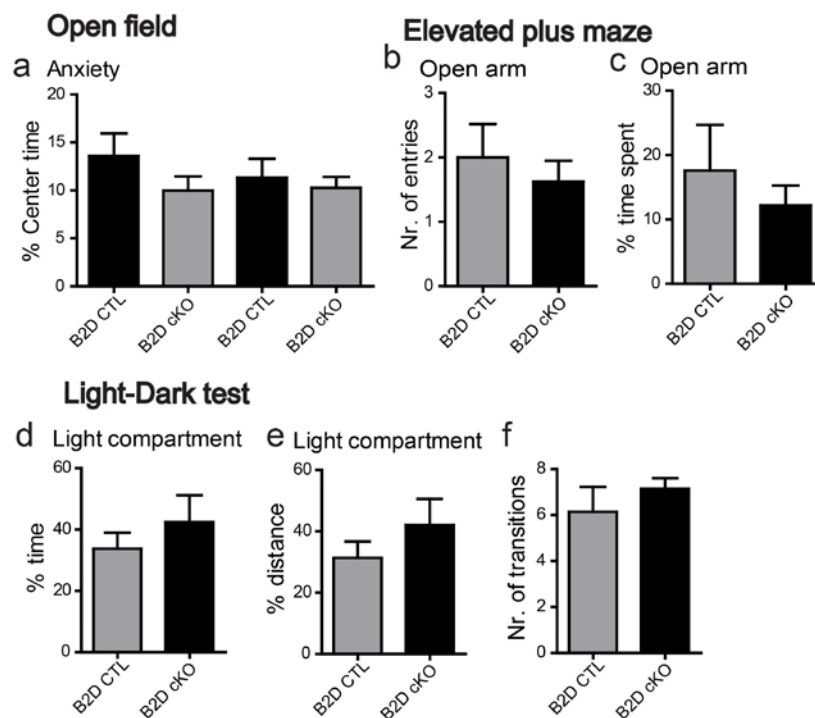

Figure 3.23. Unaltered anxiety levels in B2D cKO mice. **a,** No change in anxiety (time spent in center region of the open field arena) was observed between B2D cKO (N=8) and CTL (N=7) mice. **b,c,** In the elevated plus maze test, both the B2D cKO and CTL mice displayed comparable numbers of entries and percent of time in an open arm, indicating no change in anxiety. **d,e,** Anxiety levels were unchanged in B2D cKO mice as indicated by the percentage of time spent or distance covered in light chamber during the light-dark test (B2D cKO: N=8; CTL: N=7). **f,** Number of transitions between the light and dark compartments were also unchanged between genotypes. All values are mean ± SEM; two-way repeated measures ANOVA with Bonferroni post hoc test (**a**), Student's t-test (**b,c**) and Mann-Whitney U test (**d,e,f**).

In the light-dark test, B2D cKO mice spent similar time (%) in the illuminated compartment as CTL mice (Figure 3.23d; CTL: 33.70 ± 5.28%; B2D cKO: 42.46 ± 8.72%; U=23, p=0.6126, Mann-Whitney U test). The distance (%) travelled in illuminated compartment (Figure 3.23e; CTL: 31.36 ± 5.32%; B2D cKO: 42.03 ± 8.54%; U=20, p=0.3969) and the number of transitions between the compartments (Figure 3.23f; CTL: 6.143 ± 1.079; B2D cKO: 7.143 ± 0.459; U=16.50, p=0.3055) were also comparable between the genotypes.

3.2.2c B2D cKO mice display normal motor functions

B2D cKO and CTL mice were tested in an inverted grip strength test to measure the general muscular strength. Both groups displayed similar time periods hanging the inverted cage (Figure 3.24a. t(13)=0.7055, p=0.4929, Student's t-test).

Next, mice were tested for motor coordination and learning using an accelerating rotarod from 4-40 rpm for 5 minutes. Both B2D cKO and CTL mice displayed similar performances in terms of duration or latency to fall (Figure 3.24b; t(13)=0.1266, p=0.9012, Student's t-test) and the speed they sustained (Figure 3.24c; t(13)=0.0923, p=0.9278) on accelerating rotarod.
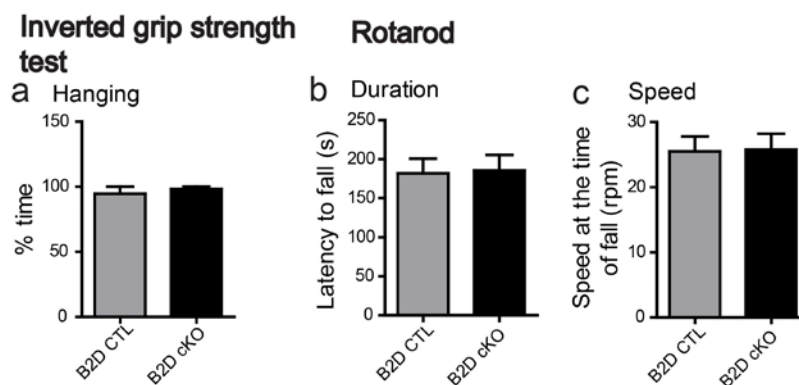

Figure 3.24. Normal motor abilities of B2D cKO mice. **a,** No change in % of time hanging to the inverted cage in the inverted grip strength test. Both the B2D cKO (N=8) and CTL (N=7) mice displayed the same time hanging. **b,c,** In the accelerating rotarod test, B2D cKO mice performed as good as CTL mice (B2D cKO: N=8; CTL: N=7) in terms of latency to fall and sustaining the speed. All values are mean ± SEM; Student's t-test.

3.2.2d B2D cKO mice display unaltered novel object recognition memory

In the novel object recognition task, both B2D cKO and CTL mice encounter two identical objects (O1 and O2) and spent comparable time with both objects during

the habituation phase (Figure 3.25a). There was no effect of object $(F_{(1,20)}=0.65$, $p=0.4302)$ or effect of genotype $(F_{(1,20)}=0.00$, $p=1.0000)$ or genotype x object interaction $(F_{(1,20)}=2.87$, $p=0.1060)$ observed. During the testing phase after 24 hrs, one of the objects was replaced with a novel object (O3) (Figure 3.25b). Here, no main effect of genotype $(F_{(1,20)}=0.00$, $p=1.0000)$ or genotype x object interaction $(F_{(1,20)}=0.12$, $p=0.7341)$ was observed. As expected, a significant effect of object $(F_{(1,20)}= 5.65$, $p=0.0276)$ was observed. However, both Bonferroni and Student's t-test, do not reveal any significance differences between novel vs. familiar objects either for B2D cKO or for CTL mice. Discrimination indices were comparable for both the groups (Figure 3.25c; $t(10)=0.2436$, $p=0.8125$, Student's t-test), indicating unchanged object recognition memory between the genotypes.
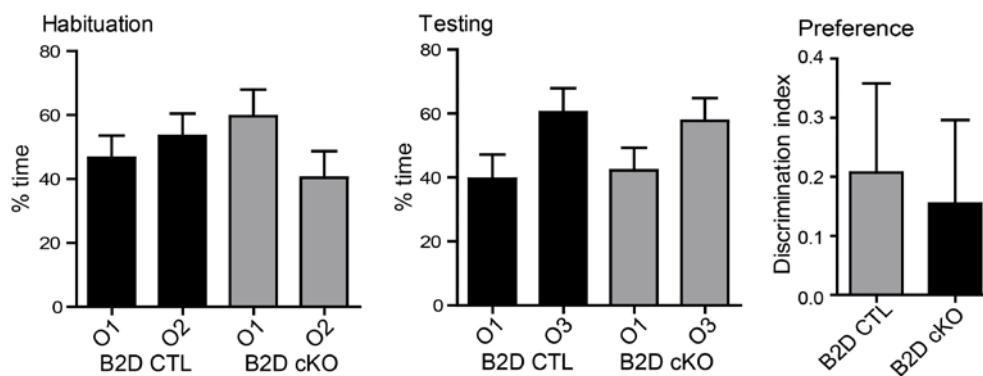

Figure 3.25. B2D cKO mice exhibit unaltered novel object recognition memory. **a,** No significant preference for any of the objects between the groups was detected during habituation (B2D cKO; N=8 and CTL; N=7). **b,** During testing both groups prefer the novel object over the familiar object. **c,** Comparable discrimination indices were calculated for both groups. All values are mean ± SEM; two-way ANOVA with Bonferroni post hoc test (**a,b**), Student's t-test (**c**).

3.2.2e B2D cKO mice display normal social recognition memory

Furthermore, mice were tested for social behavior using a 3-chambered social recognition and memory paradigm. In this social recognition and memory paradigm, during sociability period both the B2D cKO and CTL mice spent relatively more time with the social counterpart, rather than with a mouse-like object made from Lego blocks (Figure 3.26a,b). There was a significant preference for the social condition $(F_{(1,24)}=114.38$, $p<0.0001$, two-way ANOVA). However, no effect of genotype $(F_{(1,24)}=0.63$, $p=0.4345)$ or genotype x social condition $(F_{(1,24)}=0.02$, $p=0.8778)$

could be observed. During the social memory test, a novel stranger mouse was introduced replacing the mouse-like object (Figure 3.26c). Both genotypes prefer the novel stranger over the known mouse ($F_{(1,24)}=10.22$, $p=0.0039$). No main effect of genotype ($F_{(1,24)}=0.01$, $p=0.9157$) or genotype x social condition ($F_{(1,24)}=0.25$, $p=0.6203$) was observed. However, Bonferroni post hoc tests revealed a significant preference only for the B2D cKO mice towards the novel stranger ($p<0.05$), whereas CTL mice did not reach significance level. Analysis of discrimination indices revealed no genotype differences (Figure 3.26d; $t(12)=0.7873$, $p=0.4464$, Student's t-test).
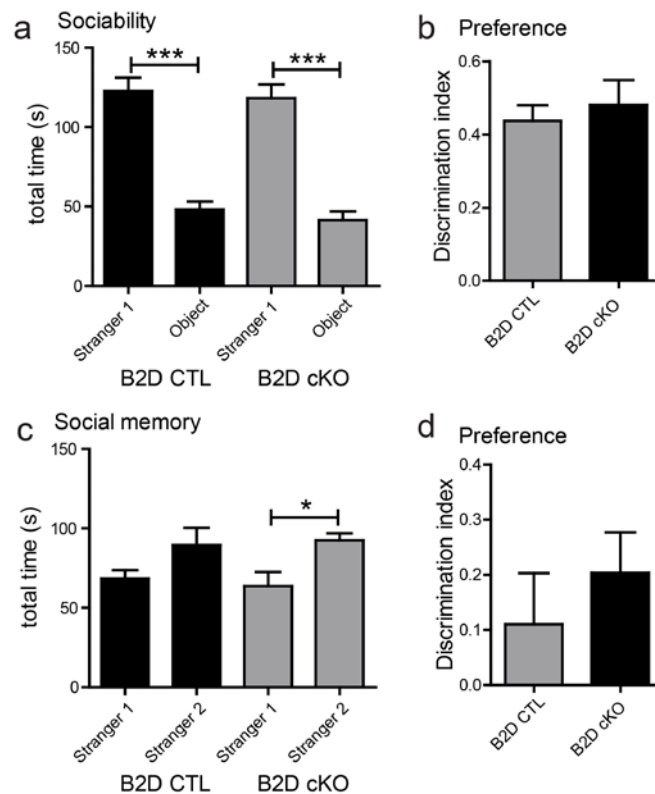

Figure 3.26. B2D cKO mice exhibit normal social recognition memory. **a,b,** Both B2D cKO (N=7) and CTL (N=7) mice prefer stranger #1 instead of a mouse like object. **c,d,** Both groups prefer stranger #2 over the familiar stranger #1. However, B2D cKO mice spent relatively more time with stranger #2. All values are mean ± SEM; *$P \leq 0.05$, ***$P \leq 0.001$ two-way ANOVA with Bonferroni post hoc test (**a,c**), Student's t-test (**b,d**).

3.2.2f B2D cKO mice do not exhibit depression-like behavior

When testing for depression-like behavior in B2D mice using the sucrose consumption test, both B2D cKO and CTL mice consume comparable amounts of sucrose solution (normalized to the water consumption) over the course of the test (Figure 3.27; $t(13)=1.655$, $p=0.1218$, Student's t-test).
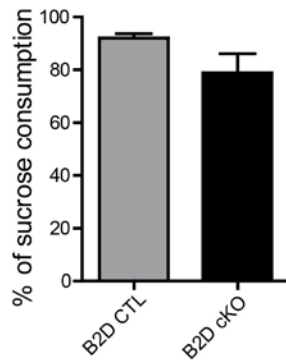
Figure 3.27. No depression-like behavior in B2D cKO mice. Both B2D cKO (N=8) and CTL (N=7) mice consumed sucrose solution in comparable amounts. All values are mean ± SEM; Student's t-test.

3.2.2g B2D cKO mice display unaltered fear memory

Furthermore, B2D cKO and CTL mice were tested in the combined contextual and cued fear conditioning paradigm. B2D cKO mice showed a slightly increased freezing towards the shock context. Baseline freezing levels were unchanged between the genotypes.
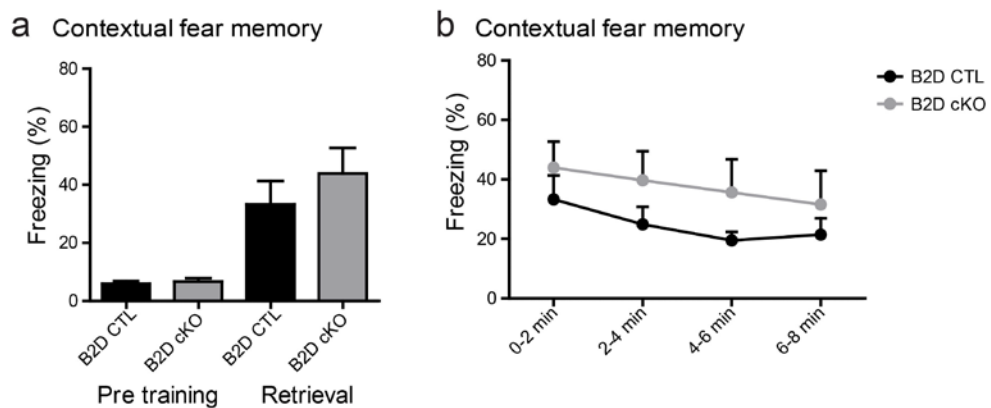

Figure 3.28. Unaltered contextual fear memory in B2D cKO mice. **a,** Both B2D cKO (N=8) and CTL mice (N=7) displayed comparable and profound freezing towards shock context compared to pre-training. **b,** Freezing (%) values throughout the contextual retrieval session, where both the B2D cKO and CTL mice displayed comparable fear response. All values are mean ± SEM; two-way repeated measures ANOVA with Bonferroni post hoc test.

The analysis revealed a significant increase in freezing towards shock context (Figure 3.28a) in both groups 24 hrs after training when compared to baseline freezing levels ($F_{(1,13)}=30.39$, $p<0.0001$, two-way repeated measures ANOVA). However, there was no effect of genotype ($F_{(1,13)}=0.84$, $p=0.3771$) or genotype x stimulus interaction ($F_{(1,13)}=0.71$, $p=0.4135$) observed. Freezing levels throughout the

contextual retrieval session indicate no genotype effect (Figure 3.28b; $F_{(1,13)}=1.38$, p=0.2612) or genotype x session duration interaction ($F_{(3,39)}=0.21$, p=0.8874).

24 hrs later, mice were tested in neutral context to assess cued memory (CS) (Figure 3.29a). Both groups exhibit similar and low freezing levels towards neutral tone (CS-) and profound freezing towards conditioned tone, CS+ (effect of test stimulus: $F_{(1,13)}=62.01$, p<0.0001, two-way repeated measures ANOVA). However, no evidence was found for a genotype effect ($F_{(1,13)}=0.00$, p=0.9657) or a genotype x test stimulus interaction ($F_{(1,13)}=0.00$, p=0.9587). Further analysis including inter stimulus intervals (ISIs) revealed comparable freezing levels between the genotypes (Figure 3.29b; genotype effect: $F_{(1,13)}=0.00$, p=0.9824).
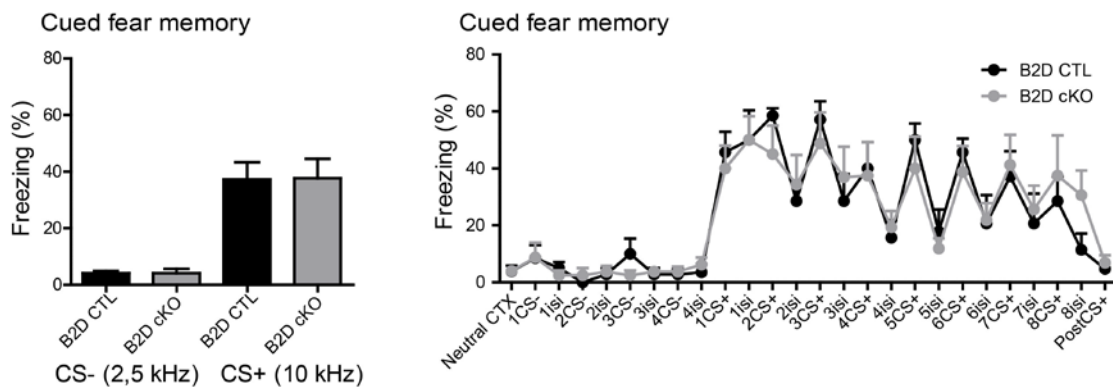
Figure 3.29. Unaltered cued fear memory in B2D cKO mice. **a,** Both B2D cKO (N=8) and CTL mice (N=7) displayed increased freezing levels towards CS+ compared to CS-. **b,** Freezing (%) values throughout the cued retrieval session, where both B2D cKO and CTL mice displayed comparable fear response. All values are mean ± SEM; two-way repeated measures ANOVA with Bonferroni post hoc test.

3.2.2h Unlike adult cKO mice, old B2D cKO mice do not show any behavioral alterations compared to control mice

In order to assess the role of Bassoon in age-dependent learning and memory functions, old (>1yr) B2D cKO and CTL littermates were tested in various behavioral paradigms. Surprisingly, the minor phenotypes observed in B2D adult cKO mice were not detectable anymore in the old mutant mice.

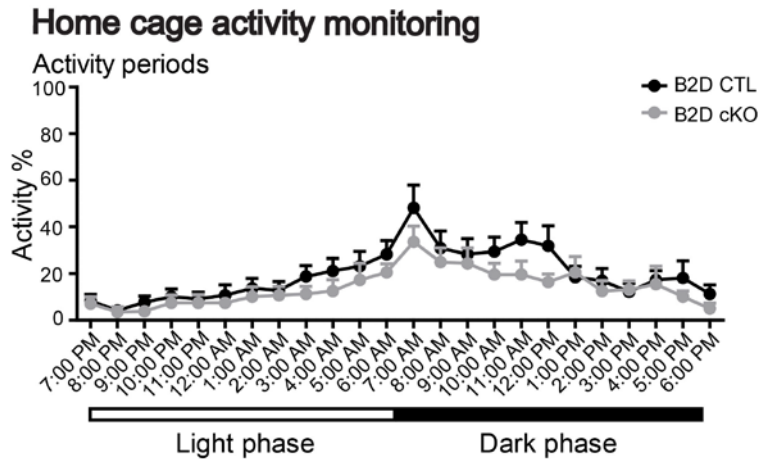## Home cage activity monitoring

Figure 3.30. Normal activity in home cage monitoring in old B2D cKO mice. Both B2D old cKO (N=7) and CTL littermates (N=7) displayed comparable and increased activity (%) during dark phase of the cycle. All values are mean ± SEM; two-way repeated measures ANOVA with Bonferroni post hoc test.

Adult B2D cKO mice displayed increased activity in their home cages during dark phase of the cycle (Figure 3.22a). In contrast, analysis of old B2D cKO and CTL mice revealed no genotype difference anymore (Figure 3.30). Both the groups displayed normal circadian activity with increased activity during dark phase ($F_{(23,276)}=14.14$, $p<0.0001$, two-way repeated measures ANOVA). But there was no effect of genotype ($F_{(1,12)}=0.99$, $p=0.3402$) or genotype x phase interaction ($F_{(23,276)}=1.01$, $p=0.4549$). Phase-wise (12 hrs of dark phase and 12 hrs of light phase) comparisons between the genotypes also revealed no major differences (dark phase: CTL: 24.80 ± 5.439%, N=7; B2D cKO: 17.96 ± 3.936%, N=7; light phase: CTL: 14.01 ± 3.342%; cKO: 9.940 ± 2.882%). Overall activity was reduced in both old B2D cKO and CTL mice when compared to adult B2D mice. This may be due to a normal ageing effect.

In social recognition and memory, during the sociability test, both old B2D cKO and CTL mice preferred social counterpart compared to mouse-like object (Figure 3.31a; $F_{(1,12)}=22.03$, $p=0.0005$, two-way repeated measures ANOVA). However, there was no effect of genotype ($F_{(1,12)}=0.66$, $p=0.4313$) or genotype x social condition ($F_{(1,12)}=0.27$, $p=0.6160$) observed. Discrimination indices do not show any significance for a genotype (Figure 3.31b; $t_{(12)}=0.3514$, $p=0.7314$, Student's t-test). During social memory, both old B2D cKO and CTL mice did not show clear preference for the novel stranger mouse (Figure 3.31c; $F_{(1,12)}=0.37$, $p=0.5554$). A main effect of genotype ($F_{(1,12)}=1.60$, $p=0.2301$) was also not observed. Discrimination indices did

not reveal any difference between the genotypes (Figure 3.31d; t(12)=0.3471, p=0.7345).
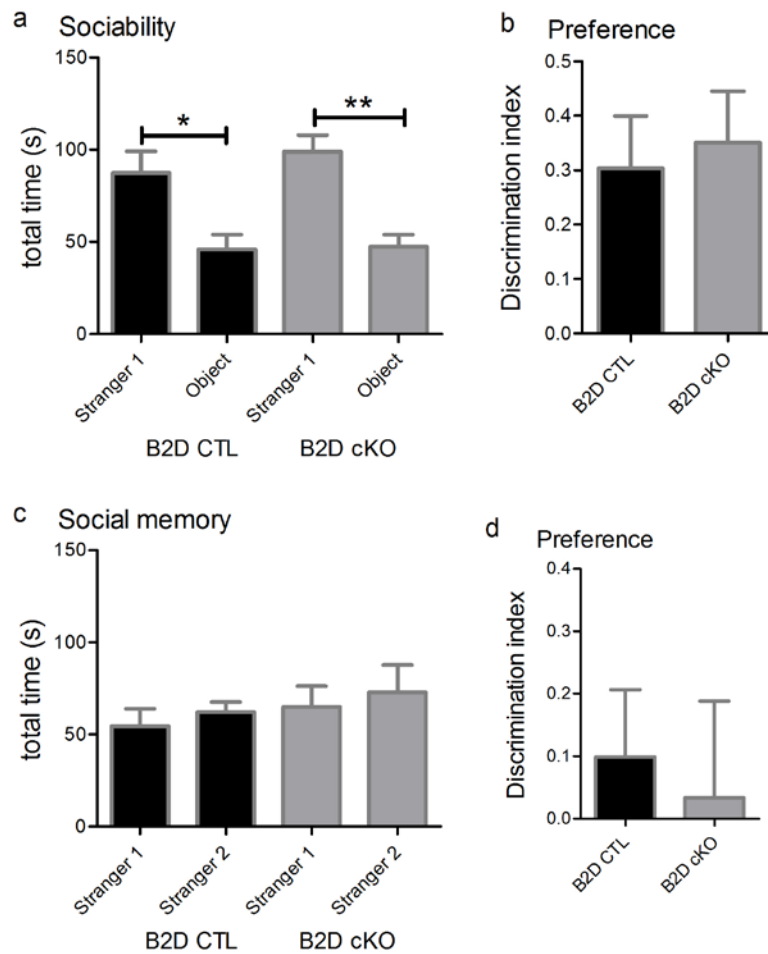
Figure 3.31. Normal social recognition and memory in old B2D cKO mice. **a,b,** Both the B2D cKO (N=7) and CTL mice (N=7) show preference for social counterpart, stranger #1 over the mouse-like object. **c,d,** No clear preference for the novel stranger mouse (#2) was observed by both groups. All values are mean ± SEM; two-way repeated measures ANOVA with Bonferroni post hoc test (**a,c**), Student's t-test (**b,d**).

3.2.2i Old B2D cKO mice do not show any alterations in other behavioral parameters assessed

Old B2D mice were further analyzed in other behavioral parameters, like activity and anxiety in an open field arena, anxiety in elevated plus maze and light-dark test, novel object recognition memory, motor strength and depression. All these behaviors were found unchanged between old B2D cKO and CTL mice.
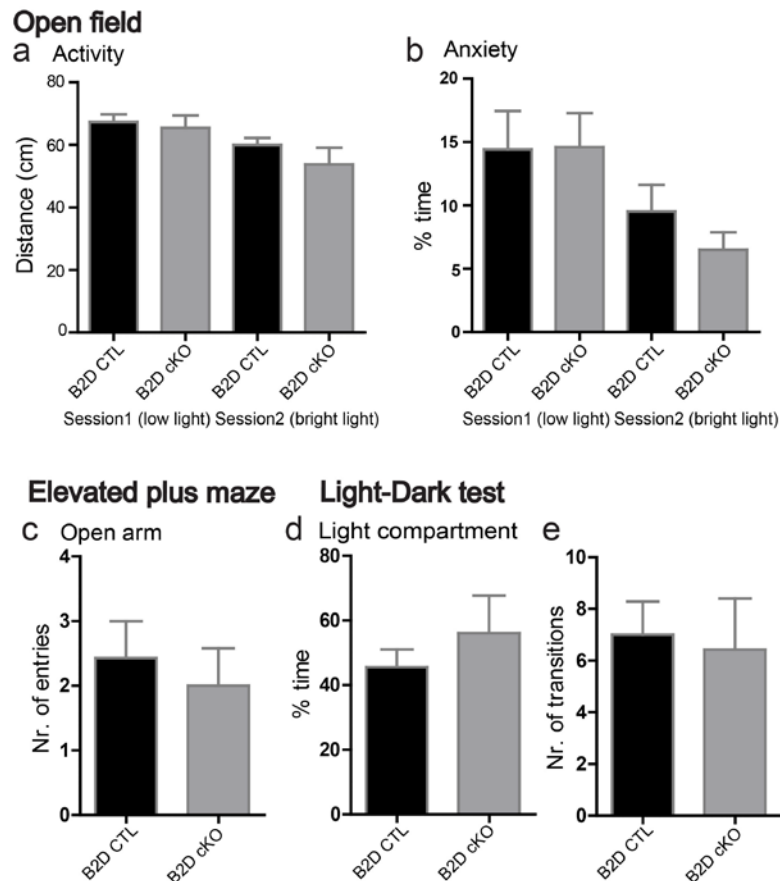
Figure 3.32. Unaltered activity and anxiety in old B2D cKO mice. **a,** Both old B2D cKO (N=7) and CTL mice (N=7) displayed no change in novelty induced activity in open field. **b,** No change in anxiety (time spent in the center region of the open field) was observed. **c,** In the elevated plus maze test, both old B2D cKO and CTL mice displayed comparable number of entries the open arm, indicating no change in anxiety. **d,** Anxiety levels were unchanged in old B2D cKO mice as indicated by the percentage of time spent in light chamber during the light-dark test (old B2D cKO: N=7; CTL: N=7). **e,** Number of transitions between the two compartments were also unchanged between genotypes. All values are mean ± SEM; two-way repeated measures ANOVA with Bonferroni post hoc test (**a,b**), Student's t-test (**c,d,e**).

Old B2D cKO and CTL mice were tested in an open field to analyze novelty induced exploratory and anxiety-like behaviors. This was done during the dark phase of the cycle under low light and bright light conditions. A significant effect of the test session was observed (Figure 3.32a; $F_{(1,12)}=14.37$, p=0.0026, two-way repeated measures ANOVA). However, there was no effect of genotype ($F_{(1,12)}=0.76$, p=0.4006) or genotype x test session interaction ($F_{(1,12)}=0.75$, p=0.4027) observed. When measured for time spent in the center of the open field arena, there was a significant effect of test session observed (Figure 3.32b; $F_{(1,12)}=22.19$, p=0.0005, two-way repeated measures ANOVA). However, no effect of genotype ($F_{(1,12)}=0.21$, p=0.6544) nor genotype x test session interaction ($F_{(1,12)}=1.36$, p=0.2669) was evident.

In elevated plus maze, old B2D cKO mice showed similar preferences like CTL mice for an open arm. Analyzed parameters, like number of entries to an open arm, did not differ between the genotypes (Figure 3.32c; t(12)=0.5276, p=0.6074, Student's t-test). In the light-dark test, old B2D cKO mice spent comparable time (%) in illuminated compartment as CTL mice (Figure 3.32 d; CTL: 45.54 ± 5.503%; B2D cKO: 56.13 ± 11.57%; t(12)=0.8264, p=0.4247, Student's t-test). The number of transitions (Figure 3.32 e; CTL: 7.000 ± 1.291; B2D cKO: 6.429 ± 1.974; t(12)=0.2422, p=0.8127) between the compartments were comparable between the genotypes.

Old B2D cKO and CTL mice were also tested in an inverted grip strength test in order to measure the general muscular strength. Both the groups displayed similar behavior in terms of percentage time hanging to the inverted cage (Figure 3.33 a; t(12)=0.7060, p=0.4937, Student's t-test). Next, mice were tested for motor coordination and learning using accelerating rotarod from 4-40 rpm for 5 minutes. Both B2D cKO and CTL mice displayed similar performance in terms of duration or latency to fall (Figure 3.33b; t(12)=0.4568, p=0.6560, Student's t-test) and the speed they sustained (Figure 3.33c; t(12)=0.4918, p=0.6317) on accelerating rotarod.
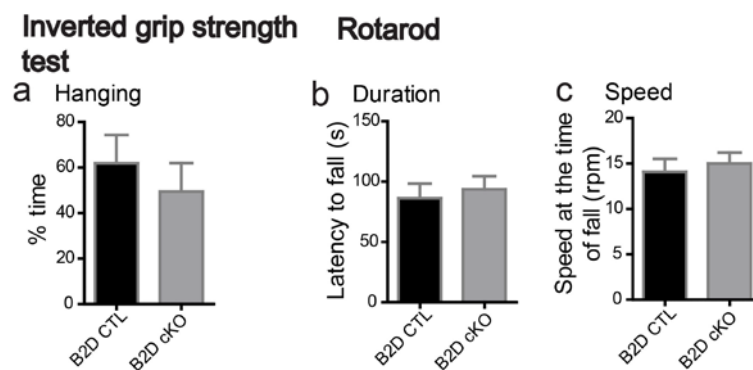
Figure 3.33. Normal motor functions in old B2D cKO mice. **a,** Both B2D cKO (N=7) and CTL mice (N=7) displayed comparable time hanging during inverted grip strength test. **b,c,** In the accelerating rotarod test, old B2D cKO mice performed comparable to CTL mice (B2D cKO: N=7; CTL: N=7) in terms of latency to fall and sustaining the increasing speed. All values are mean ± SEM; Student's t-test.

Furthermore, old B2D mice were tested for novel object recognition memory (Figure 3.34). In novel object recognition task, both B2D cKO and CTL mice encounter two identical objects (O1 and O2) and spent comparable time with both objects, during habituation phase (Figure 3.34a). There was no effect of object (F(1,22)=0.21, p=0.6477) or effect genotype (F(1,22)=0.00, p=1.0000) or genotype x object interaction (F(1,22)=0.00, p=0.9940, two-way ANOVA) to be observed. During testing phase after

24 hrs, one of the objects was replaced with a novel object (O3) (Figure 3.34b). Here, there was again no main effect of genotype (F(1,22)=-0.00, p=1.0000) or genotype x object interaction (F(1,22)=0.90, p=0. 3541) detected. No significant effect of object (F(1,22)= 0.92, p=0.3467) observed. Only old B2D CTL mice showed a slight preference for the novel object, but neither Bonferroni nor Student's t-test, does reveal any significant differences between novel vs. familiar objects. Discrimination indices were comparable for both the groups (Figure 3.34c; t(11)=0.6694, p=0.5170, Student's t-test), indicating unchanged object recognition memory between the genotypes.
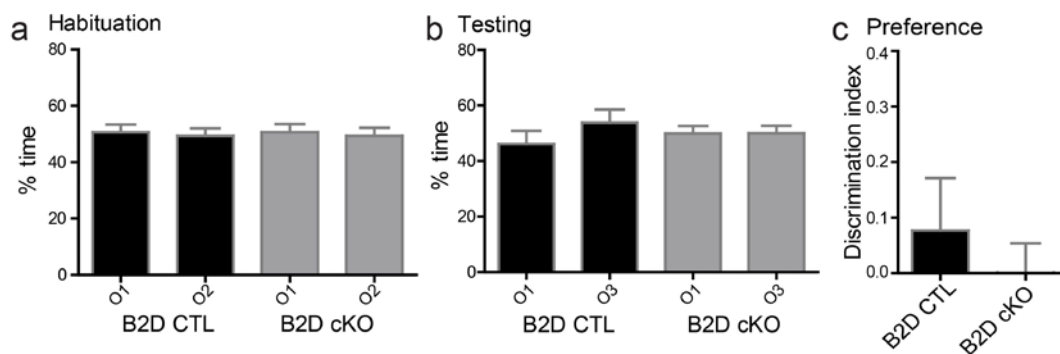

Figure 3.34. No change in novel object recognition memory in old B2D cKO mice. **a,** Both B2D cKO (N=6) and CTL mice (N=7) spent equal exploration times with both the objects during habituation phase. **b,** B2D old CTL mice spent slightly more time exploring the novel object, whereas old cKO mice did not show any preference for the novel object. **c,** Discrimination indices of B2D cKO and CTL mice displayed comparable values. All values are mean ± SEM; two-way ANOVA with Bonferroni post hoc test (**a,b**), Student's t-test (**c**).

Finally, old B2D mice were tested for depression like-behavior using sucrose consumption test. Both B2D cKO and CTL mice consumed comparable levels of sucrose solution (normalized to the water consumption) over the course of test duration (4 days) (Figure 3.35. t(12)=0.8468, p=0.4137, Student's t-test).
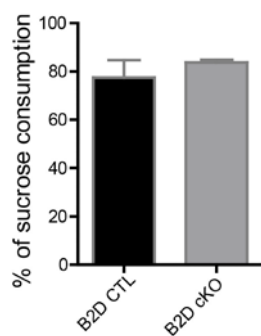

Figure 3.35. Unaltered depression-like behavior in old B2D cKO mice. Both B2D old cKO (N=7) and CTL (N=7) mice consumed the sucrose solution in a comparable manner. All values are mean ± SEM; Student's t-test.

3.2.3 Behavioral alterations were found in DAT$^{Cre/+}$ mice compared to control group

As it was already showed that insertion of Cre in 3´UTR region of the DAT gene results reduced expression of DAT protein in the striatum of homozygous and heterozygous mice compared to wild-type mice (Backman et al., 2006) and to control for genetic background, I tested DAT$^{+/+}$ (without Cre) and DAT$^{Cre/+}$ mice in the behavioral paradigms used for the characterization of B2D cKO mice. None of the analyzed parameters was different between the two driver line genotypes except for motor functions in rotarod paradigm (Figure 3.36).

In home cage activity analysis, a significant effect of the day time was observed in both groups with increased activity during the 12 hrs of dark phase of the cycle (Figure 3.36a; $F_{(23,345)}=31.55$, $p<0.0001$, two-way repeated measures ANOVA). No significant genotype effect ($F_{(1,15)}=0.68$, $p=0.4210$) and no interaction with day time ($F_{(23,345)}=1.33$, $p=0.1459$) was observed. Comparison of 12 hrs dark phase and 12 hrs light phase activity values, revealed no change between the groups. Dark phase (DAT$^{+/+}$: $44.19 \pm 3.40\%$; DAT$^{Cre/+}$: $49.63 \pm 4.98\%$, $t_{(15)}=0.9198$, $p=0.3722$, Student's t-test) and light phase (DAT$^{+/+}$: $14.53 \pm 2.08\%$; DAT$^{Cre/+}$: $15.91 \pm 2.16\%$, $t_{(15)}=0.4598$, $p=0.6523$).

Open field analysis of distance travelled during low light and bright light test sessions revealed significant effects of the test session (Figure 3.36b; $F_{(1,16)}=103.62$, $p<0.0001$, two-way repeated measures ANOVA) but no genotype effect ($F_{(1,16)}=0.01$, $p=0.9274$) or genotype x session interaction ($F_{(1,16)}=0.01$, $p=0.9358$). Furthermore, as a measure of anxiety, the time spent by both groups at the center of the open field arena was analyzed. There was a significant effect of the test session (Figure 3.36c; $F_{(1,16)}=19.01$, $p=0.0005$) as well as main effect of genotype ($F_{(1,16)}=4.55$, $p=0.0487$). However, Bonferroni posttest does not reveal any difference in significance. Statistical analysis using Student's t-test revealed a decrease of anxiety in DAT$^{Cre/+}$ mice during low light conditions, that was, however, not quite significant ($t_{(16)}=2.107$, $p=0.0512$). There was no genotype x session interaction ($F_{(1,16)}=0.36$, $p=0.5563$) observed.
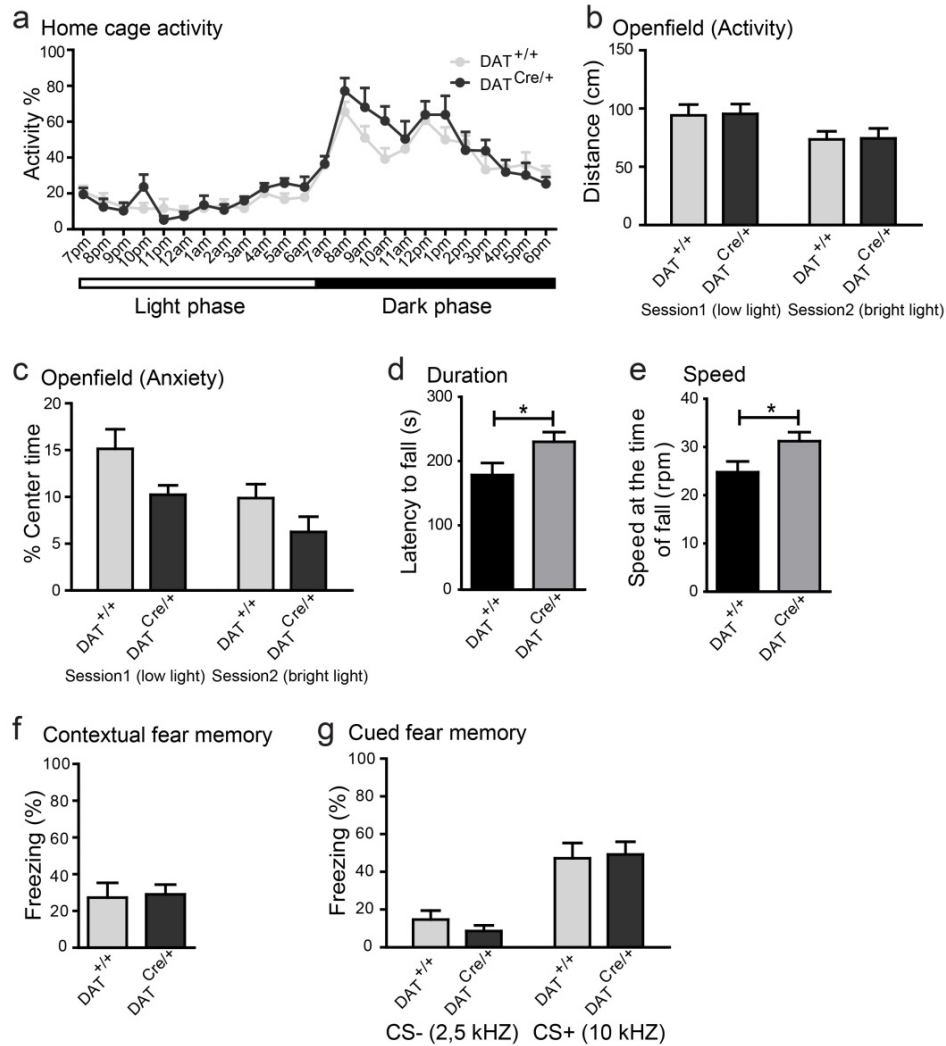
Figure 3.36. Altered motor functions in DAT$^{Cre/+}$ mice. a, Both DAT$^{+/+}$ (N=9) and DAT$^{Cre/+}$ (N=8) mice displayed comparable activity in the home cage. **b,c,** No significant change in the novelty induced activity or anxiety in both the groups (DAT$^{+/+}$: N=9, DAT$^{Cre/+}$: N=9). **d,e,** In the accelerating rotarod test, DAT$^{Cre/+}$ (N=9) mice performed better than the DAT$^{+/+}$ (N=9) mice in terms of latency to fall and sustaining the increasing speed. **f,** During contextual retrieval 24 hrs after training both the control (DAT$^{+/+}$: N=9, DAT$^{Cre/+}$: N=9) groups spent comparable time freezing in the shock context. **g,** Both groups displayed less and comparable freezing towards CS- and profound freezing towards the CS+. All values are mean ± SEM; two-way repeated measures ANOVA with Bonferroni post hoc test (**a,b,c,f,g**) Student's t-test (**d,e**).

Next, both groups were tested for motor functions using rotarod test. Accelerating rotarod from 4-40 rpm was used and mice were tested for 5 minutes. DAT$^{Cre/+}$ mice displayed superior performance in terms of duration or latency to fall (Figure 3.36d; t(16)=2.162, p=0.0461, Student's t-test) and the speed they sustained (Figure 3.36e; t(16)=2.209, p=0.0421) on accelerating rotarod.

Furthermore, mice were tested in combined contextual and cued fear conditioning paradigm. Both groups displayed comparable pre-training baseline

freezing levels and profound freezing levels in the shock context 24 hrs after training. This results in a significant session effect (Figure 3.36f; $F_{(1,16)}=25.72$, $p=0.0001$), but no genotype effect ($F_{(1,16)}=0.06$, $p=0.8129$) or genotype x session interaction ($F_{(1,16)}=0.01$, $p=0.9165$). 24 hrs after the contextual retrieval mice were tested in neutral context for auditory cued memory (Figure 3.36g). Both genotypes showed low freezing levels to the non-conditioned auditory test stimulus (CS-), but strong freezing to the CS+ resulting in significant effect of test stimulus ($F_{(1,16)}=41.39$, $p<0.0001$). There was again no effect of genotype ($F_{(1,16)}=0.11$, $p=0.7445$) or genotype x test stimulus interaction ($F_{(1,16)}=0.50$, $p=0.4883$) observed. Altogether, these results indicate that Cre insertion in 3´UTR region of DAT gene seems to influence motor function.

3.2.4 Summary of behavioral analysis

Table 3.1. List of different behavioral parameters analyzed in both B2E and B2D mice using different paradigms.

Behavioral domain	Test	Behavior of B2E cKO mice as compared to WT mice	Behavior of B2D cKO mice as compared to CTL mice
Activity and anxiety	Home cage activity	hyperactive	hyperactive only during dark phase
	Open field	no difference	no difference
	Light-dark test	no difference	no difference
Novelty recognition and Spatial learning	Novel object recognition	no difference	no difference
	Novel object location	no difference	not tested
	Pattern separation	improved performance	not tested
	Morris water maze	no difference	not tested
	Social recognition and memory	not tested	no difference

Depression	Sucrose drinking test	not tested	no difference
Motor coordination and strength	Inverted grip strength test	not tested	no difference
	Rotarod	not tested	no difference
Fear learning	Contextual fear memory	enhanced	no difference
	Cue fear memory	no difference	no difference
	Active avoidance	no difference	not tested

4 Discussion

In this study, two different conditional knockout mice for the *Bsn* gene were generated, one lacking Bassoon in excitatory forebrain synapses (B2E cKO mice) and the other lacking Bassoon in boutons releasing dopamine (B2D cKO mice) to genetically dissect Bassoon functions at different synapses and to investigate its role in behavioral and network functions. B2E cKO mice were hyperactive in their home cages and showed an increased performance in hippocampus-dependent spatial and contextual learning tasks associated with a phenotype of increased neurogenesis and reduced postnatal granule cell maturation in the dentate gyrus. In addition, in B2E cKO mice preservation of juvenile neuronal excitability at the synapse between the medial perforant path and dentate granule cells was observed. Surprisingly, B2D cKO mice displayed only minor phenotypes, such as hyperactive behavior, which was limited to the dark phase of the circadian cycle. In all the remaining tests conducted, B2D cKO mice performed like CTL mice. Moreover, the minor hyperactive behavior observed at adult stage (8-12 weeks) was not observed anymore in the old (>1 year) B2D cKO mice. Thus, behavioral analyses of both the conditional mutants argue for a very specific role of Bassoon at the glutamatergic synapses. Together, as a central organizer of the CAZ at presynaptic site, Bassoon thus seems to control specific forms of memory formation and specifically to be essential for the structural and functional maturation of the DG in the adult central nervous system.

4.1 Both cKO mice survive normally without sensory impairments

Constitutive *Bsn*$^{\Delta Ex4/5}$ mice lacking the central exons 4 and 5 have been generated previously, but the analysis of Bassoon functions in the control of behavior has been hindered by the occurrence of epileptic seizures and sensory deficits like vision and hearing problems in these animals (Altrock et al., 2003; Dick et al., 2003; Khimich et al., 2005). With the generation of B2E and B2D cKO mice, it is possible to overcome these limitations. Both these cKO mice, which apparently did not show any seizures, survived well (Figure 3.3 and 3.21b) without any difference from their respective WT or CTL (in case of B2D mice) littermates and performed equally or even superior to their WT or CTL littermates in several visual and auditory tasks. Considering the role of Bassoon in regulated neurotransmitter release (Altrock et al., 2003; Gundelfinger et al., 2016) and the importance of the GABAergic system in

epilepsy (Treiman, 2001), this might explain the lack of epileptic seizures in both the B2E and B2D cKO mice. It should be noted that an assessment of mild seizures and/or interictal spiking by EEG measurements still needs to be done.

4.2 Bassoon role in the hippocampus-dependent learning and memory

The behavioral analysis of B2E cKO mice exhibited a phenotype that is similar to an altered function of hippocampus and its sub region, DG. The B2E cKO mice showed an enhanced contextual fear memory with unaltered auditory-cued fear conditioning in a combined context/cue fear conditioning or background contextual fear conditioning paradigm. This suggests a change of hippocampus-dependent fear memory processing, as previously shown that hippocampus is required for contextual fear processing whereas amygdala is important for cue-dependent fear memory processing (Maren et al., 2013). More specifically, B2E cKO mice displayed alterations in background contextual fear conditioning, which mainly depends on dorsal hippocampal function (Phillips and LeDoux, 1994). In addition, no change in shock sensitivity was observed in these animals. Furthermore, analysis of $Emx1^{+/+}$ and $Emx1^{Cre/+}$ control mice in fear conditioning and other paradigms revealed that Cre insertion under Emx1 promoter itself does not cause any behavioral changes, indeed suggests an effect of Bassoon loss in excitatory synapses itself is responsible for contextual fear conditioning alterations in B2E cKO mice. Other behavioral parameters such as exploratory or anxiety-related behavior in an open field or responsive learning towards a shock in an active avoidance task did not differ between the B2E cKO and their WT littermates. However, these mice displayed hyperactive behavior in their home cages throughout the circadian cycle, i.e., during both light and dark phases. On the other hand, subjecting B2E cKO mice to additional hippocampus-dependent learning tasks such as the Morris Water maze, no major differences were found suggesting an unaltered spatial learning or re-learning capabilities. Considering the probe trails employed here, even the spatial memory does not seem to be changed in B2E cKO mice.

Further, a novel object location task was employed to assess intrinsically motivated spatial learning. Considering the observations in the tasks mentioned above this task was designed rather difficult for WT mice by changing object location by 90 degrees from the original position. Testing of memory was done after 24 hours. In fact, B2E cKO mice showed a stronger preference for the novel object location in this

paradigm compared to WT mice. In addition, B2E cKO mice also displayed a superior performance in a spatial pattern separation task, where again a very difficult paradigm with relatively little changes in the distance between the targeted objects was employed. WT mice indeed displayed avoidance rather than approach behavior. The very similar avoidance behavior was previously observed when the control animals failed to learn this task (Bekinschtein et al., 2013). B2E cKO mice, on the contrary, showed a strong selective approach indicative of an enhancement in this DG-dependent learning paradigm (Gilbert et al., 1998; Leutgeb et al., 2007) and/or might be due to an effect of BDNF regulation (Bekinschtein et al., 2013). So, the behavioral analysis with B2E cKO mice argues for the role of Bassoon in mediating specific forms of memory related to hippocampal glutamatergic system. Thus, it led to further investigation on potential changes in hippocampal physiology and anatomy, using B2E cKO mice.

The physiological and neuroanatomical observations in this study could explain the behavioral changes being assessed in B2E cKO mice. In fact, in hippocampal slice preparations, a higher baseline excitability and increased fEPSP to FV amplitude ratio at MPP-DG synapses was observed. These physiological changes might contribute to increase in granule cell responsiveness to stimulation during the encoding and/or retrieval of contextual and pattern separation tasks (Saxe et al., 2006; Deng et al., 2009). This is also in agreement with a role of the DG in contextual fear memory processing (Lee and Kesner, 2004; Hernandez-Rabaza et al., 2008; Liu et al., 2012; Kheirbek et al., 2013). An increased excitability at SC-CA1 synapses was also observed in B2E cKO mice (Appendix figure 5.1a,b). However, these data contrast the previous findings with Bassoon constitutive KO, $Bsn^{\Delta Ex4/5}$ mice. There, a decreased excitability and reduced LTP at CA1 synapses in $Bsn^{\Delta Ex4/5}$ mice (Altrock et al., 2003; Sgobio et al., 2010) was observed. Previous knowledge about Bassoon functions at CAZ reveals its role in regulated neurotransmitter release (Altrock et al., 2003; Gundelfinger et al., 2016). Considering this function together with the GABAergic systems role in epilepsy (Treiman, 2001), it is suggestive that the absence of Bassoon from inhibitory synapses during network development and/or epileptic seizure activity may contribute to impaired long-term plasticity in constitutive $Bsn^{\Delta Ex4/5}$ mice. $Bsn^{\Delta Ex4/5}$ mice displayed deficits in active avoidance learning paradigm (Ghiglieri et al., 2010), which is not the case in B2E cKO mice in the current study. There may be two possibilities to explain this. One possibility is that absence of epilepsy or traces of seizure activity in B2E cKO

mice along with the mentioned sensory impairments, i.e., visual and auditory impairments. The other possibility is a disturbance of GABAergic interneuron system, e.g., in the striatum of $Bsn^{\Delta Ex4/5}$ mice. This should be still intact in B2E cKO mice due to the selective ablation of *Bsn* gene from excitatory neurons of forebrain cortical areas. To understand these differences, further assessment of Bassoon function in the GABAergic system needs to be investigated.

Involvement of DG and different populations of GCs within DG in learning and memory has been widely described earlier. The structural integrity of DG is shown to be essential for contextual representations, spatial pattern separation and facilitating the encoding of spatial information (Hernandez-Rabaza et al., 2008) (Kesner, 2007; Kesner et al., 2015). Previous studies characterizing young and immature GCs have shown that high excitability as well as expanded dendrites with reduced spine density, are the typical properties of these cells (Schmidt-Hieber et al., 2004; Ge et al., 2007; Spampanato et al., 2012). In fact, using Golgi impregnation in this study, I observed an increase in dendrite branching (2-fold increase) and an accompanying decrease in spine density (approx. 2-fold reduction) in the B2E cKO mice. These changes might reflect a compensatory homeostatic response to the increased cellular excitability. These alterations are due to lack of Bassoon, which in WT mice is detectable together with Piccolo during synaptogenesis at the presynaptic active zone (Zhai et al., 2001; Gundelfinger et al., 2016). However these changes occur in a dendritic region more than 60 µm away from the soma. It might be due to alterations in the relative weight of incoming inputs to the DG, i.e. perforant path vs. commissural path. It was previously shown that the processing of information regarding object context or location involves the inputs coming from MPP and information regarding the objects itself relay on the inputs from the lateral perforant path (Eichenbaum et al., 2007; Kesner, 2007). In addition, the two populations of GCs, i.e., mature and immature GCs, mediate different aspects of learning and memory. Mature GCs of DG together with CA3 are more involved in pattern completion tasks, whereas immature GCs are mainly involved in mediating the pattern separation processes and forming long-term spatial memories (Deng et al., 2009; Nakashiba et al., 2012). They are critical components of contextual memory engrams (Liu et al., 2012; Ramirez et al., 2013) and the size of activated DG granule cells ensembles correlating with context memory strength (Stefanelli et al., 2016). All these data are in favorable agreement with the findings of this study.

Neurogenesis, on the other hand, is shown to have similar implications in learning and memory. This is a unique form of neural circuit plasticity occurring at DG and associated with improved cognitive functions (Aimone et al., 2006; Sahay et al., 2011). Augmented adult neurogenesis in mice results in improved pattern separation (Sahay et al., 2011) and ablation of neurogenesis has been reported to impair contextual fear conditioning and pattern separation in mice (Saxe et al., 2006; Clelland et al., 2009).

4.3 Bassoon involvement in maturation of hippocampal synapses and neurogenesis

Based on the physiological data, it is conceivable that the increased excitability of the adult DG may reflect an immature state of the perforant path - to - dentate gyrus circuit in B2E cKO mice. To address this question, I have used antibodies against maturation markers such as calbindin, calretinin, and doublecortin and performed immunohistochemical analyses in DG granule cell layer, which showed altered expression of these markers in B2E cKO mice compared to WT mice. It was shown earlier that, reduced calbindin staining intensity in granule cells had been associated with increased excitability of DG (Magloczky et al., 1997) and a previous study already demonstrated a reduced calbindin staining intensity in $Bsn^{\Delta Ex4/5}$ mice (Dieni et al., 2015). Here, I could show that the calbindin staining was also reduced in B2E cKO mice. Accordingly, this phenotype seems to be a consequence of Bsn gene ablation independently of epileptiform activity. I also found a profound increase in the density of immature neurons labeled by calretinin and doublecortin in the granule cell layer of B2E cKO mice, which indicates an increased number of DG granule cells in an early postmitotic differentiation stage (von Bohlen und Halbach, 2007). Furthermore, to confirm this hypothesis, I have analyzed the neurogenesis rate using Ki67, which marks the actively proliferating cells. This revealed an increased neurogenesis and could explain the increase of immature neurons in B2E cKO mice – potentially accompanied by a delay in maturation. In fact, increased neurogenesis has also been observed in $Bsn^{\Delta Ex4/5}$ mice (Heyden et al., 2011).

Bassoon is expressed in postmigratory neurons and supports the assembly of presynaptic boutons from preassembled Piccolo-Bassoon transport vesicles (PTVs) (Zhai et al., 2001; Shapira et al., 2003; Dresbach et al., 2006). By interacting with dynein light chain DLC-1, Bassoon serves as one cargo adaptor to microtubules. The disturbance of these interactions between Bassoon and DLC-1 attenuates transport of

PTVs in young axons (Fejtova et al., 2009). In the wild-type brain, Bassoon transcripts appear in late embryonic development and highest levels are seen at postnatal day 21, particularly in the pre-granule cell layer and differentiating granule cells of the DG (Zhai et al., 2000). Given the expression onset of Emx1 at embryonic day 10.5 (Gorski et al., 2002), it can be expected that Bassoon is not expressed in excitatory synapses of B2E cKO mice at any stage of development. Similarly, DAT expression starts at embryonic day 14 (Backman et al., 2006), which also suggests the lack of Bassoon in nigrostriatal DA neurons during the development. Thus, it is conceivable that Bassoon knockout may lead to a shortage of material for synapse assembly and maturation of different synapses in the brain. Recently, it was reported that Bassoon interacts with the autophagosome factor Atg5 and this interaction seems to be important for synaptic autophagy (Okerlund et al., 2017). Autophagy is a cellular digestion process that regulates protein homeostasis in the different organs of the body. In the nervous system, autophagy occurs at two distinct sites, Soma, and synaptic sites. Recent studies have shown that autophagy plays a critical role in synaptic development and homeostasis (Vijayan and Verstreken, 2017). Autophagic mechanisms involving Atgs and lysosomal activity are shown to be critical for synaptic (Tang et al., 2014) and axonal pruning during development (Song et al., 2008). The lack of decrease in FV amplitude and DG excitability during the postnatal development of B2E cKO mice may well result from a disturbance of these functions. Indeed, it was shown earlier that in $Bsn^{\Delta Ex4/5}$ mice, the rate of apoptosis is reduced at the adult stage (Heyden et al., 2011). This suggests a potential role of Bassoon in postnatal refinement processes at the hippocampus, which is known to be critical phenomena required for normal development of nervous system. Indeed, previous studies have shown behaviorally relevant implications of disturbance in axonal pruning, specifically of the infrapyramidal bundle (IPB), in the hippocampus (Pleskacheva et al., 2000; Faulkner et al., 2007). However, no studies have been reported so far regarding the disturbance of axonal pruning in MPP-DG with respect to cognitive alterations.

Another scenario to be considered is the developmental gene expression program, which is affected in Bassoon-deficient neurons. Bassoon and Piccolo can bind the chromatin-modifying transcriptional co-repressor CtBP1. This is a well-known neurodevelopmental regulator (Chinnadurai, 2007), both Bassoon and Piccolo and controls the synapto-nuclear shuttling of this repressor (Ivanova et al., 2015). Lack of

Bassoon can shift the equilibrium towards a higher CtBP1 concentration in the nucleus. This might repress the transcriptional programs during neuronal development required for controlling axonal excitability. Nevertheless, the majority of DG granule cells express calbindin rather than calretinin or doublecortin, suggesting that lack of Bassoon may delay but not completely block the maturation of these cells *in vivo*. In addition to such cell-intrinsic effects an increased neurogenesis may explain the observed maturation effect. In fact, the observed FV increment in the MPP-DG, is an indicative of enhanced axonal excitability. However, increased FV at SC-CA1 transmission (Appendix figure 5.1c,d) was balanced mostly due to synaptic adaptation. This is not the scenario at DG, may be due to the existence of neurogenic niche and activity induced enhancement of adult neurogenesis. Moreover, stimulation of the entorhinal cortex has previously been shown to stimulate hippocampal neurogenesis (Stone et al., 2011). This supports the current finding with respect to enhanced axonal excitability.

4.4 Bassoon involvement in BDNF regulation

Though it is conceivable that improved learning and memory changes occurring in B2E cKO mice are mainly mediated through the maturation disturbance in DG granule cells, an alternative or synergistic mechanism may involve the neurotrophic factor-BDNF. It was shown that $Bsn^{\Delta Ex4/5}$ mice display an increased brain size with unbalanced neurogenesis that correlates with elevated BDNF levels in the hippocampus and other forebrain regions (Heyden et al., 2011). A recent study has shown that accumulation of BDNF containing dense core vesicles are more close to the presynaptic membrane in $Bsn^{\Delta Ex4/5}$ mice (Dieni et al., 2015). Another study has reported that Bassoon and Piccolo can recruit CtBP1 to presynaptic sites upon increased synaptic activity (Ivanova et al., 2015). CtBP1, in turn, regulates the transcription of activity-dependent genes including BDNF (Garriga-Canut et al., 2006). Based on the hyperactive behavior, hyper excitable DG and the presence of Piccolo still at the presynaptic site in these cKO mice, it can be possible that majority of the CtBP1 proportion is still present at the presynaptic site, despite the lack of Bassoon. Indeed, electrophysiological rescue experiment measuring excitability at MPP-DG path using K252a (a blocker of Trk-B receptors) revealed a normalization of excitability in B2E cKO mice resulting in no change in the fEPSP between the B2E cKO and WT mice (Appendix figure 5.2). In addition, preliminary CtBP1 stainings and respective nuclear quantifications from GCs of B2E cKO DG shows a decrease of nuclear CtBP1 staining

intensity (data not shown), which might lead to the synthesis of more BDNF in cKO mice. Together with the previous studies on $Bsn^{\Delta Ex4/5}$ mice and these preliminary results suggest that Bassoon might play a potential role either in synthesis or trafficking of BDNF, making it available in excess at the presynaptic site, which might be contributing to the altered phenotype observed in B2E cKO mice. Previously, it was shown that activity-dependent release of BDNF is known to play an important role in learning and memory (Yamada and Nabeshima, 2003). BDNF interacts with immature GCs and affects the DG mediated pattern separation (Bekinschtein et al., 2013; Bekinschtein et al., 2014). The critical role of BDNF in contextual fear memories has been previously shown (Liu et al., 2004). Furthermore, an effect of BDNF on dendritic complexity and length (Horch and Katz, 2002; Tolwani et al., 2002) has also been reported.

4.5 Lack of Bassoon in dopaminergic synapses reveals no change in DA mediated learning and memory

The analysis of B2D cKO mice in different behavioral paradigms revealed a minor/no phenotype. B2D cKO mice displayed hyperactive behavior in their home cages, which was limited only to the dark phase of the circadian cycle. During light phase, which is the less active phase for nocturnal rodents, B2D cKO and respective CTL mice displayed comparable activity. Moreover, aged B2D cKO mice do not show this hyperactive behavior. In social recognition and memory task, adult B2D mice (both cKO and CTL) performed better during social memory, in differentiating novel and familiar stranger mouse. However, no significant effect was found in discrimination index between the genotypes. Aged B2D mice lack this ability in discriminating novel vs. familiar mice, what might be a general decline in cognitive abilities due to aging. Adult B2D cKO mice also displayed somewhat higher freezing levels during background contextual retrieval session, which does not reach the significance level at any time point, unlike in B2E cKO mice. From the previous findings, it is known that dopaminergic (DAergic) neurons from substantia nigra and ventral tegmental area (VTA) also project to different cortical areas including prefrontal, cingulate and entorhinal cortex (Loughlin and Fallon, 1984) and hippocampus (Gasbarri et al., 1997). DA receptor (D1/D5)-mediated stimulation of local protein synthesis can enhance the glutamatergic receptor (GluR1) expression and synaptic transmission in hippocampal

neurons (Smith et al., 2005). Studies have also been shown the connection between DAergic and glutamatergic systems in the brain circuits involved in learning and memory (Jay, 2003; Smith et al., 2005). In this context, the non-significant, but increased fear response towards the shock context in B2D cKO mice, which is similar to the much stronger effect in B2E cKO mice, might be interesting. Lack of Bassoon at both DAergic and glutamatergic synapses could have a similar effect. This argues for the role of Bassoon in a specific form of memory. Other parameters like novelty-induced activity and anxiety in an open field do not differ between the genotypes, irrespective of age. In novel object recognition memory, both adult and old B2D cKO mice performed on par with the respective CTL mice. Analysis of motor coordination and strength revealed no changes between the genotypes. However, the difference between the $DAT^{+/+}$ and $DAT^{Cre/+}$ control mice in accelerating rotarod test indicate no role for Bassoon, but rather the importance of DAT itself in coordinating the motor functions. Further analysis looking at the depression-like behavior in B2D mice, both adult and old B2D cKO mice display no change with respect to their CTL mice. Together these data suggests that lack of Bassoon alone in DAergic synapses, do not affect the DA mediated learning and memory.

4.6 Concluding remarks

In summary, data presented here document the importance of Bassoon in the maturation of the DG and in DG-dependent contextual and spatial learning. The superior performance of B2E cKO mice in contextual fear conditioning and pattern separation tasks seems to be related to an increased excitability of the DG granule cells. Disturbed maturation of the DG has been identified as a critical process in psychiatric disorders like schizophrenia and depression (Hagihara et al., 2013) Further, preliminary data on auditory cortex-dependent frequency-modulated tone discrimination learning in a shuttle box (Tischmeyer, Annamneedi et al., unpublished) point to an improved learning rate of B2E cKO mice when compared to WT littermates during initial training sessions. In this paradigm, B2D cKO mice show increased procedural learning compared to CTL mice. All together, these results raise the possibility of a more general role of Bassoon in network maturation which affects the specific forms of learning and memory.

5 Abbreviations

ANOVA	analysis of variance
Atg	autophagy-related
AZ	active zone
B2E cKO	conditional knockout of *Bsn* in forebrain excitatory neurons
B2D cKO	conditional knockout of *Bsn* in dopaminergic neurons
BDNF	brain derived neurotrophic factor
BMP	bone morphogenic protein
BSA	bovine serum albumin
CA1	cornu ammonis area 1
CA3	cornu ammonis area 3
CAST	cytomatrix at the active zone-associated structural protein
CAZ	cytomatrix at the active zone
CC	coiled coil
cKO	conditional knockout
CS	conditional stimulus
CSF	cerebro spinal fluid
CtBP1	c-terminal binging protein1
CTL	control
DA	dopamine
DAPI	4',6-diamidino-2-phenylindole
DAT	dopamine transporter
dB	decibel
DCX	doublecortin
DG	dentate gyrus
DIV	days *in vitro*
DLCs	dynein light chains
DNA	deoxy ribose nucleic acid

dNTP	deoxyribonucleotide triphosphate
EC	entorhinal cortex
Emx1	empty spiracle homeobox-1
EPM	elevated plus maze
EPSC	excitatory postsynaptic current
fEPSP	field excitatory postsynaptic potential
FRT	flippase recognition target
FS	fast spiking
GABA	gamma-aminobutyric acid
GCs	granule cells
ID	integrated density
IHC	immunohistochemistry
ISI	inter stimulus interval
kHz	kilo-hertz
LTP	long-term potentiation
mA	milliampere
MF	mossy fiber
MFB	mossy fiber bouton
MPP	medial perforant path
MS	medium spiny
NeoR	neomycin resistance
NGS	normal goat serum
PBS	phosphate buffered saline
PFA	paraformaldehyde
pH	potential hydrogen
PP	perforant path
PSD	post synaptic density
PCR	polymerase chain reaction
PTVs	piccolo-bassoon transport vesicles

PuroR	puromycin resistance
PV	parvalbumin
PVDF	polyvinylidene difluoride
RBP	RIM-binding protein
RIM	Rab3-interacting molecule
RRP	readily releasable pool
Rpm	rotations per minute
SGZ	subgranular zone
shRNA	short hairpin ribonucleic acid
SNARE	soluble N-ethylmaleimide-sensitive factor attachment protein receptor
SVs	synaptic vesicles
TA	tris-acetate
Trk	tropomyosin receptor kinase
US	unconditional stimulus
UTR	untranslated region
VGAT	vesicular GABA transporter
VGLUT 1	vesicular glutamate transporter 1
WB	western blotting
WT	wild-type
Znf	zinc finger
°C	degree centigrade
μ	micro
%	percent

6 Figures and tables

7 References

Ackermann F, Waites CL, Garner CC (2015) Presynaptic active zones in invertebrates and vertebrates. EMBO reports 16:923-938.

Aimone JB, Wiles J, Gage FH (2006) Potential role for adult neurogenesis in the encoding of time in new memories. Nature neuroscience 9:723-727.

Altman J, Das GD (1965) Autoradiographic and histological evidence of postnatal hippocampal neurogenesis in rats. The Journal of comparative neurology 124:319-335.

Altrock WD et al. (2003) Functional inactivation of a fraction of excitatory synapses in mice deficient for the active zone protein bassoon. Neuron 37:787-800.

Angenstein F, Niessen HG, Goldschmidt J, Lison H, Altrock WD, Gundelfinger ED, Scheich H (2007) Manganese-enhanced MRI reveals structural and functional changes in the cortex of Bassoon mutant mice. Cerebral cortex 17:28-36.

Augustin I, Korte S, Rickmann M, Kretzschmar HA, Sudhof TC, Herms JW, Brose N (2001) The cerebellum-specific Munc13 isoform Munc13-3 regulates cerebellar synaptic transmission and motor learning in mice. The Journal of neuroscience : the official journal of the Society for Neuroscience 21:10-17.

Backman CM, Malik N, Zhang Y, Shan L, Grinberg A, Hoffer BJ, Westphal H, Tomac AC (2006) Characterization of a mouse strain expressing Cre recombinase from the 3' untranslated region of the dopamine transporter locus. Genesis 44:383-390.

Baddeley AD, Hitch G (1993) The recency effect: implicit learning with explicit retrieval? Memory & cognition 21:146-155.

Bekinschtein P, Cammarota M, Medina JH (2014) BDNF and memory processing. Neuropharmacology 76 Pt C:677-683.

Bekinschtein P, Kent BA, Oomen CA, Clemenson GD, Gage FH, Saksida LM, Bussey TJ (2013) BDNF in the dentate gyrus is required for consolidation of "pattern-separated" memories. Cell reports 5:759-768.

Bergado-Acosta JR, Muller I, Richter-Levin G, Stork O (2014) The GABA-synthetic enzyme GAD65 controls circadian activation of conditioned fear pathways. Behavioural brain research 260:92-100.

Bergado-Acosta JR, Sangha S, Narayanan RT, Obata K, Pape HC, Stork O (2008) Critical role of the 65-kDa isoform of glutamic acid decarboxylase in consolidation and generalization of Pavlovian fear memory. Learning & memory 15:163-171.

Berke JD, Hyman SE (2000) Addiction, dopamine, and the molecular mechanisms of memory. Neuron 25:515-532.

Brose N, Rosenmund C, Rettig J (2000) Regulation of transmitter release by Unc-13 and its homologues. Curr Opin Neurobiol 10:303-311.

Burgess N, Maguire EA, O'Keefe J (2002) The human hippocampus and spatial and episodic memory. Neuron 35:625-641.

Burrone J, O'Byrne M, Murthy VN (2002) Multiple forms of synaptic plasticity triggered by selective suppression of activity in individual neurons. Nature 420:414-418.

Chinnadurai G (2007) Transcriptional regulation by C-terminal binding proteins. The international journal of biochemistry & cell biology 39:1593-1607.

Clelland CD, Choi M, Romberg C, Clemenson GD, Jr., Fragniere A, Tyers P, Jessberger S, Saksida LM, Barker RA, Gage FH, Bussey TJ (2009) A functional

role for adult hippocampal neurogenesis in spatial pattern separation. Science 325:210-213.

Cooke SF, Bliss TVP (2006) Plasticity in the human central nervous system. Brain 129:1659-1673.

Davydova D, Marini C, King C, Klueva J, Bischof F, Romorini S, Montenegro-Venegas C, Heine M, Schneider R, Schroder MS, Altrock WD, Henneberger C, Rusakov DA, Gundelfinger ED, Fejtova A (2014) Bassoon specifically controls presynaptic P/Q-type Ca(2+) channels via RIM-binding protein. Neuron 82:181-194.

Dean RB, Dixon WJ (1951) Simplified Statistics for Small Numbers of Observations. Analytical Chemistry 23:636-638.

Deng W, Aimone JB, Gage FH (2010) New neurons and new memories: how does adult hippocampal neurogenesis affect learning and memory? Nature reviews Neuroscience 11:339-350.

Deng W, Saxe MD, Gallina IS, Gage FH (2009) Adult-born hippocampal dentate granule cells undergoing maturation modulate learning and memory in the brain. The Journal of neuroscience : the official journal of the Society for Neuroscience 29:13532-13542.

Dick O, tom Dieck S, Altrock WD, Ammermuller J, Weiler R, Garner CC, Gundelfinger ED, Brandstatter JH (2003) The presynaptic active zone protein bassoon is essential for photoreceptor ribbon synapse formation in the retina. Neuron 37:775-786.

Dieni S, Nestel S, Sibbe M, Frotscher M, Hellwig S (2015) Distinct synaptic and neurochemical changes to the granule cell-CA3 projection in Bassoon mutant mice. Frontiers in synaptic neuroscience 7:18.

Dresbach T, Torres V, Wittenmayer N, Altrock WD, Zamorano P, Zuschratter W, Nawrotzki R, Ziv NE, Garner CC, Gundelfinger ED (2006) Assembly of active zone precursor vesicles: obligatory trafficking of presynaptic cytomatrix proteins Bassoon and Piccolo via a trans-Golgi compartment. The Journal of biological chemistry 281:6038-6047.

Driscoll HE, Muraro NI, He M, Baines RA (2013) Pumilio-2 regulates translation of Nav1.6 to mediate homeostasis of membrane excitability. The Journal of neuroscience : the official journal of the Society for Neuroscience 33:9644-9654.

Eichenbaum H, Stewart C, Morris RG (1990) Hippocampal representation in place learning. The Journal of neuroscience : the official journal of the Society for Neuroscience 10:3531-3542.

Eichenbaum H, Yonelinas AP, Ranganath C (2007) The medial temporal lobe and recognition memory. Annual review of neuroscience 30:123-152.

Eichenbaum H, Dudchenko P, Wood E, Shapiro M, Tanila H (1999) The hippocampus, memory, and place cells: is it spatial memory or a memory space? Neuron 23:209-226.

Ennaceur A, Delacour J (1988) A new one-trial test for neurobiological studies of memory in rats. 1: Behavioral data. Behavioural brain research 31:47-59.

Faulkner RL, Low LK, Cheng HJ (2007) Axon pruning in the developing vertebrate hippocampus. Developmental neuroscience 29:6-13.

Fejtova A, Gundelfinger ED (2006) Molecular organization and assembly of the presynaptic active zone of neurotransmitter release. Results and problems in cell differentiation 43:49-68.

Fejtova A, Davydova D, Bischof F, Lazarevic V, Altrock WD, Romorini S, Schone C, Zuschratter W, Kreutz MR, Garner CC, Ziv NE, Gundelfinger ED (2009) Dynein light chain regulates axonal trafficking and synaptic levels of Bassoon. The Journal of cell biology 185:341-355.

Frank CA, Kennedy MJ, Goold CP, Marek KW, Davis GW (2006) Mechanisms underlying the rapid induction and sustained expression of synaptic homeostasis. Neuron 52:663-677.

Frank T, Rutherford MA, Strenzke N, Neef A, Pangrsic T, Khimich D, Fejtova A, Gundelfinger ED, Liberman MC, Harke B, Bryan KE, Lee A, Egner A, Riedel D, Moser T (2010) Bassoon and the synaptic ribbon organize ca(2+) channels and vesicles to add release sites and promote refilling. Neuron 68:724-738.

Furukawa-Hibi Y, Nitta A, Fukumitsu H, Somiya H, Furukawa S, Nabeshima T, Yamada K (2010) Overexpression of piccolo C2A domain induces depression-like behavior in mice. Neuroreport 21:1177-1181.

Gage FH (2002) Neurogenesis in the adult brain. The Journal of neuroscience : the official journal of the Society for Neuroscience 22:612-613.

Garriga-Canut M, Schoenike B, Qazi R, Bergendahl K, Daley TJ, Pfender RM, Morrison JF, Ockuly J, Stafstrom C, Sutula T, Roopra A (2006) 2-Deoxy-D-glucose reduces epilepsy progression by NRSF-CtBP-dependent metabolic regulation of chromatin structure. Nature neuroscience 9:1382-1387.

Gasbarri A, Sulli A, Packard MG (1997) The dopaminergic mesencephalic projections to the hippocampal formation in the rat. Progress in neuro-psychopharmacology & biological psychiatry 21:1-22.

Ge S, Yang CH, Hsu KS, Ming GL, Song H (2007) A critical period for enhanced synaptic plasticity in newly generated neurons of the adult brain. Neuron 54:559-566.

Ghiglieri V, Sgobio C, Patassini S, Bagetta V, Fejtova A, Giampa C, Marinucci S, Heyden A, Gundelfinger ED, Fusco FR, Calabresi P, Picconi B (2010) TrkB/BDNF-dependent striatal plasticity and behavior in a genetic model of epilepsy: modulation by valproic acid. Neuropsychopharmacology : official publication of the American College of Neuropsychopharmacology 35:1531-1540.

Ghiglieri V, Picconi B, Sgobio C, Bagetta V, Barone I, Paille V, Di Filippo M, Polli F, Gardoni F, Altrock W, Gundelfinger ED, De Sarro G, Bernardi G, Ammassari-Teule M, Di Luca M, Calabresi P (2009) Epilepsy-induced abnormal striatal plasticity in Bassoon mutant mice. Eur J Neurosci 29:1979-1993.

Gilbert PE, Kesner RP, DeCoteau WE (1998) Memory for spatial location: role of the hippocampus in mediating spatial pattern separation. The Journal of neuroscience : the official journal of the Society for Neuroscience 18:804-810.

Goelet P, Castellucci VF, Schacher S, Kandel ER (1986) The long and the short of long-term memory--a molecular framework. Nature 322:419-422.

Gorski JA, Talley T, Qiu M, Puelles L, Rubenstein JL, Jones KR (2002) Cortical excitatory neurons and glia, but not GABAergic neurons, are produced in the Emx1-expressing lineage. The Journal of neuroscience : the official journal of the Society for Neuroscience 22:6309-6314.

Grubbs FE (1969) Procedures for Detecting Outlying Observations in Samples. Technometrics 11:1-21.

Gundelfinger ED, Reissner C, Garner CC (2016) Role of Bassoon and Piccolo in Assembly and Molecular Organization of the Active Zone. Frontiers in synaptic neuroscience 7:19.

Hagihara H, Takao K, Walton NM, Matsumoto M, Miyakawa T (2013) Immature dentate gyrus: an endophenotype of neuropsychiatric disorders. Neural Plast 2013:318596.

Hallermann S, Fejtova A, Schmidt H, Weyhersmuller A, Silver RA, Gundelfinger ED, Eilers J (2010) Bassoon speeds vesicle reloading at a central excitatory synapse. Neuron 68:710-723.

Haws ME, Kaeser PS, Jarvis DL, Sudhof TC, Powell CM (2012) Region-specific deletions of RIM1 reproduce a subset of global RIM1alpha(-/-) phenotypes. Genes, brain, and behavior 11:201-213.

Hernandez-Rabaza V, Hontecillas-Prieto L, Velazquez-Sanchez C, Ferragud A, Perez-Villaba A, Arcusa A, Barcia JA, Trejo JL, Canales JJ (2008) The hippocampal dentate gyrus is essential for generating contextual memories of fear and drug-induced reward. Neurobiology of learning and memory 90:553-559.

Heyden A, Ionescu MC, Romorini S, Kracht B, Ghiglieri V, Calabresi P, Seidenbecher C, Angenstein F, Gundelfinger ED (2011) Hippocampal enlargement in Bassoon-mutant mice is associated with enhanced neurogenesis, reduced apoptosis, and abnormal BDNF levels. Cell Tissue Res 346:11-26.

Holland PC, Bouton ME (1999) Hippocampus and context in classical conditioning. Curr Opin Neurobiol 9:195-202.

Horch HW, Katz LC (2002) BDNF release from single cells elicits local dendritic growth in nearby neurons. Nature neuroscience 5:1177-1184.

Hubler D, Rankovic M, Richter K, Lazarevic V, Altrock WD, Fischer KD, Gundelfinger ED, Fejtova A (2012) Differential spatial expression and subcellular localization of CtBP family members in rodent brain. PloS one 7:e39710.

Ibi D, Nitta A, Ishige K, Cen X, Ohtakara T, Nabeshima T, Ito Y (2010) Piccolo knockdown-induced impairments of spatial learning and long-term potentiation in the hippocampal CA1 region. Neurochemistry international 56:77-83.

Ivanova D, Dirks A, Fejtova A (2016) Bassoon and piccolo regulate ubiquitination and link presynaptic molecular dynamics with activity-regulated gene expression. The Journal of Physiology 594:5441-5448.

Ivanova D, Dirks A, Montenegro-Venegas C, Schone C, Altrock WD, Marini C, Frischknecht R, Schanze D, Zenker M, Gundelfinger ED, Fejtova A (2015) Synaptic activity controls localization and function of CtBP1 via binding to Bassoon and Piccolo. The EMBO journal 34:1056-1077.

Jay TM (2003) Dopamine: a potential substrate for synaptic plasticity and memory mechanisms. Progress in neurobiology 69:375-390.

Juranek J, Mukherjee K, Rickmann M, Martens H, Calka J, Sudhof TC, Jahn R (2006) Differential expression of active zone proteins in neuromuscular junctions suggests functional diversification. Eur J Neurosci 24:3043-3052.

Kahne T, Kolodziej A, Smalla KH, Eisenschmidt E, Haus UU, Weismantel R, Kropf S, Wetzel W, Ohl FW, Tischmeyer W, Naumann M, Gundelfinger ED (2012) Synaptic proteome changes in mouse brain regions upon auditory discrimination learning. Proteomics 12:2433-2444.

Kesner RP (2007) A behavioral analysis of dentate gyrus function. Progress in brain research 163:567-576.

Kesner RP (2013) Role of the hippocampus in mediating interference as measured by pattern separation processes. Behavioural processes 93:148-154.

Kesner RP, Taylor JO, Hoge J, Andy F (2015) Role of the dentate gyrus in mediating object-spatial configuration recognition. Neurobiology of learning and memory 118:42-48.

Kheirbek MA, Drew LJ, Burghardt NS, Costantini DO, Tannenholz L, Ahmari SE, Zeng H, Fenton AA, Hen R (2013) Differential control of learning and anxiety along the dorsoventral axis of the dentate gyrus. Neuron 77:955-968.

Khimich D, Nouvian R, Pujol R, Tom Dieck S, Egner A, Gundelfinger ED, Moser T (2005) Hair cell synaptic ribbons are essential for synchronous auditory signalling. Nature 434:889-894.

Kitamura T, Sun C, Martin J, Kitch LJ, Schnitzer MJ, Tonegawa S (2015) Entorhinal Cortical Ocean Cells Encode Specific Contexts and Drive Context-Specific Fear Memory. Neuron 87:1317-1331.

Kononenko N, Pechstein A, Haucke V (2013) Synaptic requiem: a duet for Piccolo and Bassoon. The EMBO journal 32:920-922.

Lanore F, Blanchet C, Fejtova A, Pinheiro P, Richter K, Balschun D, Gundelfinger E, Mulle C (2010) Impaired development of hippocampal mossy fibre synapses in mouse mutants for the presynaptic scaffold protein Bassoon. The Journal of physiology 588:2133-2145.

Laxmi TR, Stork O, Pape HC (2003) Generalisation of conditioned fear and its behavioural expression in mice. Behavioural brain research 145:89-98.

Lazarevic V, Schone C, Heine M, Gundelfinger ED, Fejtova A (2011) Extensive remodeling of the presynaptic cytomatrix upon homeostatic adaptation to network activity silencing. The Journal of neuroscience : the official journal of the Society for Neuroscience 31:10189-10200.

Lee I, Kesner RP (2004) Differential contributions of dorsal hippocampal subregions to memory acquisition and retrieval in contextual fear-conditioning. Hippocampus 14:301-310.

Leutgeb JK, Leutgeb S, Moser MB, Moser EI (2007) Pattern separation in the dentate gyrus and CA3 of the hippocampus. Science 315:961-966.

Lim DA, Tramontin AD, Trevejo JM, Herrera DG, Garcia-Verdugo JM, Alvarez-Buylla A (2000) Noggin antagonizes BMP signaling to create a niche for adult neurogenesis. Neuron 28:713-726.

Liu IY, Lyons WE, Mamounas LA, Thompson RF (2004) Brain-derived neurotrophic factor plays a critical role in contextual fear conditioning. The Journal of neuroscience : the official journal of the Society for Neuroscience 24:7958-7963.

Liu X, Ramirez S, Pang PT, Puryear CB, Govindarajan A, Deisseroth K, Tonegawa S (2012) Optogenetic stimulation of a hippocampal engram activates fear memory recall. Nature 484:381-385.

Loughlin SE, Fallon JH (1984) Substantia nigra and ventral tegmental area projections to cortex: topography and collateralization. Neuroscience 11:425-435.

Luscher C, Xia H, Beattie EC, Carroll RC, von Zastrow M, Malenka RC, Nicoll RA (1999) Role of AMPA receptor cycling in synaptic transmission and plasticity. Neuron 24:649-658.

Magloczky Z, Halasz P, Vajda J, Czirjak S, Freund TF (1997) Loss of Calbindin-D28K immunoreactivity from dentate granule cells in human temporal lobe epilepsy. Neuroscience 76:377-385.

Maren S, Anagnostaras SG, Fanselow MS (1998) The startled seahorse: is the hippocampus necessary for contextual fear conditioning? Trends in cognitive sciences 2:39-42.

Maren S, Phan KL, Liberzon I (2013) The contextual brain: implications for fear conditioning, extinction and psychopathology. Nature reviews Neuroscience 14:417-428.

Martin SJ, de Hoz L, Morris RGM (2005) Retrograde amnesia: neither partial nor complete hippocampal lesions in rats result in preferential sparing of remote spatial memory, even after reminding. Neuropsychologia 43:609-624.

Mendoza Schulz A, Jing Z, María Sánchez Caro J, Wetzel F, Dresbach T, Strenzke N, Wichmann C, Moser T (2014) Bassoon-disruption slows vesicle replenishment and induces homeostatic plasticity at a CNS synapse. The EMBO Journal 33:512-527.

Ming GL, Song H (2005) Adult neurogenesis in the mammalian central nervous system. Annual review of neuroscience 28:223-250.

Montag-Sallaz M, Montag D (2003) Severe cognitive and motor coordination deficits in Tenascin-R-deficient mice. Genes, Brain and Behavior 2:20-31.

Moser E, Moser MB, Andersen P (1993) Spatial learning impairment parallels the magnitude of dorsal hippocampal lesions, but is hardly present following ventral lesions. The Journal of neuroscience : the official journal of the Society for Neuroscience 13:3916-3925.

Mylius J, Brosch M, Scheich H, Budinger E (2013) Subcortical auditory structures in the Mongolian gerbil: I. Golgi architecture. The Journal of comparative neurology 521:1289-1321.

Nakashiba T, Cushman JD, Pelkey KA, Renaudineau S, Buhl DL, McHugh TJ, Rodriguez Barrera V, Chittajallu R, Iwamoto KS, McBain CJ, Fanselow MS, Tonegawa S (2012) Young dentate granule cells mediate pattern separation, whereas old granule cells facilitate pattern completion. Cell 149:188-201.

Nelson SB, Turrigiano GG (2008) Strength through diversity. Neuron 60:477-482.

Netrakanti PR, Cooper BH, Dere E, Poggi G, Winkler D, Brose N, Ehrenreich H (2015) Fast cerebellar reflex circuitry requires synaptic vesicle priming by munc13-3. Cerebellum 14:264-283.

Neves G, Cooke SF, Bliss TV (2008) Synaptic plasticity, memory and the hippocampus: a neural network approach to causality. Nature reviews Neuroscience 9:65-75.

Okerlund ND, Schneider K, Leal-Ortiz S, Montenegro-Venegas C, Kim SA, Garner LC, Gundelfinger ED, Reimer RJ, Garner CC (2017) Bassoon Controls Presynaptic Autophagy through Atg5. Neuron 93:897-913 e897.

Palmer TD, Markakis EA, Willhoite AR, Safar F, Gage FH (1999) Fibroblast growth factor-2 activates a latent neurogenic program in neural stem cells from diverse regions of the adult CNS. The Journal of neuroscience : the official journal of the Society for Neuroscience 19:8487-8497.

Pastalkova E, Serrano P, Pinkhasova D, Wallace E, Fenton AA, Sacktor TC (2006) Storage of spatial information by the maintenance mechanism of LTP. Science 313:1141-1144.

Phillips RG, LeDoux JE (1994) Lesions of the dorsal hippocampal formation interfere with background but not foreground contextual fear conditioning. Learning & memory 1:34-44.

Picciotto MR, Higley MJ, Mineur YS (2012) Acetylcholine as a neuromodulator: cholinergic signaling shapes nervous system function and behavior. Neuron 76:116-129.

Pleskacheva MG, Wolfer DP, Kupriyanova IF, Nikolenko DL, Scheffrahn H, Dell'Omo G, Lipp HP (2000) Hippocampal mossy fibers and swimming navigation

learning in two vole species occupying different habitats. Hippocampus 10:17-30.

Powell CM, Schoch S, Monteggia L, Barrot M, Matos MF, Feldmann N, Sudhof TC, Nestler EJ (2004) The presynaptic active zone protein RIM1alpha is critical for normal learning and memory. Neuron 42:143-153.

Ramirez S, Liu X, Lin PA, Suh J, Pignatelli M, Redondo RL, Ryan TJ, Tonegawa S (2013) Creating a false memory in the hippocampus. Science 341:387-391.

Rehberg K, Kliche S, Madencioglu DA, Thiere M, Muller B, Meineke BM, Freund C, Budinger E, Stork O (2014) The serine/threonine kinase Ndr2 controls integrin trafficking and integrin-dependent neurite growth. The Journal of neuroscience : the official journal of the Society for Neuroscience 34:5342-5354.

Richter K, Langnaese K, Kreutz MR, Olias G, Zhai R, Scheich H, Garner CC, Gundelfinger ED (1999) Presynaptic cytomatrix protein bassoon is localized at both excitatory and inhibitory synapses of rat brain. The Journal of comparative neurology 408:437-448.

Rizzoli SO, Betz WJ (2005) Synaptic vesicle pools. Nature reviews Neuroscience 6:57-69.

Roozendaal B, Hernandez A, Cabrera SM, Hagewoud R, Malvaez M, Stefanko DP, Haettig J, Wood MA (2010) Membrane-associated glucocorticoid activity is necessary for modulation of long-term memory via chromatin modification. The Journal of neuroscience : the official journal of the Society for Neuroscience 30:5037-5046.

Rosenmund C, Rettig J, Brose N (2003) Molecular mechanisms of active zone function. Curr Opin Neurobiol 13:509-519.

Sahay A, Scobie KN, Hill AS, O'Carroll CM, Kheirbek MA, Burghardt NS, Fenton AA, Dranovsky A, Hen R (2011) Increasing adult hippocampal neurogenesis is sufficient to improve pattern separation. Nature 472:466-470.

Sailor KA, Schinder AF, Lledo PM (2017) Adult neurogenesis beyond the niche: its potential for driving brain plasticity. Curr Opin Neurobiol 42:111-117.

Sanmarti-Vila L, tom Dieck S, Richter K, Altrock W, Zhang L, Volknandt W, Zimmermann H, Garner CC, Gundelfinger ED, Dresbach T (2000) Membrane association of presynaptic cytomatrix protein bassoon. Biochemical and biophysical research communications 275:43-46.

Saxe MD, Battaglia F, Wang JW, Malleret G, David DJ, Monckton JE, Garcia AD, Sofroniew MV, Kandel ER, Santarelli L, Hen R, Drew MR (2006) Ablation of hippocampal neurogenesis impairs contextual fear conditioning and synaptic plasticity in the dentate gyrus. Proceedings of the National Academy of Sciences of the United States of America 103:17501-17506.

Schacher S, Hu JY (2014) The less things change, the more they are different: contributions of long-term synaptic plasticity and homeostasis to memory. Learning & memory 21:128-134.

Schacter DL, Norman KA, Koutstaal W (1998) The cognitive neuroscience of constructive memory. Annual review of psychology 49:289-318.

Schmidt-Hieber C, Jonas P, Bischofberger J (2004) Enhanced synaptic plasticity in newly generated granule cells of the adult hippocampus. Nature 429:184-187.

Schoch S, Gundelfinger ED (2006) Molecular organization of the presynaptic active zone. Cell Tissue Res 326:379-391.

Schoch S, Castillo PE, Jo T, Mukherjee K, Geppert M, Wang Y, Schmitz F, Malenka RC, Sudhof TC (2002) RIM1alpha forms a protein scaffold for regulating neurotransmitter release at the active zone. Nature 415:321-326.

Scoville WB, Milner B (1957) Loss of recent memory after bilateral hippocampal lesions. Journal of neurology, neurosurgery, and psychiatry 20:11-21.

Selden NR, Everitt BJ, Jarrard LE, Robbins TW (1991) Complementary roles for the amygdala and hippocampus in aversive conditioning to explicit and contextual cues. Neuroscience 42:335-350.

Sgobio C, Ghiglieri V, Costa C, Bagetta V, Siliquini S, Barone I, Di Filippo M, Gardoni F, Gundelfinger ED, Di Luca M, Picconi B, Calabresi P (2010) Hippocampal synaptic plasticity, memory, and epilepsy: effects of long-term valproic acid treatment. Biological psychiatry 67:567-574.

Shapira M, Zhai RG, Dresbach T, Bresler T, Torres VI, Gundelfinger ED, Ziv NE, Garner CC (2003) Unitary assembly of presynaptic active zones from Piccolo-Bassoon transport vesicles. Neuron 38:237-252.

Sigrist SJ, Schmitz D (2011) Structural and functional plasticity of the cytoplasmic active zone. Curr Opin Neurobiol 21:144-150.

Silverman JL, Yang M, Lord C, Crawley JN (2010) Behavioural phenotyping assays for mouse models of autism. Nature reviews Neuroscience 11:490-502.

Smith WB, Starck SR, Roberts RW, Schuman EM (2005) Dopaminergic stimulation of local protein synthesis enhances surface expression of GluR1 and synaptic transmission in hippocampal neurons. Neuron 45:765-779.

Song H, Stevens CF, Gage FH (2002) Astroglia induce neurogenesis from adult neural stem cells. Nature 417:39-44.

Song JW, Misgeld T, Kang H, Knecht S, Lu J, Cao Y, Cotman SL, Bishop DL, Lichtman JW (2008) Lysosomal activity associated with developmental axon pruning. The Journal of neuroscience : the official journal of the Society for Neuroscience 28:8993-9001.

Spampanato J, Sullivan RK, Turpin FR, Bartlett PF, Sah P (2012) Properties of doublecortin expressing neurons in the adult mouse dentate gyrus. PloS one 7:e41029.

Sparkman NL, Kohman RA, Garcia AK, Boehm GW (2005) Peripheral lipopolysaccharide administration impairs two-way active avoidance conditioning in C57BL/6J mice. Physiology & behavior 85:278-288.

Squire LR, Zola SM (1996) Memory, memory impairment, and the medial temporal lobe. Cold Spring Harbor symposia on quantitative biology 61:185-195.

Stefanelli T, Bertollini C, Luscher C, Muller D, Mendez P (2016) Hippocampal Somatostatin Interneurons Control the Size of Neuronal Memory Ensembles. Neuron 89:1074-1085.

Stefanko DP, Barrett RM, Ly AR, Reolon GK, Wood MA (2009) Modulation of long-term memory for object recognition via HDAC inhibition. Proceedings of the National Academy of Sciences of the United States of America 106:9447-9452.

Stone SS, Teixeira CM, Devito LM, Zaslavsky K, Josselyn SA, Lozano AM, Frankland PW (2011) Stimulation of entorhinal cortex promotes adult neurogenesis and facilitates spatial memory. The Journal of neuroscience : the official journal of the Society for Neuroscience 31:13469-13484.

Stork O, Ji F-Y, Kaneko K, Stork S, Yoshinobu Y, Moriya T, Shibata S, Obata K (2000) Postnatal development of a GABA deficit and disturbance of neural functions in mice lacking GAD65. Brain Research 865:45-58.

Strekalova T, Spanagel R, Bartsch D, Henn FA, Gass P (2004) Stress-induced anhedonia in mice is associated with deficits in forced swimming and exploration. Neuropsychopharmacology : official publication of the American College of Neuropsychopharmacology 29:2007-2017.

Sudhof TC (2004) The synaptic vesicle cycle. Annual review of neuroscience 27:509-547.

Sutherland RJ, Weisend MP, Mumby D, Astur RS, Hanlon FM, Koerner A, Thomas MJ, Wu Y, Moses SN, Cole C, Hamilton DA, Hoesing JM (2001) Retrograde amnesia after hippocampal damage: recent vs. remote memories in two tasks. Hippocampus 11:27-42.

Tang G, Gudsnuk K, Kuo SH, Cotrina ML, Rosoklija G, Sosunov A, Sonders MS, Kanter E, Castagna C, Yamamoto A, Yue Z, Arancio O, Peterson BS, Champagne F, Dwork AJ, Goldman J, Sulzer D (2014) Loss of mTOR-dependent macroautophagy causes autistic-like synaptic pruning deficits. Neuron 83:1131-1143.

Tolwani RJ, Buckmaster PS, Varma S, Cosgaya JM, Wu Y, Suri C, Shooter EM (2002) BDNF overexpression increases dendrite complexity in hippocampal dentate gyrus. Neuroscience 114:795-805.

tom Dieck S, Altrock WD, Kessels MM, Qualmann B, Regus H, Brauner D, Fejtova A, Bracko O, Gundelfinger ED, Brandstatter JH (2005) Molecular dissection of the photoreceptor ribbon synapse: physical interaction of Bassoon and RIBEYE is essential for the assembly of the ribbon complex. The Journal of cell biology 168:825-836.

tom Dieck S, Sanmarti-Vila L, Langnaese K, Richter K, Kindler S, Soyke A, Wex H, Smalla KH, Kampf U, Franzer JT, Stumm M, Garner CC, Gundelfinger ED (1998) Bassoon, a novel zinc-finger CAG/glutamine-repeat protein selectively localized at the active zone of presynaptic nerve terminals. The Journal of cell biology 142:499-509.

Toni N, Schinder AF (2015) Maturation and Functional Integration of New Granule Cells into the Adult Hippocampus. Cold Spring Harbor perspectives in biology 8:a018903.

Treiman DM (2001) GABAergic Mechanisms in Epilepsy. Epilepsia 42:8-12.

Tulving E, Markowitsch HJ (1998) Episodic and declarative memory: role of the hippocampus. Hippocampus 8:198-204.

van Praag H, Schinder AF, Christie BR, Toni N, Palmer TD, Gage FH (2002) Functional neurogenesis in the adult hippocampus. Nature 415:1030-1034.

Vijayan V, Verstreken P (2017) Autophagy in the presynaptic compartment in health and disease. The Journal of cell biology.

von Bohlen und Halbach O (2007) Immunohistological markers for staging neurogenesis in adult hippocampus. Cell and Tissue Research 329:409-420.

Waites CL, Leal-Ortiz SA, Okerlund N, Dalke H, Fejtova A, Altrock WD, Gundelfinger ED, Garner CC (2013) Bassoon and Piccolo maintain synapse integrity by regulating protein ubiquitination and degradation. The EMBO journal 32:954-969.

Wang X, Kibschull M, Laue MM, Lichte B, Petrasch-Parwez E, Kilimann MW (1999) Aczonin, a 550-kD putative scaffolding protein of presynaptic active zones, shares homology regions with Rim and Bassoon and binds profilin. The Journal of cell biology 147:151-162.

Wang Y, Sudhof TC (2003) Genomic definition of RIM proteins: evolutionary amplification of a family of synaptic regulatory proteins. Genomics 81:126-137.

Winter C, tom Dieck S, Boeckers TM, Bockmann J, Kampf U, Sanmarti-Vila L, Langnaese K, Altrock W, Stumm M, Soyke A, Wieacker P, Garner CC, Gundelfinger ED (1999) The presynaptic cytomatrix protein Bassoon: sequence and chromosomal localization of the human BSN gene. Genomics 57:389-397.

Won H, Lee HR, Gee HY, Mah W, Kim JI, Lee J, Ha S, Chung C, Jung ES, Cho YS, Park SG, Lee JS, Lee K, Kim D, Bae YC, Kaang BK, Lee MG, Kim E (2012) Autistic-like social behaviour in Shank2-mutant mice improved by restoring NMDA receptor function. Nature 486:261-265.

Wood R, Baxter P, Belpaeme T (2012) A review of long-term memory in natural and synthetic systems. Adaptive Behavior 20:81-103.

Xavier GF, Costa VC (2009) Dentate gyrus and spatial behaviour. Progress in neuro-psychopharmacology & biological psychiatry 33:762-773.

Yamada K, Nabeshima T (2003) Brain-derived neurotrophic factor/TrkB signaling in memory processes. Journal of pharmacological sciences 91:267-270.

Zhai R, Olias G, Chung WJ, Lester RA, tom Dieck S, Langnaese K, Kreutz MR, Kindler S, Gundelfinger ED, Garner CC (2000) Temporal appearance of the presynaptic cytomatrix protein bassoon during synaptogenesis. Molecular and cellular neurosciences 15:417-428.

Zhai RG, Vardinon-Friedman H, Cases-Langhoff C, Becker B, Gundelfinger ED, Ziv NE, Garner CC (2001) Assembling the presynaptic active zone: a characterization of an active one precursor vesicle. Neuron 29:131-143.

Zhang W, Linden DJ (2003) The other side of the engram: experience-driven changes in neuronal intrinsic excitability. Nature reviews Neuroscience 4:885-900.

Zhao C, Deng W, Gage FH (2008) Mechanisms and functional implications of adult neurogenesis. Cell 132:645-660.

Ziv NE, Garner CC (2004) Cellular and molecular mechanisms of presynaptic assembly. Nature reviews Neuroscience 5:385-399.

8 Curriculum Vitae

Personal Information

Name	Annamneedi, Anil
Date of Birth	16-03-1987
Nationality	Indian

Education

Aug 2012 – Present   **Ph.D. in Neurobiology –** Leibniz Institute for Neurobiology (LIN), Magdeburg, Germany
Thesis project: Functions of Bassoon in learning and memory processes using conditional mutants

July 2012   **M.Eng. Biomedical Engineering –** Anhalt University of applied sciences, Köthen and Martin - Luther University, Halle, Germany
Thesis: Genetic crosstalk of Ret and Parkin in maintaining dopaminergic innervation of the striatum, Center for Molecular Neurobiology Hamburg (ZMNH), Hamburg, Germany

April 2009   **M.Sc. Human Genetics –** Andhra University, Visakhapatnam, India
Project: Genotyping of short tandem repeats of genomic DNA isolated from brain tissue, Andhra Pradesh Forensic Science Laboratory (APFSL), Hyderabad, India

March 2007   **B.Sc. Chemistry, Zoology and Biotechnology**
Andhra University, Visakhapatnam, India

April 2004   **Higher secondary school (Biology, Physics and Chemistry)**
Guntur, India

Scientific Presentations

- **Oral presentation** - Conditional mutants of Bassoon in excitatory forebrain synapses and dopaminergic synapses, to study its contribution in learning and memory processes- 11th German Neuroscience Society meeting, Göttingen, Germany, 2015
- **Poster presentation** - Conditional mutant of Bassoon in forebrain excitatory synapses, shows altered cortex- and hippocampus-dependent behavior, morphology and basal neurotransmission- 10th FENS (Federation of European Neuroscience Societies) Forum, Copenhagen, Denmark, 2016
- **Poster presentation** - Genetic mouse model to study Bassoon's function in excitatory forebrain synapses during learning and memory processes- Active zone meeting, Würzburg, Germany, 2014

9 Scientific Publications

- Altmüller F, Pothula S, **Annamneedi A**, Nakhaei-Rad S, Montenegro-Venegas C, Pina-Fernández E, Marini C, Santos M, Schanze D, Montag D, Ahmadian MR, Stork O, Zenker M, Fejtova A. Aberrant neuronal activity-induced signaling and gene expression in a mouse model of RASopathy. PLoS Genet. 2017 Mar 27;13(3): e1006684. doi: 10.1371/journal.pgen.1006684.

- Meka DP, Müller-Rischart AK, Nidadavolu P, Mohammadi B, Motori E, Ponna SK, Aboutalebi H, Bassal M, **Annamneedi A**, Finckh B, Miesbauer M, Rotermund N, Lohr C, Tatzelt J, Winklhofer KF, Kramer ER. Parkin cooperates with GDNF/RET signaling to prevent dopaminergic neuron degeneration. J Clin Invest. 2015 May;125(5):1873-85. doi: 10.1172/JCI79300.

10 Erklärung

Hiermit erkläre ich, dass ich die von mir eingereichte Dissertation zum dem Thema "**Functions of Bassoon in hippocampus-dependent learning and memory processes**" selbständig verfasst, nicht schon als Dissertation verwendet habe und die benutzten Hilfsmittel und Quellen vollständig angegeben wurden.
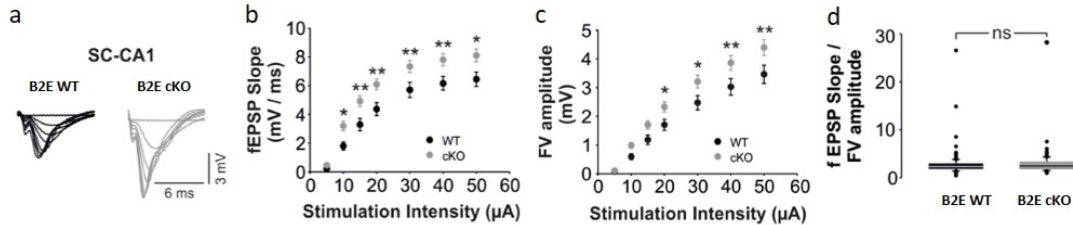
Weiterhin erkläre ich, dass ich weder diese noch eine andere Arbeit zur Erlangung des akademischen Grades doctor rerum naturalium (Dr. rer. nat.) an anderen Einrichtungen eingereicht habe.

Ort, Datum   (Anil Annamneedi)

11 Appendix

11.1 Increased excitability at Schaffer collateral (SC)-CA1 synapses but no change in fiber volley (FV) to fEPSP ratio

Appendix figure 11.1. Increased excitability but no change in synaptic efficacy at SC-CA1 synapses in B2E cKO mice. a, Merged traces of field excitatory postsynaptic potential (fEPSP) responses to increasing stimulation strengths (5-50 μA) at the SC-CA1 synapse (WT: black; cKO: gray). **b,** Summary graphs indicating increased synaptic excitability in SC-CA1 synapses of B2E cKO mice (N = 7 mice, n = 34 slices) compared to WT mice (N = 5 mice, n = 27 slices). **c,** Summary graphs indicating increased presynaptic fiber volley (FV) amplitude in SC-CA1 synapses of B2E cKO mice (N = 7 mice, n = 29 slices) compared to WT mice (N = 5 mice, n = 23 slices). **d,** Graphs summarizing fEPSP slope to FV amplitude ratios for the SC-CA1 pathway. All values are expressed as mean ± SEM. * significant difference to WT with $P \leq 0.05$; ** $P \leq 0.01$; ns = not significant (Two-way repeated ANOVA followed by posthoc comparison using Fisher LSD Method). SC: Schaffer collaterals, CA1: Cornu ammonis area 1. (This data and figure panels were provided by Dr. Gürsel Caliskan).

11.2 Increased excitability at MPP-DG is rescued by blocking TrkB receptors in B2E cKO mice
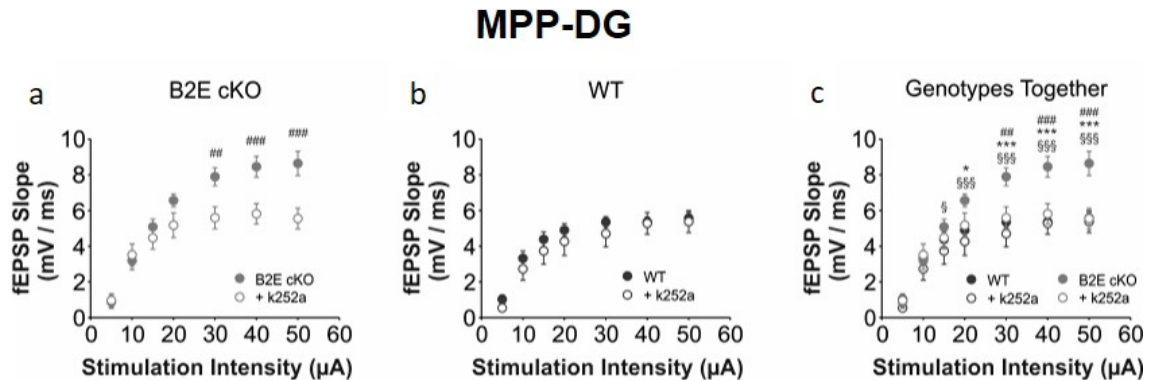
Appendix figure 11.2. Increased baseline transmission at MPP-DG is rescued in B2E cKO mice. a, Summary graphs indicating increased synaptic excitability at MPP-DG synapses of B2E cKO mice is rescued by blocking TrkB receptors using k252a treatment (200 nM). **b,** Summary graph showing no change in excitability in WT mice with or without treatment with k252a. **c,** Graph showing all the groups except B2E cKO have similar levels of fEPSP slopes, indicating the effect of BDNF at DG of B2E cKO mice. All values are expressed as mean ± SEM. * significant difference between B2E cKO vs. B2E WT, # significant difference between B2E cKO vs. B2E cKO-k252a, the § significant difference between B2E cKO vs. B2E WT-k252a. *,§$P \leq 0.05$; ## $P \leq 0.01$; ***,§§§,###$P \leq 0.001$ (Two-way repeated ANOVA followed by posthoc comparison using Fisher LSD Method). (This data and figure panels were provided by Dr. Gürsel Caliskan).